# Neuroimaging Studies of Brain Networks in Parkinson's Disease

Clare Loane

Imperial College London

Department of Medicine

Thesis submitted in fulfillment of the requirements for the degree of Doctor of Philosophy

**Abstract**

Parkinson's disease (PD) is a common, disabling, neurodegenerative disease characterised by three core motor symptoms: tremor, rigidity and bradykinesia. These symptoms arise from degeneration of dopaminergic (DA) cells in the substantia nigra (SN) and the subsequent loss of dopaminergic terminals within the striatum, and circuits to cortical areas, critical in the control of movement. Other, non-DA systems are now known to be involved in the pathogenesis of PD, defective cognitive functions and side effects of DA medication treatments. Thus, the use of non-invasive in vivo techniques such as magnetic resonance imaging (MRI) has allowed a reliable, albeit in-direct method of assessing alterations in the PD brain. It is now widely considered that motor control is dependent upon the integrated operation of large-scale distributed brain networks. Recent methodological advances in MRI techniques allow both structural and functional connectivity between critical regions of motor control to be investigated and increase our understanding of the impact of PD pathology on motor networks and its subsequent effect on symptomatology. In this thesis, I present three studies that combine both structural and functional MRI techniques to assess the neural PD motor network and to test the general hypothesis that loss of effective motor control in PD arises from disrupted connectivity. I demonstrate in a sizable cross-sectional study that as disease burden increases, effective functioning in key motor areas and functional connectivity between regions in both the active and resting state is initially compromised but does show evidence of compensatory mechanisms. In addition, I show that compensatory mechanisms are likely to possess a neural reserve property rather than permit a period of normal functioning. Next, I present a follow-up study that assessed the active and resting

neural motor network longitudinally. This study clearly shows that functional connectivity of the active and resting neural motor network is compromised as the disease progresses with evidence suggesting the initiation of compensatory mechanisms. Finally, structural properties of key regions related to PD pathology (substantia nigra and striatum) have been assessed to elucidate the effect of PD progression on diffusion indices and clinical symptoms. This work identifies the importance of multi-modal assessment of neural networks in PD to evaluate the effect of disease on neural motor control.

**Declaration of Originality**

The work presented in this thesis was carried out in the Division of Brain Sciences of the Department of Medicine at Imperial College London from September 2011.

**Copyright Declaration**

This thesis is the result of my own work and any quotation from, or description of the work of others is acknowledged. The copyright of this thesis rests with the author and is made available under a Creative Commons Attribution Non-Commercial No Derivatives licence. Researchers are free to copy, distribute or transmit the thesis on the condition that they attribute it, that they do not use it for commercial purposes and that they do not alter, transform or build upon it. For any reuse or redistribution, researchers must make clear to others the licence terms of this work.

**Acknowledgments**

Thank you to:

**Prof. Paola Piccini** for the opportunity to complete this work.

Members of the **Neurology Imaging Unit**, past and present, for their good company throughout this journey.

All the **patients** who kindly agreed to take part in my studies.

**Matt Wall** (Imanova Ltd), **Harry Rolinski** (University of Oxford) and **Flavio Dell'Acqua** (King's College London) for their advice regarding analysis of fMRI motor, resting and DTI data respectively.

**TransEuro members** from other sites for their cooperation in study procedures, sending patients to Imperial to be scanned and clinically assessing non-Imperial patients at their respective sites.

**Imanova Ltd radiographers** for assisting with scanning.

Completing this journey would not have been possible without the support of my family. A special thank you goes to my mother and brother who were always ready to give a supportive push when needed. A final thank you goes to Giampaolo who shared this experience with me.

**Publications arising from thesis**

**Loane C**, Politis M, Kefalopoulou Z, Valle-Guzman N, Bjorkland A, Paul G, Widner H, Foltynie T, Barker R, Piccini P. Aberrant nigro-striatal diffusion in Parkinson's disease: a longitudinal DTI study. Undergoing revision for Movement Disorders, 2015.

**Loane C**, Politis M, Martin-Bastida A, Wall M, Kefalopoulou Z; Valle-Guzman, N, Bjorkland A, Paul G, Widner H, Foltynie T, Barker R, Piccini P. Neural motor network decline and compensation as a consequence of disease burden in Parkinson's disease. Ready for submission.

**Loane C**, Politis M, Kefalopoulou Z, Valle-Guzman N, Bjorkland A, Paul G, Widner H, Foltynie T, Barker R, Piccini P. Parkinson's disease progression and altered connectivity in motor networks. In Preparation.

**Table of contents**


**Abstract** 2

**Declaration of originality** 4

**Acknowledgments** 5

**Publications arising from thesis** 6

**Table of contents** 7

**List of figures** 12

**List of tables** 13

**Abbreviations** 14

**CHAPTER 1: INTRODUCTION** 17

**1. Epidemiology of Parkinson's disease** 17

**2. Symptomatology of Parkinson's disease** 17

**3. Pathogenesis** 18

3.1 Dopamine and the Substantia Nigra 18

3.2 Lewy Bodies 18

3.3 Non-Dopaminergic Pathology 19

3.4 The Braak Hypothesis 19

**4. Pathophysiology** 20

4.1 The basal ganglia 20

4.2 The basal ganglia and PD 22

**5. Functional and structural neuroimaging of Parkinson's disease** 23

5.1 Introduction 23

5.2 fMRI studies of motor control in PD 23

**6. Resting state fMRI (rs-fMRI) studies in Parkinson's disease** 28

**7. Diffusion tensor imaging in Parkinson's disease** **38**

**8. Summary of Aims** **45**

**CHAPTER 2: SUBJECTS AND METHODOLOGY** **47**

**1. Patients** **47**

1.1 Recruitment 47

1.2 Inclusion and exclusion criteria 48

1.3 Clinical evaluation 49

**2. Magnetic resonance imaging (MRI)** **49**

2.1 Principles 49

2.2 Nuclear Magnetic Resonance 50

2.3 Image formation 51

**3. Functional MRI** **53**

3.1 The BOLD signal 53

3.2 Echo-planar imaging 53

**4. Analysis of fMRI data** **54**

4.1 Comparison of two major software tools 54

4.2 Pre-processing of fMRI data 57

4.3 Statistical Analysis 59

**5. Analysis approaches for rsfMRI data** **61**

**6. Diffusion Tensor Imaging (DTI)** **62**

6.1 Principles 62

6.2 Measuring diffusion with MRI 63

6.3 Diffusion measures 64

**7. Analysis of DTI data** **66**

**8. Scanning protocol** **67**

8.1 Description of scanning sessions 67

8.2 Scanner parameters 64

8.3 Motor Task Paradigm 67

8.4 The joystick 70

8.5 Behavioural Motor Data 72

**CHAPTER 3: BASELINE MOTOR NETWORKS IN PARKINSONS DISEASE** **73**

**1. Introduction** **73**

**2. Aims** **75**

**3. Hypotheses** **75**

**4. Patients and Methods** **76**

4.1 Patients 76

4.2 Scanning procedure 79

4.3 Behavioral motor data 79

4.4 Image analysis 79

4.5 Statistical analysis 80

**5. Results**

**5.1 Participants** **81**

5.2 Behavioural: Motor execution and amplitude 81

5.3 fMRI motor execution and disease burden: voxel-by-voxel-analysis 82

5.4 fMRI motor execution and disease burden: functional connectivity 85

5.5 Rs-fMRI and disease burden: functional connectivity 86

**6. Discussion** **88**

**CHAPTER 4: MOTOR NETWORKS IN PARKINSONS DISEASE OVER TIME** **94**

**1. Introduction** **94**

**2. Aims** **95**

**3. Hypotheses** **95**

**4. Subjects and methods** **96**

4.1 Patients 96

4.2 Scanning procedures 97

4.3 Behavioural Motor Data 98

4.4 Image analysis 98

4.5 Statistical analysis 98

**5. Results** **99**

5.1 Clinical changes 99

5.2 Behavioural analysis 99

5.3 fMRI motor task: ROI analysis 101

5.4 fMRI motor task: time series regional analysis 103

5.5 fMRI motor task: functional connectivity 104

5.6 Rs-fMRI: functional connectivity 106

**6. Discussion** **107**

**CHAPTER 5: LONGITUDINAL CHANGES IN DIFFUSION OVER TIME** **113**

**1. Introduction** **113**

**2. Aims** **115**

**3. Hypotheses** **115**

**4. Subjects and Methods** **115**

4.1 Patients 115

4.2 Scanning procedure 117

4.3 ROI delineation 117

4.4 Image analysis 117

4.5 Statistical Analysis 118

**5. Results 119**

5.1 Clinical changes 119

5.2 ROI Analysis 119

5.3 Clinical Correlations 121

5.4 VBA 122

**6. Discussion 125**

**CHAPTER 6: DISCUSSION 128**

**1. Summary of Key Results 128**

**2. Compensation mechanisms in PD motor networks 130**

**3. Studying networks longitudinally 132**

**4. Nigral diffusion indices in PD 133**

**5. Limitations of thesis studies and building on the current work 134**

5.1 Limitations of current studies 134

5.2 Considerations for building on current studies 135

**6. Implications for future research 137**

**References 141**

**List of Figures**

Figure 1. Braak stages in the development of Parkinson's disease. 20

Figure 2. The basal ganglia motor circuit. 21

Figure 3. T1-weighted and T2-weighted images examples 52

Figure 4. Analysis Pipeline comparison 56

Figure 5. Motor Paradigm 69

Figure 6. Extracted behavioural data from joystick 71

Figure 7. Behavioural motor results across disease burden in PD patients 82

Figure 8. BOLD signal changes as a consequence of disease burden 84

Figure 9. Functional connectivity of A) motor task fMRI and B) resting motor network 87

Figure 10. Motor execution performance in PD patients across visits 100

Figure 11. Motor amplitude performance in PD patients across visits 100

Figure 12. Regional BOLD signal reduction at follow-up vs. baseline 102

Figure 13. ROI extracted time series for movement vs. no-movement condition in PD patients. 103

Figure 14. Active functional connectivity changes over time in PD patients 105

Figure 15. Resting functional connectivity changes over time in PD patients. 106

Figure 16. Substantia Nigra ROI placement. 119

Figure 17. Alteration of nigral diffusion indices in PD patients over time. 121

Figure 18. Correlation between nigral MD and % change of UPDRS-III at follow-up. 122

Figure 19. Significant regional alterations of diffusion indices in PD patients. 124

**List of Tables**

Table 1. Main fMRI motor task studies in Parkinson's disease 26

Table 2. Main rs-fMRI publications in PD in Parkinson's disease 34

Table 3. Main DTI publications in PD in Parkinson's disease 43

Table 4. Patient characteristics undergoing motor task fMRI. 77

Table 5. Patient characteristics undergoing resting state fMRI. 78

Table 6. Significant ROIs with BOLD signal changes as a consequence of disease burden. 83

Table 7. Patient characteristics in longitudinal study. 98

Table 8. Significant ROIs with BOLD signal reduction over time in PD patients. 101

Table 9. Patient characteristics in DTI study. 116

Table 10. Diffusion indices from ROI analysis. 120

Table 11. VBA of FA and MD over time in PD patients. 123

**Abbreviations**

| | |
|---|---|
| 5-HT | Serotonin |
| ADC | Apparent Diffusion Coefficient |
| AIMs | Abnormal Involuntary Movement Scale |
| ALFF | Amplitude of Low Frequency Fluctuations |
| BDI | Beck Depression Inventory |
| BV | Blood Volume |
| BOLD | Blood Oxygenation Level Dependent Signal |
| CBF | Cerebral Blood Flow |
| CSF | Cerebral Spinal Fluid |
| CTC | Cerebello-Thalamo-Cortical Circuit |
| DA | Dopamine |
| DA-ergic | Dopaminergic |
| DLPFC | Dorsal-Lateral Pre-Frontal Cortex |
| DMN | Default Mode Network |
| DTI | Diffusion Tensor Imaging |
| EPI | Echo Planar Imaging |
| EV | Explanatory Variable |
| FA | Fractional Anisotropy |
| FDR | False Discovery Rate |
| FIX | Functional MRI of the Brain (FMRIB) centre's ICA-based Xnoiseifier |
| FLIRT | Functional MRI of the Brain (FMRIB) centre's Non-linear Registration Tool |
| fMRI | Functional Magnetic Resonance Imaging |
| FSL | Functional MRI of the Brain (FMRIB) centre Software Library |

| | |
|---|---|
| FWHM | Full Half Width Maximum |
| GCA | Granger Causality Analysis |
| GLM | General Linear Model |
| GP | Globus Pallidus |
| GPi | Globus Pallidus internal |
| GPe | Globus Pallidus external |
| H&Y | Hoehn and Yahr Scale |
| Hb | Heamoglobin |
| Hb02 | Oxyhaemoglobin |
| HRF | Haemodynamic Response Function |
| HC | Healthy Controls |
| ICA | Independent Component Analysis |
| ICD | Impulse Control Disorder |
| LED | Levodopa Equivalent Dose |
| LID | Levodopa Induced Dyskinesia |
| M1 | Primary motor cortex |
| MD | Mean Diffusivity |
| MELODIC | Multivariate Exploratory Linear Optimised Decomposition into Independent Components |
| MMSE | Mini-Mental State Examination |
| MNI | Montreal Neurological Institute |
| MPRAGE | Magnetisation Prepared Rapid Gradient Echo |
| MRI | Magnetic Resonance Imaging |
| NMR | Nuclear Magnetic Resonance |
| PD | Parkinson's Disease |

| | |
|---|---|
| PE | Parameter Estimate |
| ‘ON’ | Parkinson’s Disease patients ON medication |
| ‘OFF’ | Parkinson’s Disease patients OFF medication |
| PET | Positron Emission Tomography |
| ReHo | Regional Homogeneity Analysis |
| RD | Radial Diffusivity |
| RF | Radio Frequency |
| ROI | Region of Interest |
| RS-fMRI | Resting State functional Magnetic Resonance Imaging |
| SD | Standard Deviation |
| SMA | Supplementary Motor Area |
| SN | Substantia Nigra |
| SNc | Substantia Nigra pars compacta |
| SNr | Substantia Nigra pars reticulata |
| SPECT | Single Photon Emission Computer Tomography |
| STN | Subthalamic Nucelus |
| TE | Time of Echo |
| TBSS | Track-Based Spatial Statistics |
| TR | Time of Relaxation |
| UPDRS | Unified Parkinson’s Disease Rating Scale |
| UPDRS-III | Unified Parkinson’s Disease Rating Scale Part-III |
| VBA | Voxel-Based Analysis |

# CHAPTER 1: INTRODUCTION

## 1. Epidemiology of Parkinson's disease

Parkinson's disease (PD) affects approximately 120,000 people in the United Kingdom (UK), 1 million people in the United States of America (USA) and 4 million people worldwide (according to PD UK and PD Foundation of USA). The disease target all ethnic groups, although appears to be more prevalent in Caucasians (Van Den Eeden et al. 2003) and men are approximately 1.5 times more likely than women to develop PD. Disease onset is uncommon before 60 years of age although up to 10% of cases occur before the age of 40. Overall prevalence rates of PD in the population aged 65 and over is 1.8%, rising from 0.6% in 65-69 year olds to 2.6% in 85-89 year olds (de Rijk et al. 2000).

## 2. Symptomatology of Parkinson's disease

PD is characterised by three cardinal motor symptoms; tremor, rigidity and bradykinesia; two of which must be present for a diagnosis of PD to be made. Tremor in PD typically presents at rest with a frequency of 4-6 Hz and a characteristic 'pill-rolling' motion in the hands. Tremor initially develops unilaterally although is completely absent from symptomatology in approximately 30% of patients. Rigidity is an increase in muscle tone and stiffness which leads to resistance of passive movements of a joint, whether smooth (lead pipe) or oscillating (cogwheel). Bradykinesia is a slowness or absence of movement. This symptom can also affect handwriting (micrographia), speech (hypophonia), facial expression (hypomimia). In advanced disease, bradykinesia is usually referred to as akinesia and postural instability appears (Jankovic 2008).

PD patients often suffer from non-motor symptoms, with cognitive, autonomic and affective deficits and may be attributed to extra-striatal denervation and possibly to non-dopaminergic pathways (Politis et al. 2011).

The Unified Parkinson's Disease Rating Scale (UPDRS) is the most common scale for the clinical study of PD, which includes both motor (e.g. UPDRS-III) and non-motor subscales (e.g. UPDRS-IV).

## 3. Pathogenesis

### 3.1 Dopamine and the Substantia Nigra

PD is primarily due to a reduction of dopamine (DA) concentration in the striatum caused by the loss of DA-ergic neurons in the substantia nigra pars compacta (SNc). It is known that the ventrolateral portion of the SNc is predominately affected in PD compared to normal aging where the dorsal portion is mostly affected by DA atrophy (Fearnley & Lees 1991). Motor symptomatologies arise only following the denervation of 60% of DA SNc neurons (Gaenslen et al. 2011) and it is estimated at this point, DA levels in the PD brain are around 20% of that in a non-PD, healthy brain (Tolosa et al. 2009).

### 3.2 Lewy Bodies

Lewy bodies (LB) are neuronal intracytoplasmic inclusions of alpha-synuclein, ubiquitin and approximately 70 other proteins (Wakabayashi et al. 2007). The presence of LB are not exclusive for PD pathological criteria as it is well established that other neurodegenerative conditions also present with LB (Popescu & Lippa 2004). Furthermore, the role of LB as toxic to neurons in neurodegenerative disease is

debated due to the lack of LB presence in genetic forms of PD (Poulopoulos et al. 2012).

### 3.3 Non-Dopaminergic Pathology

Emerging evidence suggest that neurotransmitter systems, other than the DA-ergic system, play a role in PD. The pre-synaptic serotonergic (5-HT) system has been shown to be degenerate in PD in a progressive, non-linear fashion (Politis et al. 2010) and loss of 5-HT in brain regions related to motor execution result in an increase of action-postural tremor in PD patients (Loane et al. 2013). Non-DA-ergic systems have been highly implicated in investigations of the non-motor symptoms of PD. For example, 5-HT and adrenergic dysfunction in depression in PD (Politis et al. 2010; Frisina et al. 2009) cholinergic dysfunction and glutamatergic dysfunction in cognitive impairment in PD (O'Neill & Dix 2007; Mattila et al. 2001).

### 3.4 The Braak Hypothesis

The Braak hypothesis (Braak et al. 2003) (Figure 1) of PD consists of six stages beginning in the lower medulla and olfactory bulb extending to the SNc at which stage the clinical symptoms of PD becomes apparent. Later, pathology reaches the allo- and neocortex involving the primary sensory and motor areas. The Braak hypothesis offered a revolutionary view of PD pathology and the description of a multi-stage pre-symptomatic period resulted in a dramatic increase of investigations focused on early detection and preventative methods.

Figure 1. Braak stages in the development of Parkinson's disease.




*Staging of α-synuclein pathology thought to be associated with the evolution of PD, hypothesis suggested by Braak et al., 2003. Pathologic changes initially occur in the olfactory region and lower brain stem (stages 1 and 2), extending to the dopamine neurons in SNc, other midbrain regions and limbic regions (stages 3 and 4) and finally the association and primary neocortex (stages 5 and 6). Clinical motor parkinsonism appears during stages 4 and 5. Figure edited from* (Olanow et al. 2009).

## 4. Pathophysiology

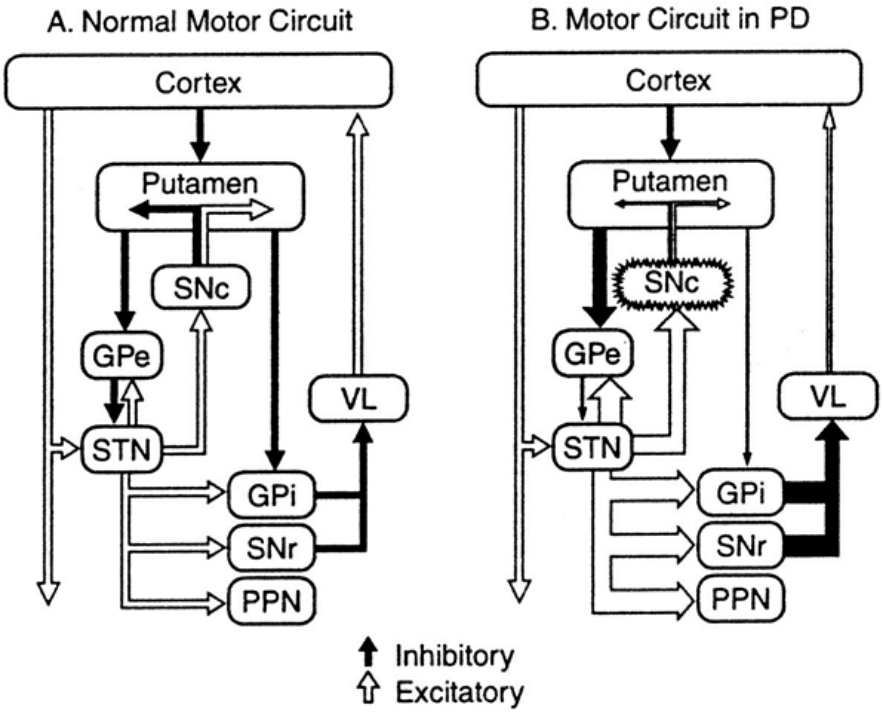
### 4.1 The basal ganglia

The basal ganglia consists of striatum (caudate nucleus and putamen), globus pallidus (GP, internal GPi, external GPe), subthalamic nucleus (STN), and SN, SNc and SN reticulata (SNr). These structures form an interconnected system that maintains multiple afferent and efferent connections with the cortex (Figure 2).

There are two main 'stations' of the basal ganglia; the input station which consists of the putamen receiving signals from the cortex and the output station which comprises the SNr and GPi inhibiting signal from the thalamus to the cortex (Obeso et al. 2013). There are two major pathways from the output station. The direct pathway has an inhibitory effect from the striatum to SNr/GPi, whereas the indirect pathway has a net excitatory effect on SNr/GPi through striatum to GPe and STN.

Initial concepts of the basal ganglia model focused on control of speed and amplitude of movement (Georgopoulos et al. 1983). Although more recent interpretations have expanded the model to involve the switching between automatic and controlled behaviour (Hikosaka & Isoda 2010) and mediating habitual actions and learning (Redgrave et al. 2010).

Figure 2. The basal ganglia motor circuit.




*Diagrammatic representation of the basal ganglia motor circuit in the healthy brain and the PD brain. A: Basal ganglia motor circuit model in health; B: Basal ganglia motor circuit model in PD. GPe – globus pallidus externa; GPi – globus pallidus interna; PPN – pedunculopontine nucleus; SNc; SNr; STN; VL- ventralis lateralis. Reproduced from* (Obeso et al. 2002).

## 4.2 The basal ganglia and PD

Typically, the direct and indirect circuits described above are balanced so that the activity of the basal ganglia output nuclei is well regulated. Facilitation of movement is associated with a reduction in the firing rate of basal ganglia nuclei output. However, loss of DA causes increased output activity of basal ganglia nuclei (i.e. hyperactivity), which in turn leads to the excessive inhibition of the thalamocortical and brain stem motor systems (Obeso et al. 2002; Rothwell, 2011). Thus, alterations of striatal neuronal excitability shift the balance of the basal ganglia circuitry toward the indirect pathway reducing the direct activity. Therefore, motor symptoms are expressed as abnormal modulations of the cortico-striatal-pallidal loops, reducing cortical activation related to the initiation of movements.

## 5. Functional and structural neuroimaging of Parkinson's disease

### 5.1 Introduction

The loss of nigro-striatal DA-ergic neurons as the pathophysiological hallmark of PD is well established. However, it is not clear how denervation of DA leads to the clinical motor symptomatology in PD. The advent of MRI has revolutionised the diagnosis and management of many neurological disorders and allowed researchers to address in vivo specific functional questions in PD by using Functional magnetic resonance imaging (fMRI).

### 5.2 fMRI studies of motor control in PD

fMRI provides a non-invasive tool for in vivo brain imaging and has been extensively applied to PD research for a wide range of important issues, not least to the assessment of brain activity related to motor execution (See Chapter 2 for a detailed description of fMRI principles).

Less than 20 studies using fMRI to comprehensively assess motor control in PD have been published to date (Table 1). Comprehensiveness refers to a sample size greater than six patients, an experimental contrast of interest i.e. patients vs. controls, an active motor task containing a baseline session and studies without DBS or atypical medication such as apomorphine due to its known effect on the sensorimotor system. These criteria were used based upon the criteria of an earlier meta-analysis (Herz et al., 2014).

In general, a subset of frontal-parietal cortical regions is associated with dysfunctional neural activity in PD patients compared to controls: supplementary motor area (SMA), primary motor cortex (M1), inferior parietal cortex (IPC) and superior parietal lobule (SPL) and putamen.

Blood oxygen level dependent (BOLD) signal is the measurement of brain activation in fMRI studies and while some studies support findings from positron emission tomography (PET) studies i.e. reduction activation in M1 and SMA (Playford et al., 1992; Jenkins et al. 1992; Buhmann et al. 2003; Haslinger et al. 2001), others are only partially consistent, such as reports of increased BOLD signal in the motor cortices (Sabatini et al. 2000). Indeed, many factors will contribute to these differences such as fMRI task specifics (gross motor, finger tapping, visual or auditory cue), narrow or heterogeneous disease population (disease duration, severity, dominant subtype), whether patients are scanned 'ON' or 'OFF' medication just to name a few.

Due to the pathophysiological hallmark of PD (nigrostriatal denervation), it is unsurprising that the posterior putamen has abnormal neural activity in PD patients 'OFF' medication. The posterior putamen receives the majority of nigral DA afferents, which are believed to facilitate effective movements, and modulate basal ganglia and cortical areas via direct pathways (Gaenslen et al. 2011). UPDRS-III scores have been correlated with abnormal putaminal neural activity in fMRI studies (Holden et al. 2006; Prodoehl et al. 2010)(Spraker et al. 2010) confirming the role of the putamen in motor control. Of particular interest, abnormal putaminal neural activity correlating with UPDRS-III can be significantly detected in mild stages of the disease i.e. mean UPDRS-III scores of 15 (Holden et al. 2006). It is of great importance to be able to detect abnormal activity in the neural motor circuit in pre-symptomatic PD brains. However, to date, no study has systematically assessed the staging of neural dysfunction in PD motor control.

Only two studies have explicitly attempted to investigate the effect of disease severity or progression on neural motor indices with fMRI (Sen et al. 2010; Tessa et al. 2012). The only longitudinal assessment was conducted using two types of motor tasks

(externally cued hand positions and sequential finger tapping) in five PD patents with highly homogenised disease severity (UPDRS-III range 2-7 at baseline and 3-10.5 at follow-up) over 2 years (Sen et al. 2010). The authors report an alteration of the cerebello-thalamo-cortical (CTC) circuit in PD patients over time but concede that the high variability in their results between PD patients and controls was extensive due to the small sample size. Tessa and colleagues (Tessa et al. 2012) report SMA hypoactivation in 19 de novo PD patients occurring as an effect of disease severity as measured by Hoehn and Yahr (H&Y) staging. Unfortunately, this study is limited buy a relatively small sample size (n = 19) and exclusion of patients with severe disease. To date, no study has used fMRI to comprehensively assess the neural basis of motor execution dysfunction as a function of disease course. In order to systematically follow the neural decline of effective motor execution, sizable cross sectional/longitudinal studies covering multiple disease stages are required.

Table 1. fMRI studies of motor control in PD

| Reference | Sample size | Motor task | Contrast | Findings |
|---|---|---|---|---|
| (Sabatini et al. 2000) | 6 PD; 6 C | Finger-to-thumb and fist clenching with external cue | OFF vs C | Decreased BOLD in SMA and DLPFC. Increased BOLD in sensorimotor cortex, premotor area and cingulate cortex |
| (Haslinger et al. 2001) | 8 PD; 8 C | Joystick-movement with free choice | OFF vs C | Impaired activation in SMA and increased BOLD in M1 and lateral PFC |
| Buhmann et al., 2003 | 8 PD; 10 C | Finger opposition task | OFF vs C | Reduced BOLD in M1 and SMA |
| Wu et al., 2005 | 12 PD; 12 C | Sequential finger tapping | OFF vs C | Increased BOLD in cerebellum, premotor area, precuneus, PFC |
| (Cerasa et al. 2006) | 10 PD; 11 C | Finger tapping with external cue | OFF vs C | BOLD increase in cerebellum, putamen, SMA, thalamus, IFG and insula |
| (Eckert et al. 2006) | 9 PD; 9 C | Opening and closing fist with external cue | OFF vs C | BOLD increase in pre-SMA |
| Holden et al., 2006 | 6 PD; 7 C | Motor switching task | OFF vs C | Reduced BOLD in striatum |
| Mallol et al., 2007 | 13 PD; 11 C | Finger-to-thumb opposition and rotation with external cue | OFF vs C | Decreased BOLD in striatum and thalamus |
| (Kraft et al. 2009) | 12 PD; 12 C | Grip-force task with external cue | OFF vs C | Increased BOLD in putamen |
| Spraker et al., 2010 | 14 PD; 14 C | Precision grip force tasks | OFF vs C | Decreased BOLD in striatum, thalamus, premotor area, SMA |
| Wu et al., 2010 | 15 PD; 15 C | In-phase movements of index fingers with external cue | OFF vs C | Increased BOLD in SMA during inphase movements but decreased BOLD |

| | | | | |
|---|---|---|---|---|
| | | | | in motor cortices during antiphase movements |
| Prodoehl et al., 2010 | 20 PD; 20 C | Precision grip force task with external cue | OFF vs C | Decreased BOLD in striatum, thalamus and motor cortices |
| Tessa et al., 2010 | 15 PD; 11 C | Continuous hand tapping with external cue | OFF vs C | Increased BOLD in cerebellum, premotor area, precuneus, PFC |
| (Pinto et al. 2011) | 9 PD; 15 C | Joystick-movements with free choice | OFF vs C | Increased BOLD in cerebellum, precentral gyrus, putamen and insula |
| (Tessa et al. 2012) | 19 PD; 13 C | Continuous writing of 'eight-figure' with external cue | OFF vs C | Decreased BOLD in somatosensory cortex and cerebellum. Increased BOLD in SMA and frontal areas |
| (Tessa et al. 2013) | 11 PD; 10 C | Continuous hand tapping with external cue | OFF vs C | Decreased BOLD in sensorimotor area and in creased BOLD in parietal and frontal areas |
| Baglio et al., 2011 | 15 PD; 11 C | Index finger button presses with external cue | ON vs C | Increased BOLD in PFC and basal ganglia during motor inhibition |
| Hughes et al., 2010 | 16 PD; 15 C | Button presses with both external cue and free choice | ON vs C | Increased BOLD in premotor areas which decreased with age |

*PD=Parkinson's disease; C = Controls; ON = ON medication; OFF = OFF medication. BOLD = blood oxygenation level dependent signal; IFG = inferior frontal gyrus; SMA = supplementary motor area; M1 = primary motor area; PFC = prefrontal cortex. Publications until the end of 2014.*

## 6. Resting state fMRI (rs-fMRI) studies in Parkinson's disease

Studying the brain at rest in an attempt to understand its spontaneous neural activity without constraints inextricably linked to task-based studies (i.e. subjects ability to perform the task, presence of attention-based stimuli) (Biswal et al. 1995; Raichle et al. 2001) is a valuable non-invasive tool for in vivo brain imaging. Task-related increases in neuronal metabolism are usually small (<5%) when compared to this large resting energy consumption. Therefore, differences in task-related changes between normal and pathological populations are even smaller. Thus, attempting to study disease or diagnose patients based on task-related changes, one is therefore focusing on only a very small fraction of the brain's overall activity. Measuring ongoing spontaneous activity may provide a window into the neural processing that appears to consume the vast majority of the brain's resources and so may prove a richer source of disease-related signal changes (Fox & Greicius 2010).

PD is one neurodegenerative disease, which has benefited from the rs-fMRI research (Table 2). The rationale of rs-fMRI focuses on low frequency (<0.1 Hz), spontaneous fluctuations in BOLD signal at rest with identification of abnormal patterns or disrupted connectivity potentially explaining PD symptoms. As detailed in Methodology (Chapter 2), analysis approaches to rs-fMRI in PD is varied, thus discrepancies in the current literature exist. However, the value of rs-fMRI in PD is reflected in the many studies that have been conducted over the past decade.

A selection of relatively established resting networks in the healthy brain have been identified: default mode network (DMN), sensorimotor network, visual, auditory and fronto-parietal networks (Damoiseaux et al. 2006). These networks have been identified using independent component analysis (ICA), a technique that separates a signal into non-overlapping spatial and time components. It is highly data-driven

permitting better removal of noisy components of the signal and has been shown to reliably extract DMN as well as many other networks with very high consistency. Rs-fMRI in neurological disease has shown promise with several studies identifying patients with Alzheimer's disease (AD). For example, graph analysis of rs-fMRI data has demonstrated sensitivity of 72% and specificity of 78% in distinguishing AD patients from controls (Supekar et al. 2008). Furthermore, distinguishing different dementia types has been demonstrated with 92% accuracy when investigating the DMN and salience network in AD patients versus frontotemporal dementia patients (Zhou et al. 2010). The clinical relevance of these findings are still to be elucidated, although large projects such as the Human Connectome Project are ongoing and attempt to understand the association between functional and structural connectivity with genetic and behavioural information in several conditions (Essen et al. 2012). Assessment of DMN in PD has revealed somewhat inconsistent findings. PD patients 'ON' medication were reported to have no difference in DMN compared to healthy controls (Krajcovicova et al. 2012), whereas a similar group imaged by Tessitore et al., demonstrated decreased connectivity in the anterior parts of DMN (Tessitore et al. 2012). The authors also suggest their findings may demonstrate resting neural dysfunction prior to cognitive decline in PD. However, no follow-up study has been conducted in this group of patients. DMN dysfunction has also been reported in a group of medicated PD patients, although areas of dysfunction differ to previous studies (Gorges et al. 2013). Further studies of PD patients 'ON' medication using ICA show increased connectivity in the sensorimotor network compared to controls (Esposito et al. 2013) and with graph theory, demonstrate decreased connectivity in caudate, orbitofrontal and occipital regions and increased connectivity in sensorimotor and parietal areas (Göttlich et al. 2013). The inconsistency of results to

date suggest a change of scanning protocol is required and future studies should consider imaging PD patients 'OFF' medication in an attempt to unify findings due to the known effect of levodopa on task-related changes in DMN (Delaveau et al. 2010). An investigation of the sensorimotor network in PD with and without medication has revealed patients imaged 'ON' medication present increased connectivity in the left dorso-lateral pre-frontal cortex (DLPFC) and decreased connectivity in the right parietal cortex, M1 and left cerebellum (Wu, Wang, et al. 2009). Furthermore, the authors report a significant negative correlation between 'OFF' UPDRS-III motor scores and SMA, putamen, thalamus, premotor area and parietal cortex in the PD patients imaged 'OFF' medication with authors suggesting that resting putamen neural activity may play a part in the motor symptoms of PD.

The majority of rs-fMRI studies in PD to date have used a seed-based approach and are also blighted by discrepant findings. Yu et al., placed seeds in SMA, putamen and caudate and reported increased connectivity between SMA and putamen but not SMA and caudate in mild-moderate PD patients (Yu et al. 2013), which is partially supported and expanded by Helmich et al., who divided the putamen into anterior and posterior portions (Helmich et al. 2010). The authors report an increased connectivity between anterior putaminal-cortical connections and reduced connectivity between posterior putamen and somatosensory and motor cortices, which is supportive of the DA loss theory (Kish et al. 1988). Further findings in a study of mild to moderate PD patients, imaged while 'ON' medication and reports increased striato-cortico connectivity which is more prominent in the dorsal striatum (Kwak et al. 2010). Baudrexel et al., reported increased connectivity between striatum and motor cortex opposed to a decreased connectivity with thalamus, midbrain, pons and cerebellum (Baudrexel et al. 2011). A similar study specifically investigating regional resting

state connectivity in motor control and execution regions (pre-SMA, M1) report increased connectivity between pre-SMA and M1 with a reduction observed between pre-SMA and insula, putamen, premotor area and inferior parietal lobule (IPL) (Wu, Long, et al. 2011). A study of early stage PD de novo patients revealed reduced connectivity between mesolimbic-striatal and cortico-striatal loops (Luo et al. 2014). Sharman et al., who used a hierarchical clustering, seed-based approach imaged PD patients 'OFF' medication (although do state they could not be certain the 12h withdrawal period had been adequately implemented by all subjects) report reduced connectivity between sensorimotor cortex and thalamus, between GP and thalamus, between putamen and GP and between SN, GP, putamen, thalamus (Sharman et al. 2013). Hacker et al., used putaminal subdivision and caudate seeds in advanced PD patients 'ON' medication reporting increased striato-cortico connectivity opposed to a 'weaker' connectivity between striatum and thalamus, pons and cerebellum (Hacker et al. 2012). Attempts to investigate PD subtype with rs-fMRI are limited although small steps have been made. Using independent component analysis (ICA) to investigate fronto-parietal and visual networks in PD patients with and without freezing of gait symptoms reveal reduced network connectivity in the presence of the symptom (Tessitore et al. 2012), while tremor dominant PD patients have been shown to have reduced connectivity between dentate nucleus and the posterior cerebellar lobe (Luo et al. 2014). Amplitude of low frequency analysis (ALFF) involves spectral decomposition of the time series data with a focus on the low frequency domain relevant to the hemodynamic response function (i.e. >0.08Hz). PD patients with apathy and depressive symptoms have demonstrated that SMA ALFF index and subgenual cingulate ALFF index is associated with clinical scores respectively, whereas UPDRS-III is predicted by right putamen ALFF index (Skidmore et al.,

2013). A study investigating medication effect on PD ALFF indices, demonstrated that while OFF medications, PD patient have increased indices in the motor and frontal regions that is normalized following medication administration (Kwak et al. 2012). However, a further study using ALFF in PD patients imaged 'OFF' medication reports a decreased index in SMA, mesial frontal regions, MTG and left cerebellum (Skidmore, Yang, Baxter, K. M. von Deneen, et al. 2013). Regional homogeneity analysis (ReHo) is is a voxel-based measure of brain activity that evaluates the similarity or synchronization between the time series of a given voxel and its nearest neighbours. This measure is based on the hypothesis that clusters of voxels rather than single voxels manifest intrinsic brain activity. The only study to date using ReHo in PD rs-fMRI investigated medication effects and found a reduction of ReHo in putamen, thalamus and SMA when 'OFF' medication which was normalised following administration of medication (Wu, Long, et al. 2009).

Using Granger connectivity analysis (GCA) is an effective connectivity analysis method for inferring directions of neural interactions and information flow directly from neuroimaging data, which can estimate the directionality of modulation from recorded time series across all nodes of a network without *a priori* assumptions. Using GCA, Wu et al., reported that SNc predicted decreased connectivity with SMA, DMN and DLPFC in mild to moderate PD patients whereby SNc predicted an increase in the same regions in healthy controls (Wu et al. 2012). Finally, the only study to date which has implemented rs-fMRI following surgical intervention, reports deep brain stimulation (DBS) results in an increased effective connection of striatal-cortico and thalamo-cortico pathways whereas all STN and striatal afferents/efferents and STN-thalamic connections were decreased in effective connectivity (Kahan et al. 2014).

It is clear from the current literature that rs-fMRI in PD needs to be ‘cleaned-up’. That is, a more cohesive analysis pipeline, more regard to medication effects and large homogenous patient groups are required to clearly identify the value of rs-fMRI in PD and determining its use in differentiating PD from other neurodegenerative disease, use as a bio-marker or use as end-points for clinical trials. It appears that prolonged use of DA-ergic medication and increased disease severity have an effect on the observed rs-fMRI networks, whether it be a natural progression of network dysfunction or reorganisation is yet to be elucidated.

Table 2. RSN. Main rsfMRI publications in Parkinson's disease

| **Reference** | **Sample Size** | **Analysis method** | **Group characteristics** | **Findings** |
|---|---|---|---|---|
| (Esposito et al. 2008) | 20 de novo PD; 18 C | ICA | 'ON' medication PD | ↑ connectivity in sensorimotor area |
| (Wu, Wang, et al. 2009) | 22 PD; 22 C | Graph theory | PD patients 'ON'/'OFF' medication and controls | 'OFF' PD patients ↓ connectivity in SMA< DLPFC, putamen and ↑ connectivity in cerebellum, M1, parietal cortex. 'ON' PD patients ↑ connectivity in left DLPFC and ↓ connectivity in parietal cortex, right M1, left cerebellum |
| (Wu, Long, et al. 2009) | 22 PD | ReHo | PD 'ON' and 'OFF' medication | ↓ ReHo in putamen, thalamus and SMA in 'OFF' PD and normalized following medication administration |
| (Kwak et al. 2010) | 24 PD; 24 C | ALFF | PD 'ON' and 'OFF' medication | 'OFF medication, ↑ALFF in primary and secondary motor areas and frontal regions. Medication administration reduced but not normalized these results. |

| | | | | |
|---|---|---|---|---|
| (Helmich et al. 2010) | 41 PD; 36 C | Seed-based (subdivion of putamen) | 'OFF' mild-moderate PD patients *vs.* controls | ↑ connectivity anterior putamen and cortex. ↓ connectivity between posterior putamen and somatosenosry and motor cortices |
| (Kwak et al. 2010) | 25 PD; 24 C | Seed-based (six striatal seeds) | 'ON' mild-moderate PD patients *vs.* controls | ↑ connectivity between striatum and cortex, more prominent in dorsal putamen. |
| (Baudrexel et al. 2011) | 31 PD; 44 C | Seed-based (STN and motor cortex) | 'OFF' PD *vs.* controls | ↑ connectivity between STN and motor cortex |
| (Wu, Long, et al. 2011) | 18 PD; 18 C | Seed-based (pre-SMA, M1) | 'OFF' PD *vs.* controls | ↑ connectivity between pre-SMA and M1. ↓ connectivity between pre-SMA and insula, putamen, premotor area and IPL |
| (Krajcovicova et al. 2012) | 18 PD; 18 C | ICA, DMN | 'ON' medication PD *vs.* controls | No differences |
| (Tessitore et al. 2012) | 16 PD; 16 C | ICA, DMN | 'ON' medication PD *vs.* controls | PD ↓ connectivity in right MTL and bilateral IPC |
| (Hacker et al. 2012) | 13 PD; 19 C | Seed-based (anterior/posterior putamen, caudate) | 'ON' Advanced PD *vs.* controls | ↓ connectivity between striatum and thalamus, midbrain , pons, |

| | | | | |
|---|---|---|---|---|
| | | | | cerebellum and ↑ connectivity with motor cortex |
| (Wu et al. 2012) | 22 PD; 22 C | GCA | 'OFF' mild-moderate PD *vs.* controls | Decreased activity of SNc on SMA, DMN and DLPFC in PD patients. |
| (Gorges et al. 2013) | 12 PD; 13 C | Seed-based, region-region, DMN | 'ON' medication PD *vs.* controls | ↓between medial prefrontal cortex and posterior cingulate. ↑ connectivity between bilateral hippocampus |
| (Göttlich et al. 2013) | 37 PD; 20 C | Graph theory | 'ON' medication PD *vs.* controls | ↓ connectivity in caudate, orbitofrontal, occipital regions and ↑ connectivity in sensorimotor and parietal areas |
| (Liu et al. 2013) | 18 PD; 18 C | Seed-based (cerebello-thalamo-cortical loop: dentate nucleus) | 'OFF' PD tremor/akinetic rigid sub groups and controls | ↑ connectivity between dentate and cerebellar posterior lobe in PD *vs.* controls. ↓ connectivity in same regions for the tremor subgroup |
| (Sharman et al. 2013) | 45 PD; 36 C | Seed-based, hierarchical clustering | 'OFF' PD *(unclear if patients actually 'OFF' medication)* | ↓ connectivity between: sensorimotor cortex-thalamus, globus pallidus-putamen- |

| | | | | |
|---|---|---|---|---|
| | | | | thalamus, substantia nigra-globus pallidus-putamen-thalamus |
| (Skidmore, Yang, Baxter, K. M. von Deneen, et al. 2013) | 22 PD | ALFF | PD with apathy/depression | UPDRS-III predicted by ALFF in right putamen and Apahy score predicted by ALFF in left SMA. Depression score predicted by ALFF in subgeneal cinglulate |
| (Skidmore, Yang, Baxter, K. von Deneen, et al. 2013) | 14 PD; 15 C | ALFF | PD 'OFF' medication | ↓ ALFF in SMA, mesial frontal regions, MFG, left cerebellum |
| (Luo et al. 2014) | 52 PD; 52 C | Seed-based (anterior/posterior putamen, caudate) | Early stage de novo PD *vs.* controls | ↓ connectivity in mesolimbic-striatal and cortico-striatal loops |
| (Kahan et al. 2014) | 12 PD | GCA | PD with and without DBS | DBS ↑effective connection of cortico-strital and thalamo-cortico pathways. ↓of all STN/striatal afferents and efferent and STN-thalamic connections |

*ICA = independent component analysis; ReHo = regional homogeneity; ALFF = amplitude low-frequency fluctuations; GCA = granger causality analysis; DMN = default mode network; PD=Parkinson's disease; IPC = inferior parietal cortex; IPL = inferior parietal lobule; SMA= supplementary motor area; M1= primary motor area; DLPFC = dorsolateral prefrontal cortex; STN*

*= subthalamic nucleus; MTG = middle temporal gyrus; MOG = middle occipital gyrus; DBS = deep brain stimulation. Publications until the end of 2014.*

## 7. Diffusion tensor imaging in Parkinson's disease

Diffusion tensor imaging quantifies the diffusional displacement of water molecules in brain tissue. In white matter, the quantification of diffusion is more complicated due to its anisotropic nature and requires a tensor. The advent of DTI provides a new image contrast, which enhances the white matter signal and yields quantitative measures that characterize the integrity of the white matter tracts. The most commonly used indices in PD research are fractional anisotropy (FA) and mean diffusivity (MD). FA measures the portion of the diffusion tensor due to anisotropy. For highly oriented structures such as white matter, FA approached one, while for isotropic diffusion (e.g. CSF) FA is zero. MD represents the overall diffusivity of molecules and indicates the overall presence of obstacles to diffusion.

These quantitative measures represent microstructure of both white and grey matter, thus their use in assessing microstructural damage in neurodegenerative disorders are potentially extremely useful. DTI analysis typically has three main approaches: ROI analysis, voxel-based analysis and tract based spatially statistics (TBSS). All three methods have been applied to data in the literature resulting in quite inconsistent findings (Table 3).

Previous studies using DTI in PD have conducted ROI-based analyses with a priori hypotheses, most commonly, the SN. In general, these studies have reported consistent findings of FA reduction in the SN. One of the earliest studies reports included subjects with PD, progressive supranuclear palsy (PSP) and healthy controls (Yoshikawa et al. 2004). By using 15 ROIs placed along areas involving nigrostrital

and extrapyramidal tracts the authors found a significant reduction of FA in the ROIs placed in nigro-striatal tract areas in the PD patients compared to controls. These findings were specific to PD patients as the PSP patients demonstrated a reduction of FA across all ROIs. The authors concluded their findings were indicative of the DA-ergic loss observed in PD reflected in white matter microstructural damage. Péran et al., reported a reduction of nigral FA and thalamic FA as well as an increase of thalamic MD (Péran et al. 2010). Rolheiser et al., (2011) also reported reduced nigral FA as well as an increase of radial diffusivity (RD) in the SN of PD patients with sensitivity to distinguish patients from controls (Rolheiser et al. 2011). A striking confirmation of reduced nigral FA and its possible use as a biomarker was reported in a group of early de novo PD patients (Vaillancourt et al. 2009). The authors were able to distinguish PD patients from healthy controls with 100% specificity and sensitivity from the findings in the caudal part of SN, although, no other study to date has been able to replicate this degree of specificity.

SN FA reduction in PD patients has also been demonstrated in a case-control study with FA inversely correlating with disease severity (Chan et al. 2007). No significant differences in FA were found in any other basal ganglia structures and an alternative measure of diffusion (apparent diffusion coefficient [ADC]) in the SN were found to be similar between PD patients and healthy controls. In addition, microstructure alterations have been reported in established motor circuit regions: SN, putamen, thalamus, M1, premotor and SMA and somatosensory areas with nigral FA correlating with disease severity (Zhan et al. 2012). The correlation of SN FA and disease severity, thus its potential use as a biomarker, is debated due to differing reports. Whereas Chan et al., (2007) and Zhan et al., (2012) find a correlation, other studies do not (Vaillancourt et al. 2009; Menke et al. 2010; Du et al. 2011). This has

lead to the question whether FA in the SN can be used as a diagnostic marker and has been tackled by two recent systematic reviews (Cochrane & Ebmeier 2013; Schwarz et al. 2013) with opposing conclusions. Cochrane et al., (2013) considered 43 studies of DTI in parkinsonian syndrome, of which nine were studies of SN diffusion indices in PD. The authors were optimistic of the use of DTI as a potential biomarker for PD as all but one of their included studies reported a reduction of FA in the SN of PD patients, seven of which were significant. Conversely, Schwarz et al., (2013) who conducted a literature review, meta-analysis and case control study were less optimistic of supporting nigral FA as a diagnostic marker. The authors propose standardisation of SN anatomical delineation to ascertain if the inclusion of peri-nigral white matter and effect of iron deposition affects the measurement of nigral FA.

A variety of tensor-derived changes in extra-nigral regions have been reported in small selection of studies (Gattellaro et al. 2009; Ibarretxe-bilbao et al. 2009; Zhan et al. 2012). FA reductions in corpus callosum genu and superior longitudinal fasciculus and MD increase in the same regions plus cingulum have been demonstrated in early stage, medicated PD patients (Gattellaro et al. 2009). This was the first study to demonstrate superior longitudinal fasciculus is impaired in PD, although it should be noted that the findings were not sufficient to discriminate the PD patients from the healthy controls. FA reduction in gyrus rectus has been reported (Ibarretxe-bilbao et al. 2009) as well as FA reductions and MD increases in motor and frontal cortices (Zhan et al. 2012) and track density indices were found to be increased in regions associated with the motor circuit (Ziegler et al. 2013). However, other studies have failed to find significant differences of extra-nigral FA or ADC in the striatum and

thalamus (Chan et al. 2007), or FA and MD in corpus callosum and cingulum (Wiltshire et al. 2010).

Studies using only whole brain diffusivity techniques also have variability in reported findings. Kim et al. (2013) employed TBSS and voxel-based analysis (VBA) and report no significant differences of FA in PD patients compared with healthy controls. Increased MD was reported in striatum, pallidum, thalamus, cingulum and fornix (Kim et al. 2013). Zhan et al., (2012) used VBA to identify a reduction of FA in the cerebellum and increased MD in the orbital-frontal cortex and inferior temporal gyrus (Zhan et al. 2012).

DTI offers a promising technique to understand changes in brain microstructure in neurodegenerative disease although there are many methodological and theoretical considerations prior to collection of data and interpretation of results. Methodologically, the scanning protocol should be optimised taking into account the subject group under examination. It has been reported that in PD patients that an emphasis on the number of diffusion directions leads to a greater sensitivity of FA measures, whereas, an emphasis on increasing the number of b values leads to a greater sensitivity to MD measures (Rae et al. 2012). Unfortunately the literature is highly varied in terms of the scanner and acquisition protocols used, leading to difficulty in interpretation of results and reliable evaluation of which parameters are optimal in DTI scanning of PD patients. Furthermore, patient disease stage may indirectly influence results. To assess the role of DTI as a potential biomarker or a marker for disease progression, more studies involving early stage patients and/or patients followed longitudinally (see chapter 5) need to be conducted. Regarding analysis, the majority of studies have conducted a priori ROI analysis, which is reliant

upon accurate delineation of ROIs and does not account for effects occurring outside the ROIs and may be subject to user-bias and partial volume effects.

The general consensus is that DTI may be a valuable tool as an imaging biomarker for PD. However, further studies focusing on premanifest disease, monitoring progression and longitudinal studies are required to enable netter assessment of preliminary findings. Furthermore, congruency across imaging protocols, use of higher field magnets and multi-modal imaging should be considered in future studies (Cochrane & Ebmeier 2013)

Table 3. Main DTI publications in Parkinson's disease

| **Reference** | **Sample Size** | **Analysis method** | **Diffusion indices Measured/ROIs Regions studies** | **Findings** |
|---|---|---|---|---|
| (Yoshikawa et al. 2004) | 12 PD; 8 C | ROI | FA/ PMC, BG | ↓ FA in SN |
| (Chan et al. 2007) | 73 PD; 78 C | ROI | FA and ADC/ Caudate, putmaen, thalamus, globus pallidus, SN | NS |
| (Karagulle Kendi et al. 2008) | 12 PD; 13 C | VBA | FA, MD/ Whole brain | ↓ FA in SN |
| (Vaillancourt et al. 2009) | 14 PD; 14 C | ROI | FA, RD, LD/ SN, cerebral peduncle | ↓ FA, LD in SN ↑ RD in SN |
| (Gattellaro et al. 2009) | 10 PD; 10 C | ROI | FA, MD/ CST, SLF, CI, CC genu, splenium | ↓ FA in CC genu, SLF ↑ MD in CC genu, SLF and cingulum |
| (Menke et al. 2010) | 10 PD; 10 C | ROI | FA/SN | NS |
| (Ibarretxe-bilbao et al. 2009) | 24 PD; 24 C | ROI, TBSS | FA/ POC, gyrus rectus, UF | ↓ FA in gyrus rectus |
| (Wiltshire et al. 2010) | 29 PD; 15 C | Tract | FA, MD/ CC, cingulum | NS |
| (Péran et al. 2010) | 30 PD; 22 C | ROI | FA, MD/ Thalamus, putamen, caudate, pallidum, red nucleus, SN | ↓ FA in SN, thalamus ↑ MD in thalamus |
| (Rolheiser et al. 2011) | 1 PD; 14 C | ROI | FA, RD/ SN, AOS | ↓ FA in SN, AOS ↑ RD in SN |
| (Du et al. 2011) | 40 PD; 28 C | ROI | FA/SN | NS |
| (Zhan et al. 2012) | 12 PD; 20 C | ROI and VBA | FA, MD/ Frontal, parietal, SN, external capsule, IC, thalamus, putamen | ↓ FA in frontal, parietal, SN, external and internal capsule, thalamus and putamen |

| | | | | |
|---|---|---|---|---|
| (Prakash et al. 2012) | 11 PD; 12 C | ROI | FA, ADC/ SN | ↓ FA in SN, asymmetric |
| (Skorpil et al. 2012) | 18 PD; 16 C | ROI | FA/ SN, Olfactory bulb | ↓ FA in SN |
| (Kim et al. 2013) | 64 PD; 64 C | TBSS, VBA | FA, MD/ Whole brain | ↑ MD in caudate, putamen, pallidum, thalamus, cingulum and fornix |
| (Ziegler et al. 2013) | 29 PD; 27 C | TBSS, VBA | FA, MD, TDI/ Whole brain | ↑ TDI in motor, cognitive and limbic networks |

*Abbreviations: AOS = anterior olfactory structures; BG = basal ganglia; CC = corpus callosum; CST = corticospinal tract; ITG = inferior temporal gyrus; LD = longitudinal diffusivity; MD = mean diffusivity; NS = not significant; OFC = orbital frontal cortex; PMC = premotor cortex; POC = primary olfactory cortex; RD = radial diffusivity; ROI = region of interest; SN = substantia nigra; TBSS = tract based spatial statistics; tract = tractography; UF = uncinate fasciculus; VBA = voxel based analysis. Publications until the end of 2014.*

## 8. Summary of Aims

To date, neuroimaging studies investigating motor execution in PD commonly report a hypoactivation and loss of connectivity between specific motor related regions when completing motor tasks in-scanner (e.g. M1, SMA, premotor area) with suggestions that this could reflect compensation mechanisms in an attempt to overcome increased difficulty for patients to complete motor actions. Furthermore, the increase of rs-fMRI studies in recent years has produced general reports of disrupted resting motor networks and potential reorganization of cortico-striatal loops. The literature clearly indicates that the assessment of both signal amplitude change and connectivity alterations need to be considered for a complete understanding of brain function in PD. Further to this, structural changes measured with DTI are also vital. Currently, the literature is not clear as to how useful DTI may be in providing a MRI biomarker in PD or how disease affects diffusion in the PD brain. It is likely that measures such as FA and MD are capable of detecting changes over time, but more robust and careful studies are required before conclusions can be made. Therefore, despite a relatively large number of neuroimaging investigations, the neural (functional or structural) course of motor execution decline and/or compensation in PD is still unclear.

In this thesis I have presented the results from three studies investigating the motor brain networks in PD from both a functional and structural perspective. The broad aims from these three studies are:

- to assess the activated and resting motor network in a sizable cross-sectional study of PD patients spanning four disease burdens in the context of both potential dysfunctional and compensatory activations. A subsidiary aim was to

investigate if collection of in-scanner behavioural data could assist interpretation of neural information.

- to assess activated and resting motor networks in a group of PD patients over time to serve as a confirmatory study of Chapter 3 by using a within-subject, longitudinal design.
- to assess nigro-striatal diffusion indices in PD patients over time to elucidate whether these measures can be informative in the investigation of aberrant diffusion in key PD related motor regions.

# CHAPTER 2: SUBJECTS AND METHODOLOGY

## 1. Patients

### 1.1 Recruitment

All PD patients included in this thesis were recruited via the TransEuro FP7 EU consortium programme. Patients were initially identified from specialist movement disorder clinics from one of four centres: Hammersmith Hospital, Imperial College Healthcare NHS trust, London; Addenbrookes Hospital, Cambridge University Hospitals NHS foundation trust, Cambridge; National Hospital for Neurology and Neurosurgery, University College London Hospitals NHS Foundation Trust, London; Skåne University Hospital, Lund, Sweden; University Hospital, Lund, Sweden. Healthy control recruitment was not included in the TransEuro study.

*TransEuro FP7*

The TransEuro programme was set up to conduct a clinical trial of fetal cell transplantation in the PD brain. The results from previous trials have provided a proof of principle that cell replacement can work in humans, with some patients reporting a huge improvement of motor symptoms with reduced 'off' period, motor complications and some patients even requiring less or complete withdrawal from DA-ergic therapy post-operatively. However, they also revealed troublesome adverse effects, the so-called graft induced dyskinesia. The current trial aimed to counter previous unknowns which may have contributed to the variable results and conduct uni-lateral and bi-lateral grafts in the caudate and putamen of 20 patients. At the time of thesis submission, only one subject had successfully undergone graft surgery (May 2015).

1.2 Inclusion and exclusion criteria

All patients were required to fulfill the following criteria at time of recruitment to be eligible.

Inclusion:

- PD as defined using Queen's Square Brain Bank criteria.
- Disease duration ≥ 2 years and ≤ 13 years.
- Aged ≥ 30 years and ≤ 68 years at the time of grafting.
- Hoehn & Yahr stage 2.5 or better when 'on'.
- On standard anti PD medication without significant LIDs (levodopa induced dyskinesia) defined as a score of >2 on the abnormal involuntary movement scale (AIMS) dyskinesia rating scale, in any body part.
- Patients must be right handed.

Exclusion:

- Atypical or secondary parkinsonism including F-DOPA PET patterns consistent with this.
- No clinically significant response to Levodopa (as evaluated by the clinician) and/or apomorphine challenge.

  Mini-Mental State Examination (MMSE) score of less than 26.
- Unable to do normal copying of interlocking pentagons and semantic fluency score for naming animals of less than 20 over 90 seconds as these have recently been associated with the earlier onset of dementia in PD.
- Ongoing major medical or psychiatric disorder including depression and psychosis.

- Other concomitant treatment with neuroleptics (inc. Atypical neuroleptics) and cholinesterase inhibitors.
- Significant drug induced dyskinesia defined as a score of >2 on the AIMS (abnormal involuntary movement scale) dyskinesia rating scale, in any body part.
- Previous neurosurgery, cell therapy or organ transplantation.
- Unable to be imaged using MRI.
- Any contraindication to immunosuppression therapy.
- Patients on anticoagulants
- Patients who are left handed

1.3 Clinical evaluation

As part of the TransEuro programme, all PD patients recruited and included in this thesis were clinically evaluated every 6 to 12 months. Evaluations included: Neurological examination, total UPDRS (including ON and OFF medication UPDRS-III scores), AIMS and MMSE.

**2. Magnetic resonance imaging (MRI)**

2.1 Principles

MRI is a non-invasive and safe technique to generate internal images of the body to be used in either clinical or research settings. Images are generated using a strong magnetic field based upon principles of nuclear magnetic resonance (NMR). Changing magnetic gradients and oscillating electromagnetic fields, known as pulse sequences are used to detect different tissue properties leading to the generation of

images differentiating between low and high proton density, grey and white matter or fluid and tissue.

## 2.2 Nuclear Magnetic Resonance

Protons and neutrons within atoms spin on their axis producing an angular momentum. If an atom has an uneven number of protons and neutrons, the vector will be different from zero. Due to protons mass property, spin phenomenon and positive charge, a small magnetic field is produced and named a magnetic moment. This magnetic moment is orientated similarly to the angular momentum thus producing a ratio constant, gyromagnetic ratio ($\gamma$), which is specific to each magnetically active nucleus. Due to hydrogen possessing a significant magnetic moment and existing in a high abundance in the human body, MRI scanners can be configured to detect it. The hydrogen nucleus atom contains a single proton, which behaves as a tiny bar magnet. As such, the spin properties align parallel or anti-parallel to the direction of the magnetic field when placed inside a large magnetic field ($b_0$). When protons are aligned in a parallel state, they are said to be in a low energy state compared to an anti-parallel alignment and in a high energy state. Thus the higher the $b_0$, the more protons that are in a low energy state. It is this ratio that produces a net magnetisation vector (M) proportional to the $b_0$. Additionally, protons precess at a particular frequency that is equal to the strength of $b_0$ multiplied by the gyromagnetic ratio: the Lamour frequency ($\omega_0$).

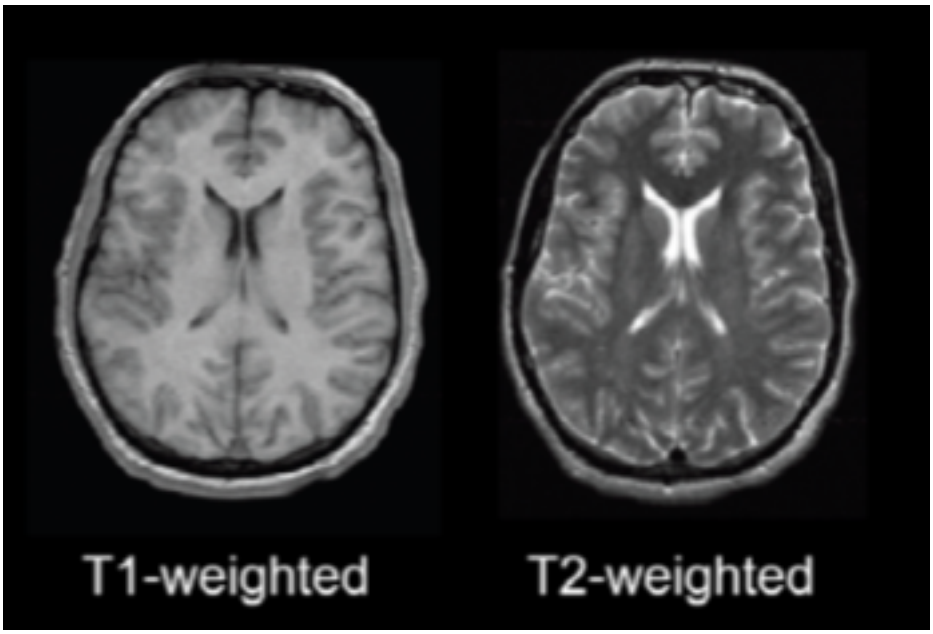
Different tissues possess differing amounts of hydrogen, thus their behaviour in a magnetic field will vary. For example, water has one of the strongest magnetic fields due to its high abundance of hydrogen compared to brain tissue. The use of MRI to differentiate tissue types involves orienting M away from the $b_0$ axis (z axis) toward a

perpendicular plane (transverse xy) and its constants associated with its reorientation to the z axis is what is measured by the scanner. To do this, a radio frequency (RF) wave oscillating at the lamour frequency is administered resulting in the spins beginning to precess in phase: a phenomenon known as resonance. On continuation of the pulse, spins in the low energy state will absorb the RF field energy and become 'excited' into the high energy state, causing these proton to 'flip' M away from the z axis. Spins that had moved to the high energy state will now return to the low energy state causing a reorientation of M to the z axis. This phenomenon is known as relaxation and is described by two constants: T1 and T2 (Figure 3). T1 longitudinal relaxation time is the decay constant for recovery of z to M. T2 is the decay constant for the xy component of M. T2* is a related constant of T2 which accounts for the inhomegnieties in $b_0$ and neighbouring spin-spin interaction. Due its rapid processing time, this constant is very useful in functional MRI.

## 2.3 Image formation

Identification of the origin of MR signal (spatial information) is acquired through the use of gradients. Gradients are spatially linear variations in the static field strength and can be applied in orthogonal directions and the speed of precessing determines detection of higher or lower MR signal. Gradient coils inside the scanner, generate a magnetic field increasing in strength across a single direction, thus multiple coils are applied. Therefore, image reconstruction can occur in three dimensions via frequency measurements in different positions in space.

Figure 3. T1-weighted and T2-weighted image examples.




*Images of a single subject. A: T1-weighted image which shows the grey matter bright and the cerebral spinal fluid (CSF) darker and hypointense lesion. B: T2-weighted image highlighting the CSF*

## 3. Functional MRI

### 3.1 The BOLD signal

Blood-oxygen-level-dependent (BOLD) signal is the MRI contrast of blood deoxyhemoglobin. Neurons do not store internal reserves of glucose and oxygen, which are essential to their proper function. Increases in neuronal activity, typically in response to a demand for information processing, require more glucose and oxygen to be rapidly delivered via the blood stream. The processes of this heamodynamic response (explained below) can be exploited and as such provide a localizer marker of activity for fMRI.

The haemodynamic response corresponds to an increase of cerebral blood flow (CBF), blood volume (BV) and blood oxygenation. During neuronal firing, oxygenation increases by approximately 5%, and CBF to the local area by 20-40%. Increases of CBF can take up to 6 s, therefore the time course of this change is a ratio of oxyhaemoglobin (HbO2) to haemoglobin (Hb), know as the haemodynamic response function (HRF). The magnetic properties of Hb alter depending on whether or not it is oxygenated. Thus changes of Hb and HbO2 are detectable via BOLD response directly. Hb presence leads to microscopic field inhomogenenities that have a destructive effect on the signal from a voxel. This effect has a tendency to shorten the T2* relaxation time. Therefore, brain areas, which have currently enhanced blood flow due to greater neuronal activity, will have a longer T2*. This can then be seen as areas of increased signal relative to baseline.

### 3.2 Echo-planar imaging

Imaging the functioning brain rather than a structural image, requires rapid acquisition in order to capture the physiological change of interest at a similar rate.

Echo planar imaging (EPI) is a T2* sequence which collects data from an entire image slice following one RF pulse and introducing a rapidly changing magnetic field gradient. The benefit of EPI is the rapid acquisition of data, however it is at a cost of spatial resolution and increased risk of image artifacts and distortion. It is for these reasons that it is imperative to collect a standard T1 image at a higher resolution for registration purposes.

## 4. Analysis of fMRI data

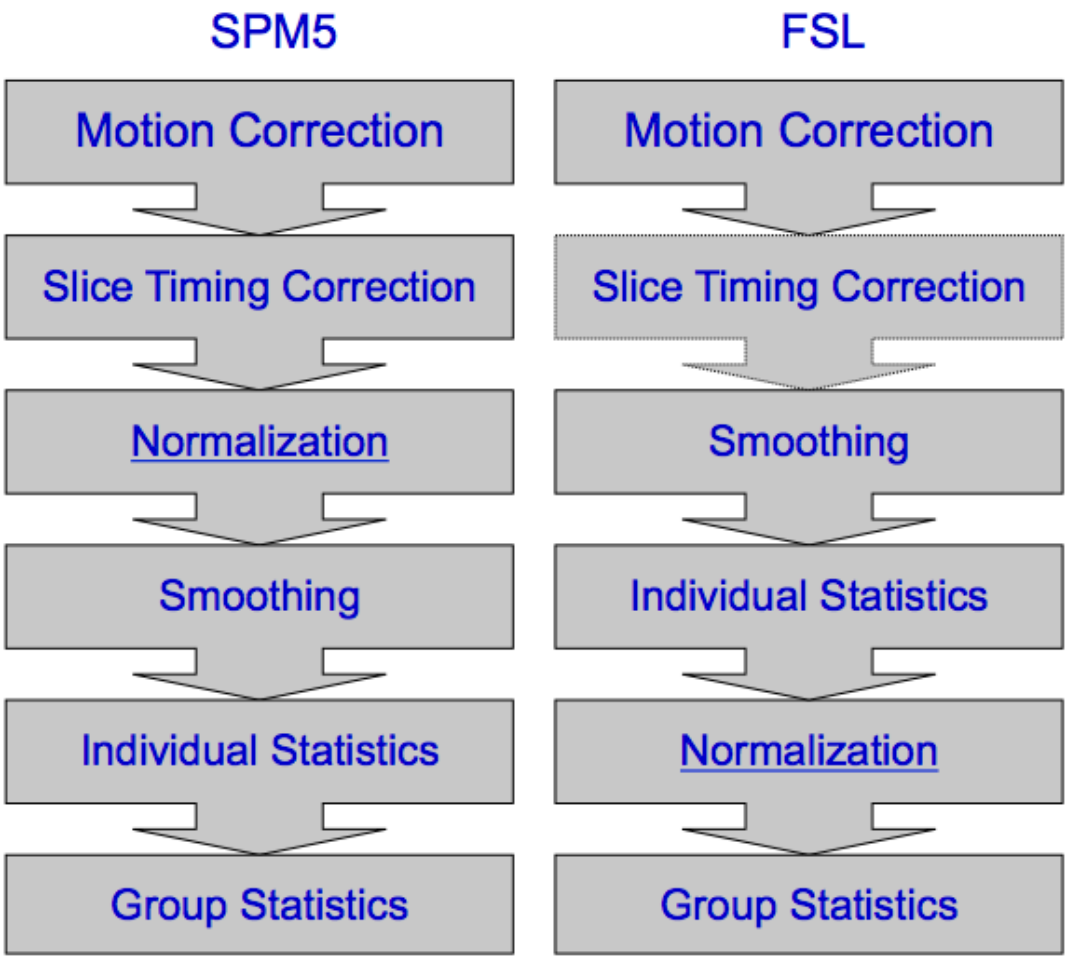
There are multiple methods of analysis for fMRI data which depend upon the type of data collected (i.e. task-based or resting state), design protocol used (i.e. block, event related) and the existence of an a priori hypothesis or not (i.e. region-of-interest vs. whole brain). Two major software packages are commonly used for fMRI data analysis: Statistical Parametric Mapping (SPM; http://www.fil.ion.ucl.ac.uk/spm/) and FMRIB Software Library (FSL; http://fsl.fmrib.ox.ac.uk/fsl/fslwiki/).

### 4.1 Comparison of two major software tools

Both SPM and FSL are well recognised and cited in the literature confirming their validity as software analysis tools. It has also been reported that the results between the two software packages for various analysis techniques are similar although the analysis pipeline does differ slightly. For example, FSL performs normalisation after initial statistics in order to view activation on raw scans. Realignment consists of rigid body registration in both softwares but differ in cost functions used (SPM uses variance; FSL uses normalised correlation). Spatial smoothing is applied in both software packages differing in stage of implementation of temporal filtering; SPM at individual statistics using high pass filter 128s and FSL earlier with 100s.

Normalisation does differ between the SPM and FSL. SPM initially uses linear transforms before applying non-linear transforms whereas FSL uses only linear transformation. The latter approach is very robust but does produce a lot of residual error compared to SPM which is much more aggressive and requires a good structural scan for success. Both software packages adopt the general linear model (GLM) for individual statistics. At the group level, SPM uses only the estimates of contrasts whereas FSL uses both the estimates and the variability. The latter approach will be slightly more sensitive although will be more time consuming.

Figure 4. Analysis pipeline comparison




*Diagrammatic representation of a basic analysis pipeline for the SPM and FSL software packages. The main difference being the timing of the normalisation process.*

## 4.2 Pre-processing of fMRI data

*Brain extraction*

Non-brain structures that cannot be accurately aligned in functional scans must be removed. This can be done using the brain extraction tool (BET) in FSL which removes the eyes, skull, tongue, sinuses etc from structural images using a surface model approach: a tessellated mesh of triangles is fitted to the brain surface (Smith 2002). It is necessary to do this step, as functional scans will be normalised into standard space based on the structural scan information.

*Temporal filtering*

Temporal filtering allows the removal of noise from data with the aim to increase the signal to noise ratio. By using a high pass filter, low frequency noise that could be due to slow changes of the overall signal intensity, can be removed. Here, a high-pass filter of 128s (default setting) was implemented.

*Motion Correction*

Head movement is inevitable during a long scanning session despite the use of immobilising equipment, such as padding. This gradual shift needs to be rectified in order for registration into standard space to be accurate, as each voxel is required to be in the same location throughout the scanning session. Subject head movement is removed by aligning the EPI images to a common reference point (in FSL, this is the middle volume and in SPM the first volume) using rigid body transformation (six degrees of freedom). Motion outliers can be created and used in design matrices as an additional confound (nuisance regressors). Here, when using SPM, realignment

option was used and in FSL, the McFLIRT function was implemented (Motion Correction FMRIB's Linear Registration Tool) (Jenkinson et al. 2002).

*Regressors for WM and CSF*

In order to eliminate noise generated from spurious activations in WM and CSF, masks were generated using FAST (FMRIBs Automated Segmentation Tool) which is part of the FSL software package. The FAST tool extracts the mean time series using fslmeants command and generates a text file for each mask to be included as a regressor in preprocessing steps.

*Spatial smoothing*

Signal-to-noise ratio can be improved via smoothing. This process reduces variation in structural scans between-subjects and high frequency nose within-subjects. Typically a smoothing kernel of 5mm full-width half-maximum is applied to each volume of functional data and this parameter was applied to the data in this thesis.

*Registration and Normalisation*

Prior to group comparisons, the runs of each session need to be registered together and then all subject data is required to be registered into standard space. SPM uses a direct normalisation approach whereby the fMRI data is directly normalised to steroeotaxic space. FSL uses an indirect method involving the normalisation of the structural image into stereotaxic space. The parameters produced in the former step are then used for the normalisation of fMRI data into stereotaxic space.

## 4.3 Statistical Analysis

The GLM is used to produce summary statistics at each level before being passed onto the next level. First level analysis considers individual sessions of data ('runs'). In SPM, all runs can be analysed at the same time during one stage of first level analysis, however FSL requires individual runs are analysed separately, then combined in an intermediate level before moving on the higher level analyses. Higher level averages data across subjects or groups for comparisons.

*First level analysis*

Each run is analysed separately using voxelwise time series analysis within the framework of GLM. A synthetic HRF is generated as well as its first temporal derivative in order to shift the waveform in time to create a better fit to the data. A design matrix, requiring explanatory variables (EVs) is created describing the time course of each experimental condition within a run. For example, in this thesis I present a GLM design matrix for movement and no movement conditions and contrasts comparing EV's such as movement vs. no movement. Each EV will result in a parameter estimate (PE) image that reflects how strongly the EV fits to the voxels within the image. To create a t-statistic image, the PE image is divided by its standard error and at this point a z-statistic image can be created.

*Higher level analysis*

During higher level analysis, the variance of each subject is accounted for, resulting in the probable group mean of the cohort and can be conducted using analysis of variance and post hoc t-tests. Comparisons between groups can be carried out using independent samples t-tests.

*Thresholding*

Carrying out statistical tests at higher level analysis requires thresholding to show only voxels or clusters of voxels significantly activated. If all of the voxels in an image were to be considered independent then a Bonferroni correction could be applied. However, due to approximately 20,000 voxels within an image, the risk of type II error (falsely rejecting true activation) is increased. Thus, an alternative approach is to consider that each voxel is not independent and correcting according to the number of possible independent observations in a spatially smoothed area, which is biologically plausible. This cluster-based thresholding method is applied to neuroimaging data whereby a voxel can be considered significant if surrounded by a thresholded number of adjacent voxels. Therefore, the cluster-level threshold is dependent upon the level set for the peak-level threshold. In this thesis, a threshold of 20 voxels was implemented.

*Region of interest (ROI) analysis*

When there is a clear a priori hypothesis, ROI analysis can be performed. First, a region needs to be defined which can be done via manual delineation or from atlases such a WFU Pickatlas, which contains pre-defined ROIs, based on a number of standardised anatomical scans. ROI analysis can also be used to extract data upon, i.e. such as time series information, which statistical analysis can be performed. In this thesis, anatomical ROIs for the fMRI data were used and manual delineation for the DTI data.

## 5. Analysis approaches for rsfMRI data

A testament to its relative youth in neuroscience, there are as yet, no clear consensus for the optimal approach rs-fMRI data analysis. Numerous methods have been developed and applied to rs-fMRI data in PD populations to assess functional connectivity and within-voxel oscillations. Seed based functional connectivity analysis involves placing a 'seed' in a specific ROI from which fluctuations of ROI BOLD signal are correlated with BOLD signal fluctuations in all other voxels of the resting brain. Hierarchical clustering has expanded seed-based functional connectivity analysis by using a correlation matrix of multiple seeds to determine which seeds are most closely related. These functional connectivity approaches require strong a priori hypotheses and are advantageous from the perspective of interpretation in the context of neuroanatomy and disease processes. Data driven approaches consider all activation across the whole brain, such as graph theory, which mathematically derives global and local connectivity between brain regions resulting in a collection of 'nodes', which are representative of brain regions, interconnected both spatially and functionally (Wang et al. 2010). ICA decomposes BOLD signal into separate source signals in a network-based approach (Esposito et al. 2008). The assumption that individual source signals will be statistically independent, each component therefore represents an independent network. Graph theory and ICA are free of a priori hypotheses and can remove physical noise from the rs-fMRI signal. ReHo analysis is dissimilar to ICA in that it considers short-distance functional connectivity by measuring time series similarity of one voxel with its nearest neighbour voxels (Zang et al. 2004). ALFF analysis provides an index of the amplitude of a given region within its network or location within a specified low-frequency range (Zang et al. 2007). To date, only one analysis approach provides information on the directionality

of information flow: GCA or effective connectivity, due to its assumption that activity in one region causes activity in another region (Delaveau et al. 2010).

It is clear that given the variety of analysis techniques and the heterogeneity of the PD population, effective comparison of the resting state literature and determining the optimal analysis approach in PD is complicated. However, in this thesis, a seed-based approach has been used due to the strong a priori hypotheses.

## 6. Diffusion Tensor Imaging (DTI)

### 6.1 Principles

DTI offers a unique, non-invasive technique to assess the microstructure and anatomy of brain tissue through the characterisation of diffusion processes in water molecules. Diffusion is the random movement of particles i.e. water molecules, following thermally driven molecular collision. Within an unrestricted environment, water molecules are more equally able to travel in all directions. Conversely in a restricted environment, such as brain tissue, which contains myelin sheaths and cell membranes, such obstacles restrict diffusion. The amount of diffusion restriction varies among tissue types. For instance, white matter typically causes water molecules to travel along a specific direction due to the densely packed and homogenously oriented myelinated axon bundles. This is considered anisotropic diffusion whereas isotropy is a property referring to the orientation independence of diffusion.

FA is a measure of anisotropy and refers to a value, between zero and one, which is used to quantify relative directional properties of the diffusion process. A higher fractional anisotropic value would indicate an ellipsoid that was ‘cigar shaped’, and indicative of a strong, linear directional diffusion, a value closer to zero would indicate a higher degree of isotropy.

Therefore, DTI can quantitatively measure diffusion properties within different tissue types and gather information regarding any degeneration, insult or reorganisation within brain tissue.

## 6.2 Measuring diffusion with MRI

Diffusion weighted MRI uses pairs of magnetic gradient pulses to detect water diffusion. The first gradient results in the dephasing of protons along the gradient axis, which is amount dependent upon the protons position along the magnetic gradient. After approximately 20-50 ms, the second gradient is applied which cancels out the dephasing caused by the first gradient. This rephrasing is also dependent upon the position of the proton along the gradient axis, therefore complete rephrasing the initial status does not occur and leads to a detectable loss of signal. The more diffusion along the direction of the applied gradient leads to a higher attenuation of signal compared to that obtained with no applied gradient (b=0). As such, a diffusion coefficient (D) can be calculated based on the signal intensity within each imaging voxel, where S is the signal intensity in the diffusion image and S0 is the signal intensity in the reference image ($b_0$ image) and b is the diffusion weighted gradient factor (Mori et al. 2006):

$$S = S_0 e^{-bD}$$

Critically, gradients must be applied along multiple axes to allow detection of water diffusion in different directions. Therefore, a DTI experiment will apply several diffusion gradients and the strength of these gradients is known as b (b-value). B values, which depend on the strength and duration of gradients, are critical to ensure enough signal can be detected whist attenuating the signal-to-noise ratio. The most

commonly used b value is 1000 sec/mm2 and can be adequately used in a variety of applications.

6.3 Diffusion measures

Basser et al., introduced diffusion tensor application as a description of anisotropic diffusion behaviour by a multivariate normal distribution model (Basser et al. 1994). This model reflects diffusion properties in both anisotropic and isotropic mediums meaning diffusion measures can be derived regardless of the location or direction of neural fiber. Therefore, the diffusion tensor is a 3 x 3 x 3 covariance matrix:

$$\bar{D} = \begin{vmatrix} D_{xx} & D_{xy} & D_{xz} \\ D_{xy} & D_{yy} & D_{yz} \\ D_{xz} & D_{yz} & D_{zz} \end{vmatrix}$$

As such, to describe the tensor in each voxel, six diffusion weighted images and one b value equal to zero are required (Bammer & Bammer 2003). Therefore, more diffusion directions applied increases the accuracy of the tensor measurement. The diffusion can be visualised as an ellipsoid with eigenvectors ($v_1$, $v_2$, $v_3$) and eigenvalues ($\lambda_1\lambda_2\lambda_3$) defining the diagonalisation and directionality of diffusivity at a given time. If the eigenvalues are (almost) equal then diffusion is considered isotropic and anisotropic if significantly different in magnitude.

The main diffusion tensor measures are:

• Fractional anisotropy (FA), which measures the proportion of directionality in the tensor. Highly anisotropic structures will have an FA approaching '1.0' while isotropic structures will have an FA approaching 'zero'.

$$\mathrm{FA} = \sqrt{\frac{1}{2}}\frac{\sqrt{(\lambda_1-\lambda_2)^2+(\lambda_2-\lambda_3)^2+(\lambda_3-\lambda_1)^2}}{\sqrt{\lambda_1^2+\lambda_2^2+\lambda_3^2}}$$

• Mean diffusivity (MD), which is the sum of eigenvalues and represents overall diffusivity of molecules

$$MD = \frac{\lambda_1+\lambda_2+\lambda_3}{3},\ trace(D) = \lambda_1+\lambda_2+\lambda_3$$

DTI does have its limitations. Water diffusion in the brain is perhaps a rather simplistic approach of study to a complicated organ such as the brain. Partial volume effects may be present due to tissues/substances other than white matter existing in an identified voxel. Areas of crossing fibres such as the centrum semiovale, where fibres of the corpus callosum, corona radiata, and superior longitudinal fasciculus form a three-fold crossing present issues in accurately defining the directionality within a voxel. However, sophisticated methods of analysis are being developed to over come problems such as crossing fibers, hopefully allowing greater assessment of diffusion indices in these problematic areas. DTI data is prone to artifacts, particularly related

to motion of the subject, as well as eddy currents due to the rapid switching of diffusion gradients, which are high in amplitude.

**7. Analysis of DTI data**

There are four basic approaches for DTI data analysis: VBA, ROI analysis, whole brain histogram analysis and tractography.

Pre-processing steps for DTI data analysis are broadly similar to those previously described for fMRI (Chapter 2). In general, raw data is transformed to the appropriate format depending upon the software of use and brain extraction is applied to remove all non-brain voxels. For DTI data, it is particularly important to apply motion correction for subject motion and eddy current correction for image distortions. Eddy currents are localized electric currents induced by varying the magnetic field in the scanner, which can cause stretches, and shears in the diffusion weighted images. Geometric distortions may be caused due to misalignments in the individual diffusion weighted images comprising a total data set. Eddy current correction will correct for these artifacts. Furthermore, data is corrected by affine registration to the $b_0$ image, which is of particular importance when scanning tremulous PD patients. Finally, calculating a diffusion tensor within each voxel generates FA and MD maps.

In this thesis, two approaches were used. Due to a strong a priori hypothesis, ROI analysis using DTIExplore and TrackVis were implemented to extract measures of diffusion (FA and MD) from individual diffusion maps to be used for statistical group analyses. ROIs were manually delineated by two experienced imaging scientists for caudate, putamen and SN using the co-registered T2-weighted image of the selected individual for anatomical guidance. Anatomical borders for SN followed that of outlining hypointense region between cerebral peduncles and posterior tegmentum on

three slices. VBA was also performed in SPM12 to examine the entire brain in single subjects and perform group statistics.

**8. Scanning protocol**

8.1 Description of scanning sessions

All patients underwent a baseline scanning session, which consisted of structural brain imaging including T1 and a 64-direction DTI scan. Functional imaging consisted of two runs of a motor task paradigm interjected by a single rs-fMRI sequence. A proportion of the subjects returned for a follow-up scanning session that consisted of the exact same protocol. All scanning sessions were conducted on a 3T Trio Siemens scanner (Siemens Magneton, Erlangen, Germany) equipped with a 32-channel head coil at Imanova Ltd.

8.2 Scanner parameters

*Structural T1*

One high-resolution T1-weighted turbo field echo structural scan was collected (TE 2.98 ms; TR 2300 ms; 9° flip angle; FOV 256 mm).

*Functional MRI*

Whole-brain data were acquired with 160 volumes of T2*- weighted gradient-EPI in ascending order with an automated higher-order shim procedure [slice thickness 3.0 mm; repetition time (TR) 2500 ms; alternating long and short echo time (TE) 13 ms, 31 ms; 80° flip angle; field of view (FOV) 192 mm]. The slice acquisition angle was set at 0° from the anterior-posterior commissure (AC–PC) line to reduce frontal lobe

signal dropout due to the air sinuses, with a z-shim gradient correction to compensate for through-plane susceptibility gradients (Deichmann et al. 2003).

*DTI*

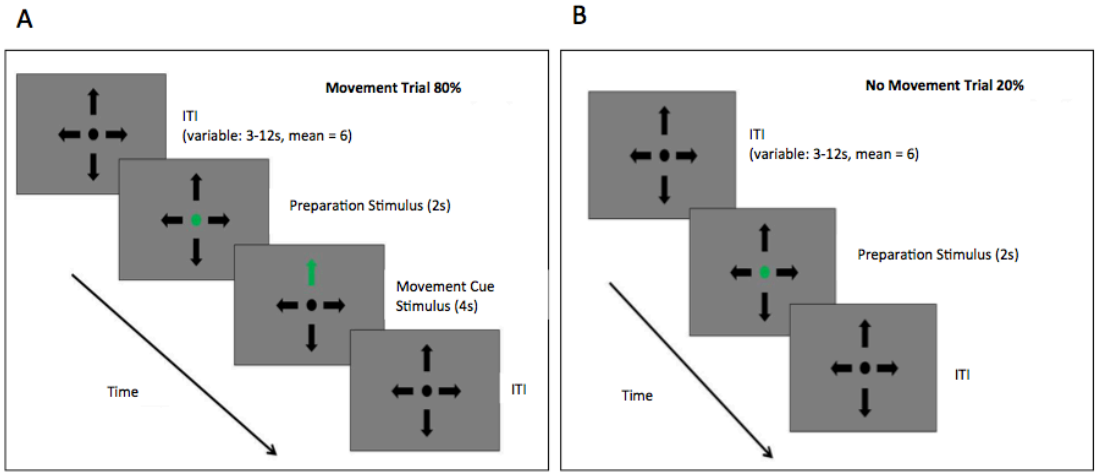
Integrated parallel imaging (GRAPPA) was used with two-fold acceleration. Seventy axial slices were obtained: TR = 9300 ms; TE = 88ms; acquisition matrix: 128 x 128; FOV= 240 mm; voxel size = 1.875 x 1.875 x 1.9mm and 1.9mm slice thickness. Diffusion sensitizing gradients were applied to 64 non-collinear directions with a b-value of 1000s/ mm2 and a non- diffusion weighted image with b = 0s/ mm2 was obtained. The present protocol was optimal at time of sequence development; however, advances regarding higher b0 values suggest the current protocol may reduce accuracy of tissue characterisation.

## 8.3 Motor Task Paradigm

All PD patients completed a motor execution paradigm in the scanner using an in-house built joystick, placed on the most clinically affected side, consisting of two conditions: “movement” and “no-movement”. Trials were presented on a screen starting with a centered black circle and four directional black arrows (north, east, south, west) on a grey background (Figure 5). During the movement condition the patient was presented with a preparation stimulus (black circle turning green) for 2 s followed by a movement cue stimulus of one directional arrow turning green for 4 s. PD patients were requested to move the joystick in a single movement following the cue in the direction presented. This condition accounted for 80% of the trials (80 trials; 20 north, 20 east, 20 south, 20 west). The no-movement condition consisted of the patients holding the joystick and looking at the preparation stimulus but not

instructed to make a movement. This condition accounted for 20% of the trials (20 trials). The paradigm consisted of a single run lasting twenty minutes, interjected with a rest period half way through, totaling 100 trials.

Figure 5. Motor Paradigm

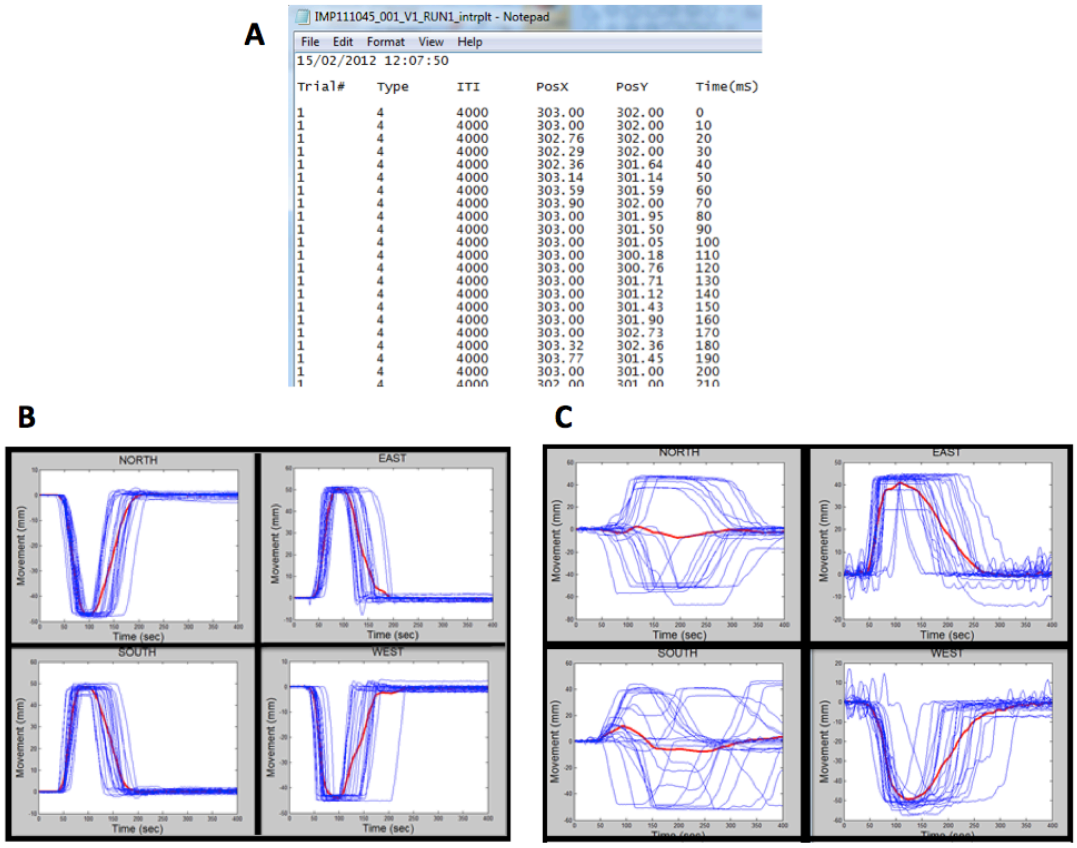



*A = Example of a 'north' movement trial i) Subject is presented with a grey background with a black centering circle and four directional black arrows for an inter-trial interval (ITI) (mean 6 s, due to event-related design) ii) Following the ITI, the preparation stimulus of the black circle turning green is presented for 2 s iii) The north arrow turns green for 4 s, during which time, the subject is required to move the joystick in a single movement, north iv) The ITI is presented again before the next trail begins. B = Example of a 'no-movement' movement trial i) Subject is presented with a grey background with a black centering circle and four directional black arrows for an inter-trial interval (ITI) (mean 6 s, due to event-related design) ii) Following the ITI, the preparation stimulus of the black circle turning green is presented for 2 s iii). The ITI returns, i.e. none of the arrows turn green indicating no movement is expected.*

## 8.4 The joystick

The in-house joystick was designed specifically for this motor paradigm to allow collection of behavioural data. The joystick location in relation to its axes was recorded every 10ms throughout each movement trial for each run, ultimately producing a log file (Figure 6, A). The data within each logfile from each run could then be averaged and visualized through an in-house Matlab code (Figure 6, B and C) permitting quality control and extracting of individual performance for motor execution and amplitude to be used in group statistics.

Figure 6. Extracted behavioural data from joystick




*Examples of log files produced from in-house joystick programme. A = screenshot of logfile portion. Positional data at each 10 ms time point is collected throughout the scan which can be collated to provide motor execution and motor amplitude data for each subjects.. B = well performed task with movements in the correct direction and in a smooth manner and C = poorly performed task with errors of direction and tremor.*

## 8.5 Behavioural Motor Data

Measures of motor execution and motor amplitude were collected from the joystick during the motor task scanning session. Motor execution was defined by the time (ms) it took each subject to move from starting position to their peak movement (furthest point from initial position before returning the joystick, thus completion of movement). The peak movement described above defined motor amplitude. These measurements were collected for each movement trial for both runs and averaged for statistical analyses.

# CHAPTER 3: BASELINE MOTOR NETWORKS IN PARKINSONS DISEASE

## 1. Introduction

Parkinson's disease (PD) is a neurodegenerative disease characterized by the presence of Lewy bodies resulting in the loss of dopamine (DA) neurons in the substantia nigra pars compacta (SNc) and the subsequent deficiency in striatal DA, which is required for the effective execution and control of movements. Neuroimaging studies using PET and functional magnetic resonance imaging (fMRI) to investigate motor execution in PD commonly report a hypoactivation of the supplementary motor area (SMA) and hyperactivation of primary motor area (M1), premotor area, parietal lobes and cerebellum (Playford et al. 1992; Jahanshahi et al. 2010; Rascol et al. 1992; Haslinger et al. 2001; Buhmann et al. 2003). It is suggested that findings of hyperactivation may reflect compensation mechanisms attempting to overcome the extra difficulty for patients to complete motor actions (Grafton 2004). However, despite a relatively large number of neuroimaging investigations, the neural course of motor execution decline and/or compensation in PD is still unclear. In recent years, a move away from solely investigating changes in magnitude of brain activity but the relationships and interactions between regions during motor execution has become an important component of PD research. Assessing interregional associations of the multi-regional motor network will provide valuable information of neural processes underlying PD pathophysiology. As such, studies of altered motor network connectivity in PD with conclusions of compensatory mechanisms have been reported in recent year (Wu & Hallett 2005; Wu, Wang, et al. 2011). The aforementioned studies are blighted by small sample sizes compared to healthy controls only thus inferences of connectivity as a result of the disease course cannot be made.

A further advancement of functional connectivity in PD has been made in recent years in the form of resting-state fMRI (rs-fMRI). Studying the brain at rest in an attempt to understand its spontaneous neural activity without constraints inextricably linked to task-based studies (i.e. subjects ability to perform the task, presence of attention-based stimuli) (Biswal et al. 1995; Raichle et al. 2001) is a valuable non-invasive tool. Thus a number of rs-fMRI studies in PD have been undertaken with general reports of disruption of the motor networks in PD (Wu, Wang, et al. 2009) and possibly reorganisation of cortico-striatal loops due to disease processes (Helmich et al. 2010). From the previous literature it is clear that it is important to continue considering magnitude of brain activity changes but to also investigate functional connectivity in both the active and resting state. It is presumed that a disrupted resting network will have a deleterious effect on the active state, such that it may not be effectively primed to initiate or execute future movements. Similarly, a resting state network experiencing compensatory mechanisms may be beneficial to the active motor network. Furthermore, to elucidate the effect of disease processes and symptomatology on these networks, sizable cohorts of varying stages of disease are required. To date, no study has used fMRI to comprehensively assess the neural basis of active and resting motor execution dysfunction or compensation as a function of disease course.

Here, we have undertaken an established motor task fMRI paradigm (Jenkins et al. 1992) in 76 PD patients divided by quartiles according to their Unified Parkinson Disease Rating Scale Part-III (UPDRS-III) score. By completing voxel-by-voxel analysis and a functional connectivity analysis across groups, we aimed to explore regional BOLD signal reductions across the disease course as well those, which

possess compensation activity. Assessment of functional connectivity of the resting network has also been investigated in a sub-set of 56 PD patients to ascertain if underlying intrinsic networks are related to the functioning of the active neural state. There is no consensus on sample size in fMRI studies. However, reports suggest between 12 and 36 subjects could be optimal (Friston et al. 1999; Desmond & Glo 2002). It is likely larger sample sizes are required for multiple comparisons (considering both voxel-by-voxel comparison and subject/group comparison). Division of the current cohorts into four groups is currently within the realms of acceptability regarding sample size.

**2. Aims**

The aims of this chapter were to:

- Identify the neural motor network in a large group of PD patients;
- Characterise stages of aberrant neural motor dysfunction in PD as a consequence of disease severity;
- Identify possible compensatory processes occurring as a response to the loss of normal motor neural functioning.
- Use behavioural in-scanner information to assist interpretation of neural findings.

**3. Hypotheses**

The hypotheses were that:

- The joystick paradigm will sufficiently elicit recruitment of the neural motor network;

- There will be gradual decline of BOLD signal in these regions as disease severity increases;
- PD patients with greater disease severity will recruit neighbouring regions to compensate for neural motor network dysfunction.

## 4. Patients and Methods

### 4.1 Patients

Seventy-six non-depressed, non-demented PD patients underwent a single fMRI scanning session involving an in–scanner motor task and 56 PD patients underwent rs-fMRI. Twenty rs-fMRI datasets were excluded due to a high degree of signal dropout surrounding the frontal sinuses area and deemed unfit for analysis. PD patients were recruited from three UK centers (Imperial College London, London, University College London, London and University of Cambridge, Cambridge) and one European center (Skäne University Hospital, Lund, Sweden) of the FP7 EC TransEuro. Recruitment onto the study was dependent upon at least one year disease duration and less than 10 years, ability to be MR imaged and an AIMS (abnormal involuntary movement scale) score less than 2. All PD patients fulfilled the UK brain bank criteria for PD (Hughes et al. 1992). The clinical battery included H&Y staging, the motor part of UPDRS (UPDRS-III), MMSE and calculation of L-dopa-Equivalent-Dose (LED). PD patients were divided into four groups according to disease severity, as measured by UPDRS-III and assigned a disease burden score (1 being the lowest and 4 being the highest) (Tables 4 and 5). Groupings were created according to quartiles calculations.

PD patients were divided into four groups according to disease severity, as measured by the UPDRS-III and assigned a disease burden score (1 being the lowest and 4 being the highest). Groupings were created according to quartiles calculations.

Table 4. Patient characteristics undergoing motor task fMRI.

| | **DB 1** | **DB 2** | **DB 3** | **DB 4** | ***P* value DB 1 vs DB 2*** | ***P* value DB 2 vs DB 3*** | ***P* value DB 3 vs DB 4*** |
|---|---|---|---|---|---|---|---|
| **No of subjects** | 19 | 19 | 19 | 19 | - | - | - |
| **Sex Male:Female** | 15:4 | 13:6 | 15:4 | 17: 2 | - | - | - |
| **Age (years ± SD)** | 55.1± 7.3 | 56.6 ± 6.9 | 56.1 ± 6.1 | 57.1 ± 8.5 | ns | ns | ns |
| **Disease Duration (years ± SD** | 4.16 ± 1.45 | 4.38 ± 2.1 | 5.7 ± 2.9 | 6.78 ± 2.5 | ns | ns | ns |
| **H&Y OFF** | 1.7 ± 0.4 | 2.0 ± 0 | 2.0 ± 0 | 2.0 ± 0 | >0.05 | ns | ns |
| **UPDRS-III OFF** | 17.5 ± 2.6 | 25 ± 2.4 | 33.4 ± 2.2 | 46.6 ± 5.1 | >0.000 | >0.000 | >0.000 |
| **Total LED** | 410 ± 191.2 | 414.8 ± 200.5 | 562.4 ± 331.3 | 637 ± 288.9 | ns | ns | ns |

*Patient characteristics demonstrating subjects are matched for demographic and clinical data apart form UPDRS-III OFF score which was the grouping criteria. *All p values derived from unpaired t tests; SD = standard deviation; UPDRS-III = Unified Parkinson's Disease Rating Scale Part III; LED = Levodopa equivalent dose; MMSE = mini mental state examination; DB = disease burden.*

Table 5. Patient characteristics undergoing resting state fMRI.

| | **Group 1** | **Group 2** | **Group 3** | **Group 4** | ***P* value Group 1 vs Group 2*** | ***P* value Group 2 vs Group 3*** | ***P* value Group 3 vs Group 4*** |
|---|---|---|---|---|---|---|---|
| **No of subjects** | 14 | 14 | 14 | 14 | - | - | - |
| **Sex Male:Female** | 11:3 | 9:5 | 10:4 | 12: 2 | - | - | - |
| **Age (years)** | 54.7 ± 7.8 | 56.3 ± 7.3 | 58.1 ± 5.6 | 59.4 ± 6.8 | ns | ns | ns |
| **Disease Duration (years ± SD)** | 3.99 ± 1.6 | 4.59 ± 2.2 | 4.52 ± 2.6 | 5.6 ± 1.6 | ns | ns | ns |
| **H&Y OFF** | 1.7 ± 0.4 | 2.0 ± 0 | 2.0 ± 0 | 2.0 ± 0 | >0.05 | ns | ns |
| **UPDRS-III OFF** | 17.9 ± 2.9 | 24.07 ± 1.6 | 31. 4 ± 2.7 | 46.1 ± 6.6 | >0.000 | >0.000 | >0.000 |
| **Total LED** | 329.1 ± 158.4 | 455.27 ± 189.7 | 418.2 ± 294.5 | 672.2 ± 288.5 | >0.05 | ns | >0.05 |

*Patient characteristics demonstrating subjects are matched for demographic and clinical data apart form UPDRS-III OFF score which was the grouping criteria and H&Y scores. *All p values derived from unpaired t tests; SD = standard deviation; UPDRS-III = Unified Parkinson's Disease Rating Scale Part III; LED = Levodopa equivalent dose; MMSE = mini mental state examination; DB = disease burden.*

## 4.2 Scanning procedure

PD patients were scanned in morning sessions (between 10.00 and 13.00 h) in the practically defined OFF condition following withdrawal of medication at least 18h prior to scanning, or 36h if using a prolonged released form of medication. Image acquisition was conducted as per the descriptions detailed in Chapter 2. All subjects conducted the motor task paradigm as detailed in Chapter 2 and a single rs-fMRI acquisition.

## 4.3 Behavioral motor data

Measures of motor execution and motor amplitude were collected from the joystick during the motor task scanning session. Motor execution was defined by the time (ms) it took each subject to move from starting position to their peak movement (furthest point from initial position before returning the joystick, thus completion of movement). The peak movement described above defined motor amplitude. These measurements were collected for each of the trials for both runs and averaged for statistical analyses.

## 4.4 Image analysis

Rigorous quality control was done on all images. Image analysis for motor task fMRI data was conducted with using Statistical Parametric Mapping version 8 (Wellcome Department of Imaging Neuroscience, UCL, UK). Preprocessing stages included, discarding the first five volumes of each fMRI run to allow for equilibrium effects, realignment of all functional scans to the first scan of the run and then again to the mean of the all the volumes for motion and slice-time correction (all scans were included in the final analysis due head movement in any direction being <2 mm),

coregistration of the mean functional image to the T1 structural scan, normalization to MNI space using parameters for the segmented T1 structural scan and smoothed using an 8 mm full-width at half-maximum Gaussian filter.

Image analysis for rs-fMRI data was completed using MELODIC, part of the FSL package (release 5.0.4, http://fsl.fmrib.ox.ac.uk/fsl/fslwiki/FSL). The images were motion corrected and un-warped using the field map and were subsequently submitted to the standard processing steps: skull stripping, grandmean scaling (putting all time series on a common scale by normalising the mean of all voxels [over space and time]t to 100), temporal filtering (0.01-0.1 Hz), normalization and registration.

4.5 Statistical analysis

Voxel- based comparisons for motor task activation differences were performed between groups using two sample t-tests in SPM8. Contrasts created in a general linear model (GLM) for each movement vs. no movement condition, which included motion and movement parameters. These contrasts were used for the second level, group random effects analysis. Initially a statistical threshold of $p < 0.001$ uncorrected and cluster extent over 20 voxels was used for activation using whole brain analysis with corrections for multiple comparisons using the false discovery rate at $p< 0.05$. Peak voxel activation was determined at the group level for four groups divided according to severity.

Functional connectivity analyses for both motor and rs-fMRI analyses were performed with FSL. A mean time series was obtained from each a priori seed region (caudate, putamen, M1, premotor area, SMA, thalamus, pallidum, dorsolateral prefrontal cortex [DLPFC], somatosensory cortex) by averaging the time series of every voxel within the ROI prior to smoothing in functional native space. A Pearson

r correlation coefficient map was produced for each comparison. There is an acknowledged degree of variance in task-activated fMRI time-series data (Gavrilescu et al. 2008). Therefore, motor task data were converted to z maps using Fisher's r to z transformation to account for this variance.

Behavioural motor data were extracted from the scanner output logfiles using an in-house code for Matlab. Statistical analyses for behavioural motor data, clinical and demographic data were performed using SPSS (version 16, SPSS Inc) for Macintosh. Comparisons between groups were performed using two sample t-tests.

## 5. Results

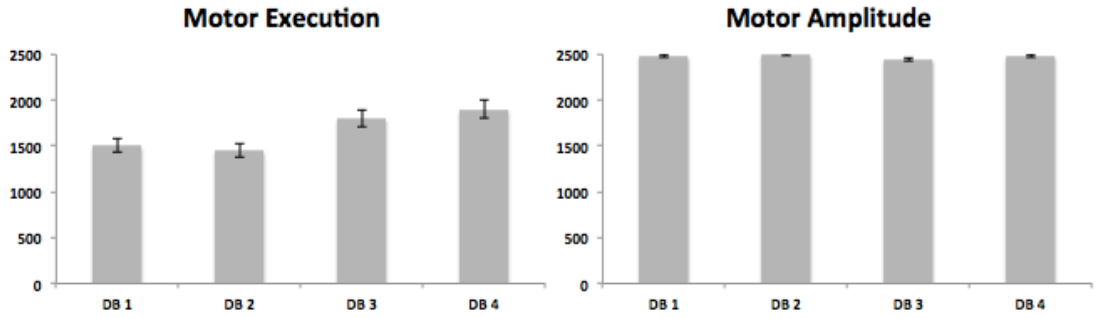
### 5.1 Participants

PD patients undergoing motor task fMRI analyses were not significantly different between groups for age, disease duration, total LED. DB 1 and DB 2 were marginally significantly different for H&Y scores ($p < 0.05$) and all groups were significantly different for UPDRS-III scores ($p<0.0001$). PD patients undergoing the rs-fMRI analyses were not significantly different between groups for age or disease duration. Similar to the motor-task fMRI group, DB1 and DB2 were marginally significantly different for H&Y scores ($p < 0.05$), as well as total LED ($p< 0.05$). All groups were significantly different for UPDRS-III score ($p <0.0001$)

### 5.2 Behavioural: Motor execution and amplitude

PD patients generally showed deficits in both motor execution and amplitude between lower and higher disease burdens indicated by the slower reaction time and less distance respectively. Both motor measures indicate a worsening between DB 2 and DB 3, although the observed effect was no significant (figure 7).

Figure 7. Behavioural motor results across disease burden in PD patients




*Motor Execution = mean reaction time (ms) for subject to move the joystick from its starting position to its peak movement (furthest point form initial starting position) with standard deviation. Motor Amplitude = mean distance from initial starting point to furthest point indicating completion of movement. Measurements taken from 'movement' conditions only and averaged across all trials in both runs. Results show lower DB stages have slower reaction time and have lower amplitude compared to higher DB stages.*

## 5.3 fMRI motor execution and disease burden: voxel-by-voxel-analysis

Whole brain analysis revealed that PD patients with DB 2 *vs.* DB 1 have reduced BOLD signal in M1, caudate, putamen, somatosensory cortex, premotor area, SMA and thalamus ($p < 0.01$) during motor execution *vs.* no movement. Patients with DB 3 *vs.* DB 2 show significant BOLD signal reductions, which were detected in M1, premotor area ($p<0.01$), putamen and left somatosensory cortex ($p<0{\cdot}05$) with an additional decrease in the right DLPFC ($p<0.05$).

PD patients with DB 4 *vs.* DB 3 no longer revealed significant BOLD signal decreases but rather, BOLD signal increases are detected in the same or neighboring

regions (premotor area, SMA, DLPFC [0<0.01], caudate, thalamus [p<0.05]). ROI analysis confirmed findings of the whole brain analysis (Table 6, Figure 8).

Table 6. Significant ROIs with BOLD signal changes as a consequence of disease burden

| **Disease burden comparison** | **Region** | **MNI** | **Z Score** |
|---|---|---|---|
| 2< 1 | M1 | 413, -19, 40 | 3.58** |
| | Left Caudate | -10, -2, -24 | 2.70** |
| | Left Putamen | -28, -16, 12 | 3.46** |
| | Right Somatosensory | 42, -22, 40 | 3.45** |
| | Thalamus | 10, -24, 6 | 3.09** |
| | Left Premotor area | -62, 8, 46 | 2.83** |
| | Right SMA | 12, -6, 46 | 3.03** |
| 3 < 2 | M1 | -24, -16, 48 | 2.45** |
| | Right DLPFC | 54, 10, 22 | 2.39** |
| | Putamen | -22, -2, 4 | 2.17* |
| | Left Somatosensory | -42, 20, 56 | 2.28* |
| | Premotor | 8, -16, 66 | 2.55** |
| 4 < 3 | No significant regions | | |
| 4> 3 | Premotor area | -40, 08, 36 | 3.48** |
| | SMA | 6, -14, 52 | 2.72** |
| | DLPFC | 44, 26, 22 | 2.99** |
| | Caudate | 18, 9, 13 | 2.59* |
| | Thalamus | -9, -14, -4 | 1.94* |

*Significant BOLD signal changes in the motor network during movement vs rest in PD patients. Lower DB stages have significant hypoactivations in motor areas which appears to be restored at higher DB stages. All cluster corrected, thresholded at 20 voxels; * p<0.05; **p<0.01; MNI Montreal*

*Neurological Institute coordinate space; M1 = primary motor area; DLPFC = dorsolateral prefrontal cortex; SMA = supplementary motor area;*

Figure 8. BOLD signal changes as a consequence of disease burden




*Transverse sections of parametric maps showing significant BOLD signal decreases (blue-white) in 2 > 1: M1 **; left caudate**; left putamen**, right somatosensory cortex**; thalamus**; left premotor**, right SMA**. 3 < 2: M1**; right DLPFC*; premotor**; putamen*; left somatosensory*. 4 > 3: premotor**; SMA**; DLPFC**; caudate*; thalamus*. 1 = disease burden 1; 2 = disease burden 2; 3 = disease burden 3; 4 = disease burden 4. Results show significantly reduced activations in motor related regions in lower DB stages compared to significantly increased activation in motor region at the higher DB stage. Colour bar indicates z scores. * = $p < 0.05$; ** = $p < 0.01$; *** = $p < 0.001$, cluster corrected, thresholded at 20 voxels.*

5.3 fMRI motor execution and disease burden: functional connectivity

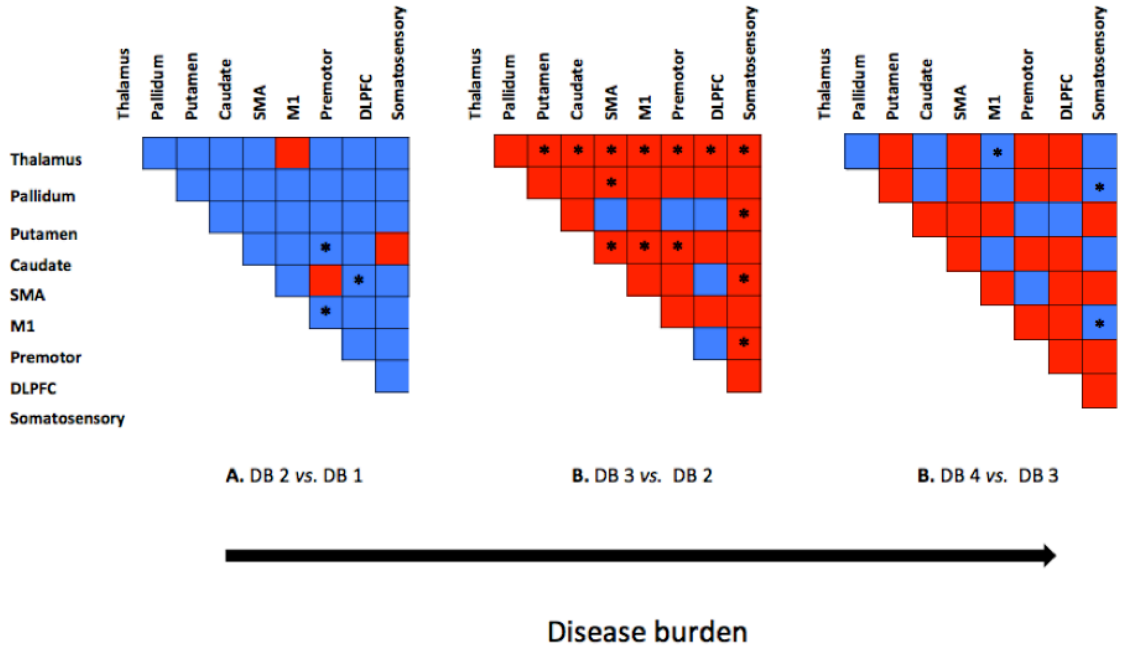
DB 2 vs. DB 1 showed generalized reduction of functional connectivity in motor networks with significant decreases between premotor and caudate ($p < 0.05$), premotor and M1 ($p < 0.03$) and DLPFC and SMA ($p<0.03$). As DB increases (DB 3 vs. DB 2) there are significant increases in connectivity between thalamus and putamen ($p < 0.01$), caudate ($p < 0.01$), SMA ($p < 0.05$), M1 ($p< 0.01$), premotor ($p< 0.01$), DLPFC ($p<0.01$) and somatosensory cortex ($p< 0.01$); SMA and pallidum ($p<0.05$), caudate ($p< 0.04$); M1 and caudate ($p<0.02$); premotor an caudate ($p<0.01$); somatosensory cortex and putamen ($p<0.02$), SMA ($p<0.01$) and premotor ($p< 0.01$). At the highest DB (DB 4 vs. DB 3), a generalized increase of connectivity remains but a significant loss of previously restored regions is observed between M1 and thalamus ($p<0.02$); somatosensory cortex and pallidum ($p<0.02$) and M1 ($p<0.05$) (Figure 9).

## 5.5 Rs-fMRI and disease burden: functional connectivity

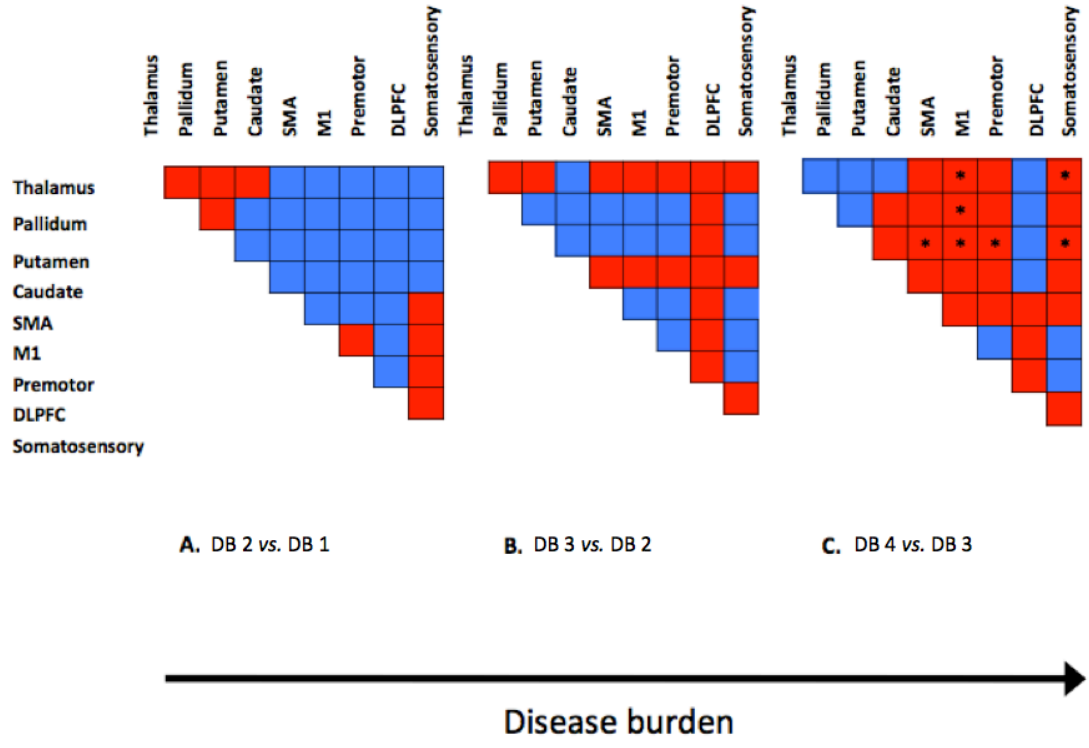
ROIs identified during the motor fMRI task as being involved in significant BOLD changes within the motor network were used to define the rs-fMRI motor network. Correlation analysis applied to the extracted time-series data revealed a generalized decrease of connectivity at lower disease burdens (DB 2 vs DB 1) which gradually and regionally increases as disease burden increases (DB3 vs. DB 2) becoming significantly increased at the highest disease burden (DB 4 vs. DB 3) for seven ROI pairs: M1-thalamus, $p < 0.03$; M1-pallidum, $p < 0.03$; M1- putamen, $p < 0.01$; putamen-SMA, $p < 0.02$; putamen-premotor area, $p < 0.01$; putamen- somatosensory cortex, $p < 0.03$; somatosensory cortex-thalamus, $p < 0.03$ (figure 10).

Figure 9. Functional connectivity of A) motor task fMRI and B) resting motor network

A.




B.



*Functional connectivity analyses. A) Fisher z-transformed correlation co-efficients for the functional connectivity between motor related regions during the fMRI motor task. Showing significant decreases between DLPFC, caudate, premotor and M1 at lower DB stages. Significantly increased connectivity primarily from thalamus and somatosensory areas to the rest of the network at middle DB stages and then significant loss of connectivity M1, somatosensory, DPFC and premotor area at the higher DB stages. B) Pearson r correlation maps for the functional connectivity between motor related regions during the rs-fMRI scan. Showing significant increases in connectivity between M1, premotor, somatosensory, pallidum, putamen and caudate at higher DB stages. Groups according to disease burden (DB). Red = increased connectivity as disease burden increases; blue = decreased connectivity as disease burden increases. SMA = supplementary motor area; M1 = primary motor area; DLPFC = dorsolateral prefrontal cortex. Significant correlation indicated by bold asterisk. Pearson r correlation, $p < 0.05$.*

## 6. Discussion

The present study, for the first time to our knowledge, investigated the change in magnitude of motor related neural activity as well as functional connectivity of the motor network in both its active and resting state in large cohort spanning four disease burden levels.

Our results demonstrate that behaviorally, PD patients' performance of motor execution and motor amplitude is defected as a consequence of DB. Specifically, there is a significant decline in motor execution performance as measured by reaction time between DB 2 and DB 3, which is maintained at DB 4. A similar trend is observed for motor amplitude performance.

Following a voxel-by-voxel-analysis of the fMRI motor task, significant changes of BOLD signal (regional amplitude) are observed at DB 2 compared to DB 1 with reductions in M1, premotor area, somatosensory cortex, SMA, putamen, caudate and

thalamus. Significant reductions in M1, premotor, somatosensory cortex and caudate persist at DB 3 with additional reductions found in DLPFC. Interestingly, at DB 4, no significant reductions are found compared to DB 3 but rather significant increases are located within premotor area, SMA, DLPFC, caudate and thalamus.

To investigate further and elucidate the relationship between these regional changes, functional connectivity analyses of the fMRI motor task were undertaken. Regional correlations reveal a generalized decrease of functional connectivity at DB 2 compared to DB 1. Significant reductions were located between premotor area, M1, caudate, DLPFC and SMA. Conversely DB 3 compared to DB 2 revealed a multitude of significantly increased functional connections existing between thalamus, putamen, caudate, M1, premotor, DLPFC, somatosensory cortex, pallidum. These results are highly indicative of compensatory mechanisms occurring to account for the increased difficulty to complete motor activities due to disease processes. This theory is upheld by the behavioral data not showing an increase in motor performance, thus increased connectivity in the active motor network is not permitting increased motor performance but more likely possessing a reserve property to allow continuation of motor abilities at a reasonable level. However, by DB 4, this reserve capacity appears to be declining with significantly reduced connectivity between M1, thalamus, somatosensory cortex and pallidum. The functional connectivity results are in line with the voxel-by-voxel-analysis but do show that the underlying functional connectivity may be altering in a more dynamic fashion, which is not observable at an isolated regional neural level until sometime later. This is evidenced by the observed increases at DB 4 in the voxel-by-voxel-analysis compared to the already declining connectivity analysis in the same group comparison.

Identification of compensatory mechanisms in PD is important for the development of biomarkers and to tailor endpoints and interpretation of clinical trials. However, compensatory mechanisms at the macroscopic level in PD are under-researched. This is mainly a consequence of the difficulty regarding methodology but the advances made in neuroimaging techniques enables better investigation of such processes. Indeed, animal models of PD suggest parkinsonian syndromes cannot be solely attributed to dysfunction within the basal ganglia (Chesselet & Delfs 1996) with strong evidence of biochemical changes in the nigrostriatal pathway serving as maintenance of DA transmission homeostasis (Zigmond et al. 1990). Neuroimaging techniques do not appear to correlate well with clinical measures of disease severity i.e. UPDRS-III and the progression of PD is affected by many factors such as age of onset, disease sub-type. (Marras & Lang 2008) However, it cannot be excluded that individual compensatory mechanisms are responsible for the variable rate of disease progression (Palmer et al. 2010). Indeed, recent fMRI studies have attempted to investigate compensatory mechanisms in PD with reports of cerbello-thalamo-cortico loop recruitment as a compensation of dysfunctional basal ganglia loops (Palmer et al. 2010). The concept of motor reserve in PD; the ability of the brain to continue functioning *via* enhanced recruitment of typical regions and/or recruitment of novel regions until the dysfunction reaches a critical threshold, has been previously investigated in one fMRI study (Palmer et al. 2009). The authors demonstrated that when performing a motor task, PD patients maximally recruited the motor network and compensated for task difficulty by recruitment of novel areas (Palmer et al. 2009). Conclusions from the authors are in line with the current study as well as similar work in stroke (Mulder et al. 2002); increased effort required to maintain a suitable functional output leads to the activation of motor reserve.

Functional connectivity analysis of the resting motor network revealed theoretically agreeable findings to that of the active motor network. In general, there is a decrease of connectivity at lower disease burden, which gradually increases until significantly increased connectivity between M1, pallidum, putamen, SMA, premotor area, somatosensory cortex and thalamus are detected at DB 4. The active motor network is hypothesized to be dependent upon the resting motor network by virtue of modulating the effectiveness to prepare, initiate and execute any given action. In the healthy brain, motor networks are required to maintain a resting state equilibrium in order to perform future motor tasks (Bressler & Kelso 2001). Thus, a disrupted or compensated resting motor network should have an effect on the effective initiation and execution of movements. It should also be considered that the presence of dyskinesia could have an influence on motor networks (active or resting) through further disruption of reorganisation. Due to the lack of dyskinesia in the current cohort, this could not be explored in the current study.

Multiple brain regions are well established as being part crucial in the effective control of movements, namely M1, premotor area and SMA. The SMA is indeed important for motor preparation and initiation. Typically this region is reported to possess a hypoactivation or decrease in activation rather than the increase that we have reported. Our motor paradigm was more focused on motor execution than preparation or initiation, thus a decrease may not be completely expected. It has also been previously suggested that an increase in SMA activity could be directly proportional to speed of movement (Riecker et al. 2003). Considering our patients had a significant reduction in reaction times for movement completion, we are confident that our increased SMA finding is not related to an increased speed of movement

effect. However, one of the few rs-fMRI studies in PD does corroborate our findings (Wu et al., 2010b). The premotor area is involved in selection and generation of movements (Grafton et al. 1997) and has been reported to demonstrate decreased connectivity in the resting motor network (Wu et al. 2010). Here, we report an increase but not in M1. Thus it is likely that the disruption of the central motor region (M1) may lead to compensatory mechanisms in associative motor cortices.

The DLPFC has also been previously reported as possessing decreased functional connectivity with other motor related regions (Wu, Long, et al. 2009). The DLPFC is typically involved in processes related to attention of action performance monitoring. The fact we found an increase and not a decrease in this region in isolation and within connectivity analysis, could simply indicate that our subjects were of a high cognitive ability or that compensatory mechanisms are also in place for non-motor and motor-related processes.

It should be noted that the current data detected an apparent delay between the restoration of functional connectivity in the active motor network and resting network. This could be due to a genuine delay in the restoration of networks or due to methodological reasons related to the extraction of highly correlated time courses in the resting data. An alternative explanation could be related to the increased attentional load likely to be required for the completion of motor tasks, thus the active motor network is detecting an increase of functional connectivity in motor- attentional areas to compensate for the higher demand motor tasks require as disease burdens increases.

Due a strong *a priori* hypothesis regarding ROIs for this study, our results directly answer the question at hand: how are motor related networks affected in PD due to disease burden. However, it should be noted that pre-chosen ROIs always present the

possibility of bias and complete removal of physiological noise is limited. Therefore, future studies may wish to take a whole brain approach whereby robust de-noising approaches can be applied to the data to ensure the effects of non-neural physiology, scanner artefacts and other confounds are accounted for. By doing so, the data can be less likely to contain spurious correlations.

Here, we have shown for the first time, magnitude and connectivity changes in the active and resting motor network in a large cohort of PD patients across various DB stages. Collection of in-scanner behavioral data not only aids quality control of data i.e. ensuring subjects are completing the task effectively, but allows cross-checking of neural information with actual symptomatology, i.e. increased activation in a certain brain region does not necessarily mean an enhanced performance on the task. This study is limited by the lack of control subjects thus not permitting the comparison of normalization effects. Furthermore, conducting whole brain connectivity analyses could enhance the study because despite possessing strong *a priori* hypotheses, it cannot be discounted that region-to-region introduced bias.

This study highlights the need to utilise all stages of PD to fully elucidate the underlying neural mechanisms due to and coping with the disease process. Future studies should consider the use of cohorts with multiple disease stages to investigate motor network evolution in PD in both the active and resting state. Furthermore, this study indicates the importance of using more than one imaging modality and analysis technique to capture the full extent of PD network alterations.

# CHAPTER 4: MOTOR NETWORKS IN PARKINSONS DISEASE OVER TIME

## 1. Introduction

In line with Chapter 3, the focus of the current chapter is to elucidate the course of neural motor network dysfunction in PD patients. To date, fMRI investigations of motor control and the motor network in PD have elucidated significant differences in BOLD signal between PD patients and healthy controls in the striatum and cortical areas such as M1, SMA and IPL (Buhmann et al. 2003; Haslinger et al. 2001; Kwak et al. 2012) whilst performing a variety of motor tasks in the scanner. A serious concern in the motor activation in PD literature is the heterogeneity of findings. For example, the pre-SMA has been consistently observed in fMRI studies of motor control as significantly different from controls. However, whether the difference was an increase or decrease of BOLD signal in PD patients varies across studies. Certainly, one issue for these discrepancies could be the variety of motor tasks implemented in the scanner i.e. finger tapping vs. ankle movement. An alternative approach for assessing motor networks in PD could be the investigation of brain activity in the absence of a task. By doing so, performance related confounds are eliminated. In the healthy brain, motor networks are required to maintain a resting state equilibrium in order to perform future motor tasks (Bressler & Kelso 2001), thus the resting brain or the intrinsic activity of the brain may be disrupted in neurodegenerative disease and in turn, disrupt the active motor network. Rs-fMRI studies have also been blighted by discrepant findings that may well be due to differences in preprocessing or statistical analysis of the data.

The majority of these studies have consisted of a cross-sectional design that is vulnerable to greater inter-individual variability in regard to BOLD signal. Thus,

conducting within-subject longitudinal studies needs to be exploited to robustly assess activation changes in motor networks across PD progression. Furthermore, it is believed that brain regions involved in motor control do not act in isolation. Therefore, investigating functional connectivity changes over time is also crucial to motor network alterations in PD.

Here, a subset (n = 29) of PD patients from Chapter 3 underwent a second scanning session on average 19.8 months following the baseline scan. The fMRI motor paradigm and rs-fMRI were repeated in all subjects to investigate within subject changes in both the active and resting motor network over time as a function of PD progression.

**2. Aims**

The aims of this chapter were to:

- Characterise regional and connectivity alterations of the active and resting neural motor network in PD patients over time.
- Investigate whether neural motor network alterations over time significantly correlated with clinical parameters.

**3. Hypotheses**

The hypotheses of this chapter were:

- PD patients will show a decline in behavioural motor performance over time.
- Regional decreases of BOLD signal identified in Chapter 3 will be confirmed longitudinally.

- Functional connectivity between regions will be altered as a function of disease progression.

## 4. Subjects and methods

### 4.1 Patients

Twenty-nine PD patients included in Chapter 3 returned for the follow-up scanning session, which was an average 19.8 months (SD = 3.8 months) after the baseline scan (Table 7). PD patients demonstrated significantly increased disease severity as measured by the UPDRS-III ($p<0.0001$) and had significantly higher LED ($p<0.001$). All PD patients still fulfilled the UK brain bank criteria for PD at follow-up (Hughes et al. 1992). The clinical battery included H&Y staging, UPDRS-III, MMSE and calculation of LED.

Table 7. Patient characteristics in the longitudinal study

| | Baseline | Follow-up (mean ± SD; 19.8m ± 3.8m) | P value* |
|---|---|---|---|
| N | 29 | 29 | - |
| Male:Female | 22:7 | 22:7 | - |
| Age (mean±SD) | 55.5 ± 7.44 | 57.2 ± 7.37 | - |
| Disease duration (years ± SD) | 4.19 ± 2.24 | 5.5 ± 2.3 | - |
| UPDRS-III OFF (mean±SD) | 27.38 ± 9.6 | 35.7 ± 12.1 | P < 0.0001 |
| UPDRS-III OFF % change over time (mean±SD; range) | 37.83% ± 43.71; 0 – 152.63% | | |
| LED (mean±SD) | 464.53 ± 265.6 | 564 ± 286.9 | P < 0.001 |
| MMSE (mean±SD) | 29.7 ± 0.6 | 29.7 ± 0.6 | ns |

*Patient characteristics showing that UPDRS-III OFF and LED significantly increased over time.*

**paired t test; m= months; SD = standard deviation; UPDRS-III = Unified Parkinson's Disease Rating Scale Part III; LED = Levodopa equivalent dose; MMSE = mini mental state examination.*

## 4.2 Scanning procedures

Scanning procedures were as previously described (Chapter 3. In brief, PD patients underwent a T1 structural scan, two runs of the fMRI motor paradigm interjected with a single rs-fMRI scan. All scans took place on a morning session (between 10.00 and

13.00 h) in the practically defined 'OFF' condition following withdrawal of medication between 18 h and 36 h pre-scan.

4.3 Behavioural motor data

Measures of motor execution and motor amplitude as earlier described (Chapter 3) were collected during the fMRI motor paradigm. These data were used to for statistical comparison against the baseline performances.

4.4 Image analysis

All scans underwent rigorous quality control and were analysed as described in Chapter 3. In brief, fMRI motor task data were analysed using SPM version 8 following preprocessing steps of realignment, motion and slice time correction, coregistration, nomalisation and smoothing.

Rs-fMRI data analyses were completed using MELODIC in FSL with preprocessing steps: motion corrected, skull stripping, grandmean scaling, temporal filtering (0.01-0.1 Hz), normalization and registration.

4.5 Statistical analysis

Following pre-processing of image data, voxel-based comparisons between baseline and follow-up visits of the fMRI motor paradigm were performed using paired t tests in SPM8. The GLM included contrasts for each movement vs no movement condition and included motion parameters. These contrasts were used for second level, group analysis. An initial statistical threshold of $p<0.001$ and a voxel threshold of 20 voxels were used for the ROI analysis. Anatomical ROIs were taken from the WFUPickatlas using a priori hypotheses based on findings form the baseline study (Chapter 2). Peak

voxel activation was determined at the group level for two groups according to scan visit.

Functional connectivity analyses for both motor and rs-fMRI were completed in FSL as described in Chapter 3. In brief, regional timeseries were extracted and Pearson r correlation coefficient maps were generated. Motor task fMRI data were converted to z maps due to variance in the data.

Statistical analyses of the motor behavioural data were completed using SPSS for Macintosh. Paired t tests were used for statistical comparisons between scan visits.

## 5. Results

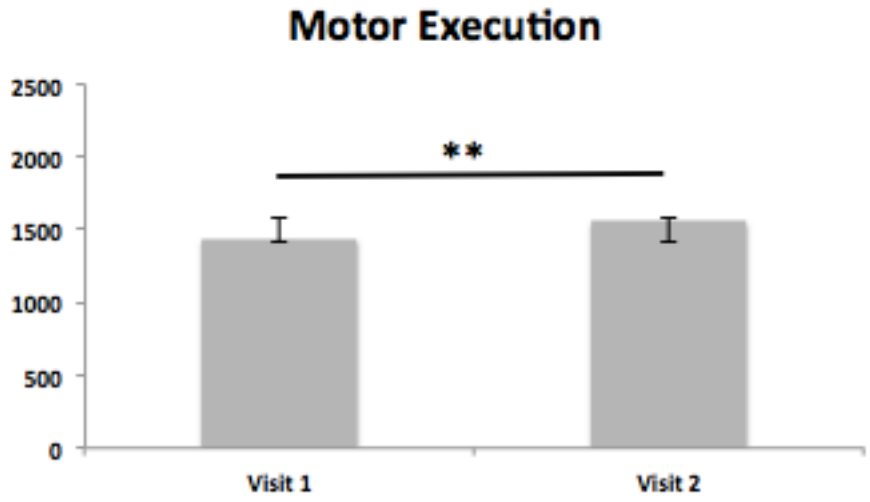
### 5.1 Clinical changes

Over an average 19.8 months, PD patients presented a decline in motor function evidenced by significantly higher levels of disease disability as measured by UPDRS-III and a significantly increased intake of LED (Table 7). There was no apparent cognitive decline as measured by the MMSE.

### 5.2 Behavioural analysis

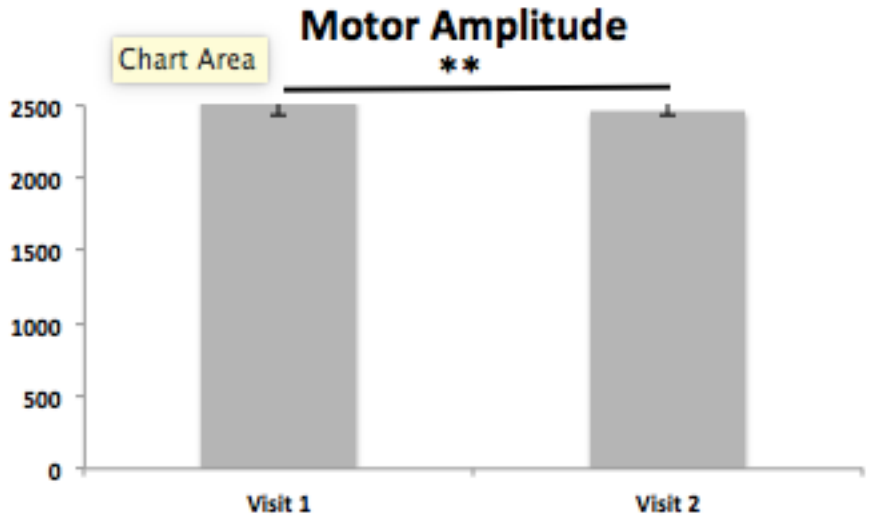
PD patients demonstrated a significant decline in both motor execution ($p = 0.002$) and amplitude ($p= 0.0001$) whilst performing the fMRI motor task over time (Figures 10 and 11).

Figure 10. Motor execution performance in PD patients across visits (mean Interval 19.8 months)




*Performance of motor execution over time showing that patients had significantly declined in visit 2 versus visit 1 with standard deviation. Motor Execution = mean reaction time (ms) for subject to move the joystick from its starting position to its peak movement (furthest point form initial starting position). ** = p < 0.002, paired t-test.*

Figure 11. Motor amplitude performance in PD patients across visits (mean Interval 19.8 months)



*Performance of motor amplitude over time showing that patients had significantly declined in visit 2 versus visit 1 with standard deviation. Motor Amplitude = mean distance from initial starting point to furthest point indicating completion of movement. Measurements taken from 'movement' conditions only and averaged across all trials in both runs. *** = p < 0.0001, paired t-test.*

## 5.3 fMRI motor task: ROI analysis

ROI analysis confirmed the whole brain analysis results. Further ROIs were placed bilaterally in the pallidum due to a priori hypothesis of the potential role of the pallidum in a functional network of motor execution in PD. All ROIs showed a significant reduction of BOLD signal over time ($p<0.01$) (Table 8; Figure 12).

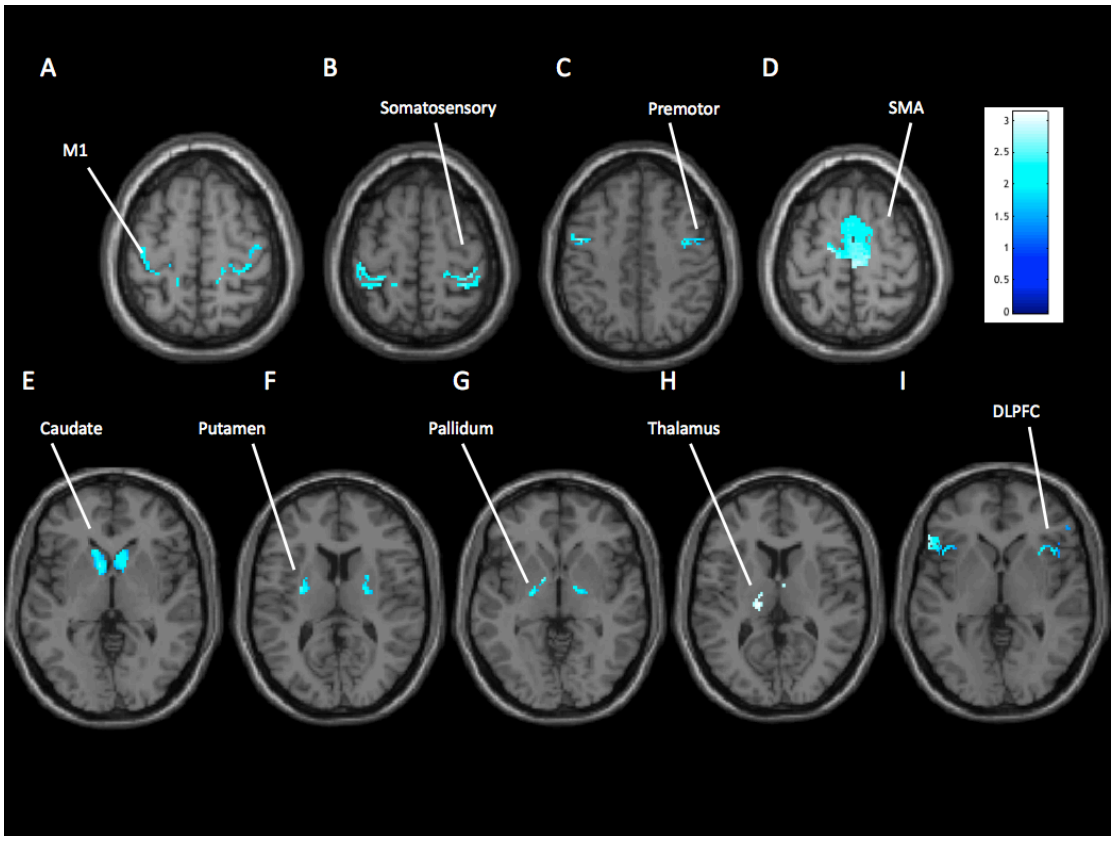
Table 8. Significant ROIs with BOLD signal reduction over time in PD patients.

| **Region** | **MNI** | **Z score** |
|---|---|---|
| Caudate | -10, 20, -6 | 3.03** |
| DLPFC | -54, 26, 22 | 3.51** |
| Pre-motor | -44, 2, 40 | 3.52** |
| M1 | -28, -28, 72 | 3.42** |
| Somatosensory | -14, -36, 76 | 3.19** |
| SMA | -16, -12, 64 | 3.02** |
| Pallidum | -22, -12, 4 | 2.52* |
| Putamen | -24, -12, 4 | 2.63* |
| Thalamus | -14, -20, 10 | 1.89* |

*BOLD signal reductions in motor ROIs in PD patients from visit 1 to visit 2. Shows significant BOLD signal reduction in all key motor related regions. All cluster corrected, thresholded at 20 voxels;*

**p<0.05, **p<0.01; MNI Montreal Neurological Institute coordinate space; M1 = primary motor area; DLPFC = dorsolateral prefrontal cortex; SMA = supplementary motor area.*

Figure 12. Regional BOLD signal reduction at follow-up vs. baseline

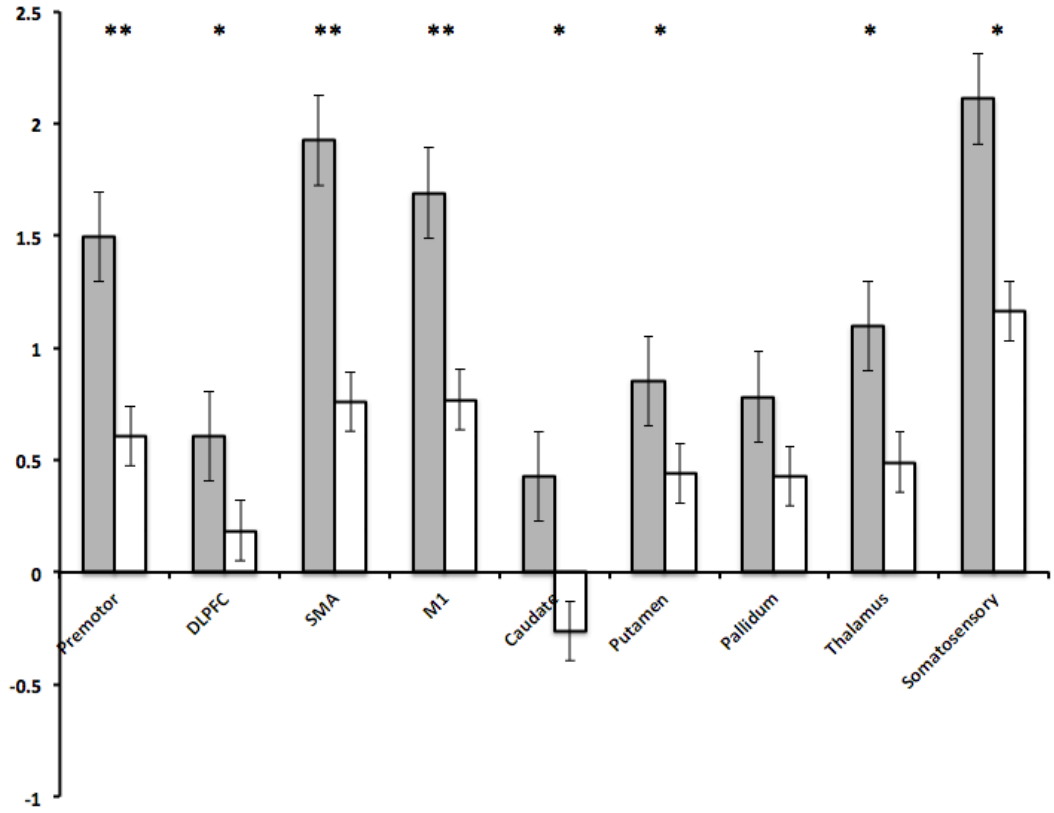



*Transverse sections of statistical parametric maps showing significant BOLD signal decreases (blue - white) associated with movement versus rest in PD patients over time. A = bilateral M1**; B = bilateral somatosensory cortex**; C = bilateral premotor area**; D = bilateral SMA**; E = bilateral caudate**; F = bilateral putamen**; G = bilateral pallidum**; G = right thalamus*; I = bilateral DLPFC**. Colour bar indicates z scores. * = p < 0.05; ** = p < 0.01, cluster corrected, thresholded at 20 voxels.*

5.4 fMRI motor task: time series regional analysis

The mean time series (mean run1 + mean run2) for each ROI was extracted to evaluate whether observed reduction in the voxel-based analysis was due to a significant reduction only or whether a deactivation occurred. The time series analysis confirmed the voxel-based analysis but provided further information regarding the caudate which demonstrated a deactivation (Figure 13).

Figure 13. ROI extracted time series for movement vs. no-movement condition in PD patients.

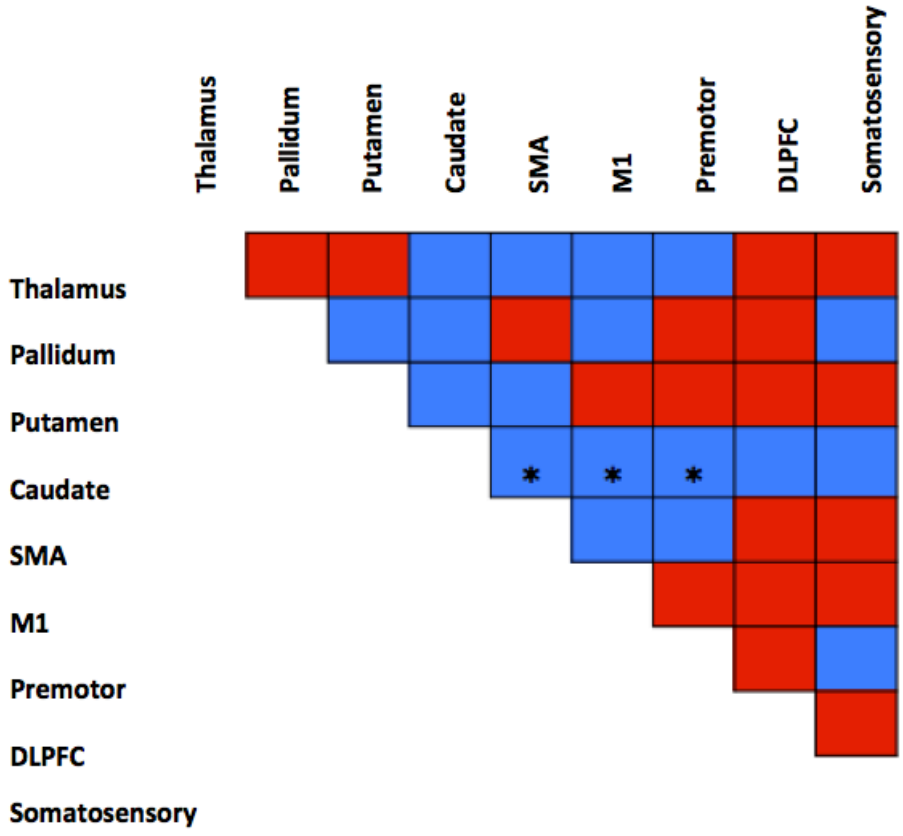



*Extracted time series z scores for motor network ROIs. Shows all ROIs significantly declined in activation over time with caudate demonstrating a hypoactivation over time. DLPFC = dorsolateral prefrontal cortex, SMA = supplementary motor area, M1 = primary motor cortex. * = p <0.05; ** = p < 0.01. Paired t tests.*

## 5.5 fMRI motor task: functional connectivity

Regional functional connectivity in the motor network of PD patients altered over time. There was a generalised increase of connectivity within DLPFC and putamen connections and a decrease of caudate connectivity (Figure 14). Significant reductions of connectivity between caudate and cortical regions: M1, premotor area and SMA were detected as a consequence of disease progression ($p < 0.05$). No other decreases and no increases of connectivity were found to be significant.

Figure 14. Active functional connectivity changes over time in PD patients



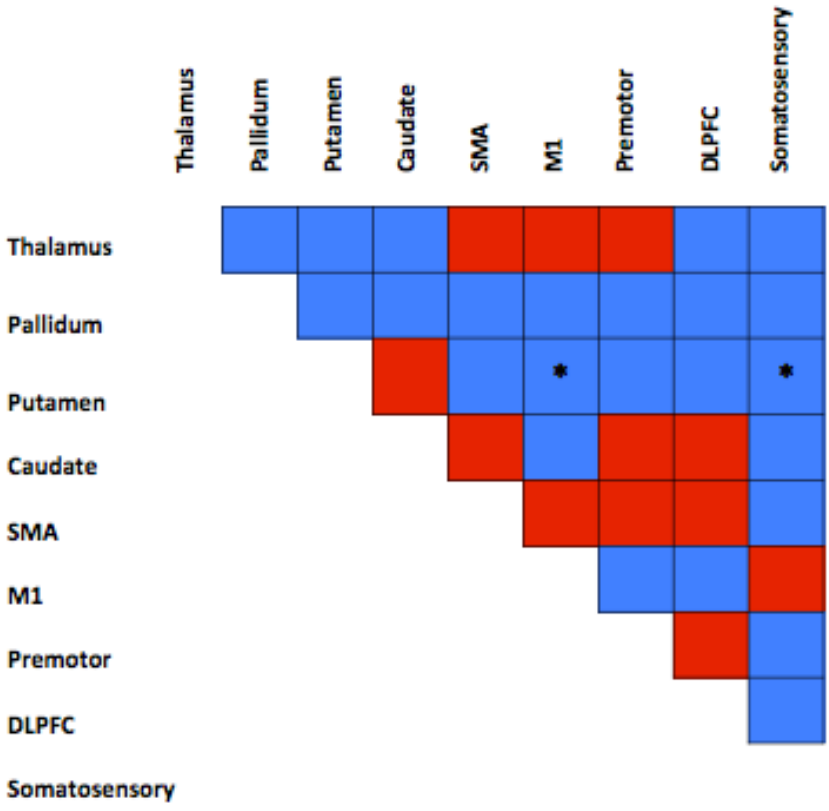

*Functional connectivity analyses. Fisher z-transformed correlation co-efficients for the functional connectivity between motor related regions during the fMRI motor task. Showing significant decreases between, caudate, premotor and M1 and SMA from visit 1 to visit 2. Groups according to disease burden (DB). Red = increased connectivity as disease burden increases; blue = decreased connectivity as disease burden increases DLPFC = dorsolateral prefrontal cortex; M1 = primary motor area; SMA = supplementary motor area. Changes in correlation r values over time indicated by colour scale: red = increased correlation over time; blue = decreased correlation over time. Significant changes in functional connectivity from baseline to follow-up are indicated by a black asterisk *= $p < 0.05$.*

*. Significant correlation indicated by bold asterisk. Pearson r correlation, $p < 0.05$ (corrected for multiple comparisons, bonferroni).*

## 5.6 Rs-fMRI: functional connectivity

Regional functional connectivity in the resting motor network of PD patients altered over time. There was evidence of decreased connectivity within the network between putamen with M1 (p = 0.5) and somatosensory cortex (p = 0.05) (Figure 15). Interestingly, the direction of changes was generally in opposition to findings within the active motor network.

Figure 15. Resting functional connectivity changes over time in PD patients




*Functional connectivity analyses. Pearson r correlation maps for the functional connectivity between motor related regions during the rs-fMRI scan. Showing significant decreases in connectivity between putamen, M1 and somatosensory area between visit 1 to visi 2. Groups according to disease burden (DB). Red = increased connectivity as disease burden increases; blue = decreased connectivity as disease burden increases DLPFC = dorsolateral prefrontal cortex; M1 = primary motor area; SMA =*

*supplementary motor area. Changes in correlation r values over time indicated by colour scale: red = increased correlation over time; blue = decreased correlation over time. Significant changes in functional connectivity from baseline to follow-up are indicated by a black asterisk *= $p < 0.05$.*

*. Significant correlation indicated by bold asterisk. Pearson r correlation, $p < 0.05$.*

## 6. Discussion

This study presents for the first time a combined assessment of both the active and resting motor network in PD over time. Twenty-nine PD patients undertook two scanning sessions consisting of fMRI a motor paradigm and rs-fMRI on average 19.8 months apart. The current cohort returning for the follow-up scan had significantly declined in motor function as measured by UPDRS-III and were receiving significantly more DA-ergic medication, which is a sensible clinical assumption to make and enables assessment of neural network alterations in relation to disease progression. Behavioural in-scanner data reveal a significant decline in motor execution and motor amplitude performance in the PD patients over time. All PD patients were able to complete the task efficiently but were slower and completed more restricted movements at follow-up compared to baseline. These findings are clinically in line with disease progression averaging ~38% increase of UPDRS-III scores over time.

Investigation of regional BOLD signal change over time during the fMRI motor task across time revealed significant reductions in key cortical and subcortical areas involved in the motor network (striatum, thalamus, motor cortices, DLPFC, somatosensory cortex). These findings were corroborated following extraction of regional time series data and no significant regional increases in BOLD signal were detected. Indeed, evaluation of time series data reveals that whilst all regions had a

reduction of activity, the caudate demonstrated a deactivation. The known connections between caudate and prefrontal areas and its role in goal directed movements, could explain the deactivation. The motor task completed by PD patients in the scanner required patients to view an external cue and purposefully initiate and complete a movement in a specific direction, thus possessed goal directed behavior. The greater difficulty experienced by patients to perform these movements as observed by the significant decline in behavioural performance appears to be reflected in the deactivation of a key region critical in both motor control and higher order executive functioning enabling goal directed behaviour. Furthermore, interrogation of clinical correlations reveals a significant negative correlation between percentage change of UPDRS-III with BOLD signal change in premotor, M1, SMA and somatosensory cortices, i.e. the greater decline in motor function correlates with a greater loss of BOLD signal over time. To date, the vast majority of fMRI studies of motor control in PD have been cross-sectional, change of amplitude studies. As previously mentioned, results have been varied and could be a reflection of heterogeneous samples, tasks implemented or an indication that multimodal imaging applications and/or analysis methods are required to fully elucidate the mechanisms underlying neural motor networks in PD. Prior to the current study, only one fMRI study has attempted to assess neural alteration longitudinally (Sen et al. 2010). Sen et al., investigated CTC motor circuitry in 5 PD patients over 2 years compared against 5 control subjects. It was reported that PD patients had an increased recruitment of CTC circuits during a motor task using the most clinically affected hand, that is, the side which was most clinically affected over 2 years required increased activity in CTC circuits to complete the tasks compared to the less clinically affected side which showed no changes compared to control subjects. Sen et al., concluded that this

evidenced compensatory mechanisms over time in CTC due to dysfunction in the striato-thalamo-cortical circuits. Although providing the first attempt of to assess neural motor network alterations as a function of disease progression, this study is limited through its small sample size and its inability to be certain the patient cohort had adequately withdrawn from medication. It is generally accepted that scanning PD patients following 12 hours post medication withdrawal (Quinn et al. 1996) is sufficient for patients to be in the practically defined 'OFF' medication state. The current study exceeding this by withdrawing from medication at least 18 hours previously (36 hours if receiving a prolonged-released form), we are confident that potential medication effects would be eliminated from effects on BOLD signal. Furthermore, the current sample size is larger than Sen et al., (n = 29 vs. 5) and covered a wider range of disease severity (UPDRS-III mean at baseline = 27 vs 4). The concept of connectivity between regions has provided a theoretical framework for identification of brain network interaction thus providing an additional source of information for identifying regional changes in magnitude of brain activity. PD induced modifications of brain networks have been explored in multiple studies (Rowe et al. 2002; Palmer et al. 2009). To date, only one study has investigated this in relation to self-initiated movements in PD (Wu et al. 2010). A reduced connectivity between striatal-cortical interactions and an increased connectivity between cortico-cerebellar structures was reported. Patients were performing the motor task at the same level as the healthy volunteers; therefore the authors hypothesised the increased connectivity to be a compensatory mechanism resulting from the striatal-cortico dysfunction. The current study demonstrates both increases and decreases of connectivity in the active motor network suggestive of a dynamic neural network, which may reflect compensatory mechanism initiation with significant decreases of

connectivity between caudate and SMA, M1 and premotor area which corroborate BOLD signal decreases in the regional amplitude analysis. These findings are in line with the caudate hypoactivation observed in the current regional amplitude analysis and highlight the importance of including multiple analysis techniques to further interrogate neural changes in the context of a network, as it is clear that brain regions do not act in isolation.

Rs-fMRI has shown promise as a technique for development of a neurodegenerative biomarker. A basal ganglia resting network has been previously identified as possessing the ability to differentiate PD from healthy controls (Szewczyk-Krolikowski et al. 2014) and recently the same network has provided evidence that resting state basal ganglia dysfunctions are specific to PD and not representative of a generalised neurodegenerative process (Rolinski et al. 2015). Despite the basal ganglia clearly playing a critical role in PD pathophysiology, when considering a relatively novel imaging modality (rs-fMRI), it is important to understand its dynamics on a larger scale in relation to the entire brain. The current study attempted to investigate resting connectivity of key motor regions, identified during the active motor task, thus, the resting motor network. Analyses revealed significant decreases in putaminal connectivity with M1 and somatosensory cortex and a trend toward increased connectivity of caudate with cortical regions that could be an indication of intrinsic brain networks attempting to compensate for the declining active motor network from caudate to cortical regions. However, it must be noted that the observed changes in the caudate were not significant and may be the result of spurious correlations in the rs-fMRI data due to the limited de-noising that was applied to the current dataset. Future studies should apply robust de-noising approached to the data prior to model-based analyses in rs-fMRI data. Previous rs-fMRI studies specifically

identifying motor networks through activation of motor networks in PD are lacking. Wu et al., (Wu, Long, et al. 2011) identified in 18 PD patients compared to 18 control subjects, altered connectivity between pre-SMA and M1 (increased), and between pre-SMA and putamen, insula, premotor area and IPL (decreased). The authors concluded that the disrupted connections represented a lack of readiness for movement and suggest that their findings are more pertinent in light of motor initiation rather than motor execution. The only study to report longitudinal changes of the resting motor network used whole brain functional ALFF (fALFF) over 2 years in 17 PD patients compared to 20 control subjects (Wang et al. 2015). The authors report increased ALFF in the right temporal and occipital gyri over 2 years and decreased ALFF in the cerebellum, striatum, thalamus, superior and inferior parietal lobule, precentral and postcentral gyri. These results are interesting, as they do not include the potentially expected primary or secondary motor areas.

The current study found decreased resting connectivity between putamen with M1 and somatosensory cortex. The putamen is located in a key position in the basal ganglia circuit which is responsible for the effective initiation and execution of movements. The significant decrease of putaminal-M1 connectivity in our cohort over time fits in with basal ganglia models of PD an well as previous studies reporting similar less functional synchronization of the putamen in PD at cross-sectional level (Wu & Hallett 2005).

It is clear that the body of work currently existing for regional amplitude alterations and functional connectivity in PD is complicated to interpret and certainly requires further studies to define network interactions and effects of disease on these interactions. Our findings add to the general view that the PD pathological process interrupts regional functional connectivity as seen by the loss of significant functional

connectivity between caudate and cortical motor regions in the active state, the trend toward regaining connectivity in the resting state and significant loss of connectivity between putamen and cortical regions in the resting state. This study serves to increase sensitivity compared to previous studies due to the longitudinal design and to highlight the importance of multimodal imaging and multiple analysis approaches to a data set. The current study is limited by the lack of whole brain analyses and/or region of no interest to control for potential nonspecific changes over time. Future studies should consider this.

Currently, a wide range of methodological approaches for functional connectivity analysis exist which are yet to be tested in large cohorts or across a wide variety of disease stages to allow clear identification of the optimal approach. Thus, further validation of these methodologies and the current findings of active and resting motor networks in PD are required.

# CHAPTER 5: LONGITUDINAL CHANGES IN DIFFUSION OVER TIME

## 1. Introduction

DTI provides a non-invasive in vivo method to estimate diffusion metrics. Neurodegenerative cell loss results in a loss of diffusion barriers and orientational dependence, thus DTI is a useful method to assess neurodegenerative processes. Multiple DTI studies have attempted to clarify its use as a biomarker for PD (Yoshikawa et al. 2004; Péran et al. 2010; Rolheiser et al. 2011; Vaillancourt et al. 2009). To date, no study has systematically assessed multiple groups of PD across various disease stages or followed patients over time. However, there have been attempts to identify an index of diffusion that correlates with disease severity. Chan et al., (2007) reported an inverse correlation of nigral FA with disease severity and no significant differences of FA in any other basal ganglia structure (Chan et al. 2007). Further FA alterations have been reported in established motor circuit regions: SN, putamen, thalamus, M1, premotor area and SMA and somatosensory areas that significantly correlated with disease severity (Zhan et al. 2012). Conversely, further reports did not find a correlation between disease severity and diffusion indices (Vaillancourt et al. 2009; Menke et al. 2010; Du et al. 2011), thus leading to a debate regarding the potential for DTI to be a reliable technique for tracking disease progression or its use as a biomarker. This debate is solidified in two recent systematic reviews (Cochrane & Ebmeier 2013; Schwarz et al. 2013) with opposing conclusions.

Attempts to characterise extra-nigral diffusion indices have also resulted in variable findings. FA reductions in corpus callosum genu and superior longitudinal fasciculus and MD increases in the same areas have been reported in early stage medicated PD

patients (Gattellaro et al. 2009). FA reduction in gyrus rectus has been reported (Ibarretxe-bilbao et al. 2009) as well as FA reductions and MD increases in motor and frontal cortices (Zhan et al. 2012) and track density indices were found to be increased in regions associated with the motor circuit (Ziegler et al. 2013). However, other studies have failed to find significant differences of extra-nigral FA or ADC in the striatum and thalamus (Chan et al. 2007), or FA and MD in corpus callosum and cingulum (Wiltshire et al. 2010). Kim et al. (2013) employed TBSS and VBA and report no significant differences of FA in PD patients compared with healthy controls (Kim et al. 2013). Increased MD was reported in striatum, pallidum, thalamus, cingulum and fornix. Zhan et al., (2011) used VBA to identify a reduction of FA in the cerebellum and increased MD in the orbital-frontal cortex and inferior temporal gyrus (Zhan et al. 2012).

DTI offers a promising technique to understand changes in brain microstructure in neurodegenerative disease and much is known about nigral FA in PD, however it is not clear how diffusion indices progress over time and their relevance to the progression of clinical symptomatology in PD. Here, we have undertaken a longitudinal DTI study in 18 PD patients followed up over 19.8 months. This study aims to assess how FA and MD in the substantia nigra and striatum change over time as a consequence of early disease progression using a manual delineation ROI approach and VBA.

## 2. Aims

- To examine nigro-striatal diffusion microstructure in PD patients over time.
- To assess whether alteration in nigro-striatal microstructure correlate with clinical symptomatology.

## 3. Hypotheses

It is hypothesised that measures of diffusion (fractional anisotropy, FA and mean diffusivity, MD) will be significantly altered over time and that motor control in PD patients will be significantly correlated with diffusion measures.

## 4. Subjects and Methods

### 4.1 Patients

Eighteen non-demented patients with idiopathic PD (Hughes et al. 1992) were studied with a longitudinal two-scan DTI protocol (mean: 19.5m between scans; standard deviation, SD: 3m). These 18 patients were selected from a possible 43 patients. Twenty-five patients were excluded due to poor data quality (high signal dropout in frontal sinuses area and motion artefacts). The clinical assessment battery included the motor part (Part III) of Unified Parkinson's Disease Rating Scale (UPDRS), Mini-Mental Sate Examination (MMSE) and calculation of daily L-dopa-Equivalent-Dose (LED) (Table 9). A larger sample size would be desirable, however, using a longitudinal design will increase power.

Table 9. Patient characteristics in the DTI study.

| | **PD Baseline** | **PD Follow-up (When?)** | ***P* value** |
|---|---|---|---|
| Number of Subjects | 18 | 18 | - |
| Age (years ± SD) | 56.8 ± 6.8 | 58.3 ± 6.8 | - |
| Sex | 12M/6F | 12M/6F | - |
| Disease Duration (years ± SD) | 3.9 ± 2.2 | 5.5 ± 2.2 | - |
| UPDRS OFF motor (Part III) score (mean ± SD) | 26.2 ± 9.2 | 34.6 ± 12.5 | P = 0.0003 |
| % change in UPDRS OFF motor score (mean ± SD; range) | 28.6 ± 24.9%; 0 – 80% | | P = 0.0002 |
| MMSE (mean ± SD) | 29.6 ± 0.6 | 29.7 ± 0.6 | P = 0.4 |
| Daily $LED_{TOTAL}$ (mg ± SD) | 442.4 ± 245.6 | 564.0 ± 286.9 | P = 0.008 |

*Patient characteristics from visit 1 to visit 2 showing significant increases in UPDRS-III OFF scores, and LED. * Paired t test; m= months; SD = standard deviation; UPDRS-III = Unified Parkinson's Disease Rating Scale Part III; LED = Levodopa equivalent dose; MMSE = mini mental state examination.*

## 4.2 Scanning procedure

Subjects were scanned on two separate mornings (between 10.00 and 13.00 h) on average, 19.5 months apart. All subjects were scanned in the practically defined 'OFF' condition having withdrawn from medication at least 18 h previously (or 36 h if receiving a prolonged released form). Image acquisition for DTI was conducted as per the descriptions detailed in Chapter 2.

## 4.3 ROI delineation

Caudate and putamen were manually drawn on the FA map using the co-registered T1-weighted image of the selected individual for anatomical guidance. SN was drawn manually on the co-registered B0 (T2) image for guidance (Figure 16).

## 4.4 Image analysis

All data were analysed with two approaches: manual ROI analysis and VBA.

ROI analysis was conducted using ExploreDTI and TrackVis. Data were converted from DICOM (Digital Imaging and Communications in Medicine) to NifTI (Neuroimaging Informatics Technology Initiative) format. In ExploreDTI, bvec and bval files were generated and converted to B-matrix text files (128 x 128 x 70). DTI.mat files with the scanner parameters and b-matrix information were created which output the MD, FA maps for each subject. Eddy-current motion correction was applied to the data. ExploreDTI data were converted to TrackVis data via a code executed in Matlab (NBL_ExpDTi2TrakV (0, 'T',2,[])). MD and FA maps were then visualized in TrackVis to allow delineation of our ROIs. Our a priori hypothesis dictated the putamen, caudate nucleus and SN as ROIs. Two experienced raters (C. Loane and another imaging scientist) drew all ROIs manually on both the MD and FA

maps for each subject. Data was re-coded to ensure both raters were blind to the subject and visit information of each scan. The interrater reliability was Kappa = 0.68 ($p < .0.001$), 95% CI (0.504, 0.848).

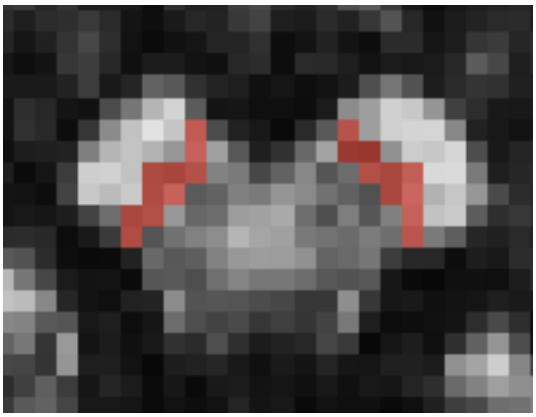
VBA was used to compare MD and FA maps between groups. All FA and MD maps were aligned using FMRIB's Nonlinear Registration Tool (FNIRT) with a threshold of 0.2 to exclude peripheral tracts with significant inter-subject variability and/or partial volume effects with GM. Following spatial normalization, the FA and MD maps were smoothed with 8mm isotropic Gaussian kernel to reduce noise and correct misalignments.

4.5 Statistical Analysis

Statistical analyses for FA/MD clinical correlates and clinical and demographic data were performed using SPSS (version 16, SPSS Inc) for Macintosh. Comparisons within groups were performed using paired t-tests.

Statistical comparisons for VBA were performed using statistical parametric mapping (SPM12, http://www.fil.ion.ucl.ac.uk/spm) and paired t tests between baseline and follow-up visits. An uncorrected $p<0.001$ at voxel level for multiple comparisons and a cluster extent of 20 voxels was used.

Figure 16. Substantia Nigra ROI placement.



*Example of a DTI scan of a patient and substantia nigra ROI placement. ROIs defined by two scientists blinded by visit number and patient ID. The interrater reliability was Kappa = 0.68 (p <.0.001), 95% CI (0.504, 0.848).*

## 5. Results

### 5.1 Clinical changes

UPDRS-III scores had significantly declined over 19.8 months (mean change of 28.6 % on UPDRS-III; p=0.0003) and LED significantly increased (average increase of 121.6mg; p=0.0002). MMSE remained unchanged and within normal limits over time indicating no decline in cognitive functioning. No other significant health concerns were reported by the subjects at follow-up.

### 5.2 ROI Analysis

Regional MD values were stable in caudate (1.1 vs 1.1; p=0.4) and putamen (0.7 vs 0.7; p=0.2) but significantly increased in SN (0.3 vs 0.9; p=0.01) from baseline to follow-up. Similarly, FA values remained stable at follow up in caudate (0.188 vs

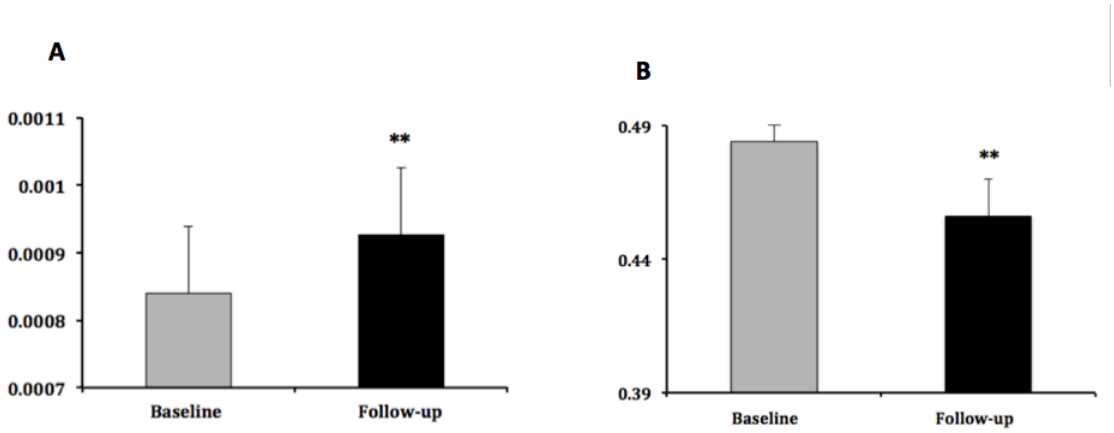
0.183; p = 0.3) and putamen (0.22 vs 0.22; p = 0.2) but significantly reduced in SN (0.48 vs 0.45; p=0.008) (Table 10, Figure 17).

Table 10. Diffusion indices from ROI analysis

| | Baseline | | | Follow-Up | | | P value |
|---|---|---|---|---|---|---|---|
| | Caudate | Putamen | SN | Caudate | Putamen | SN | |
| FA ± SD | 0.18831 ± 0.0519 | 0.2221 ± 0.028 | 0.4839 ± 0.048 | 0.1833 ± 0.0481 | 0.2254 ± 0.0281 | 0.4561 ± 0.0451** | **0.008[a] |
| MD ± SD | 1.1 ± 0.3 | 0.76 ± 0.1 | 0.83 ± 0.2 | 1.1 ± 0.3 | 0.75 ± 0.04 | 0.93 ± 0.13* | *0.014[a] |

Diffusion indices over time form visit 1 to visit 2 in caudate, putamen and SN. Showing significant decline in FA and MD in the SN. [a]paired t test; SD = standard deviation; FA = fractional anisotropy; MD = mean diffusivity (displayed 10(-3); SN = substantia nigra. Values are mean from rater 1 and rater2 .

Figure 17. Alteration of nigral diffusion indices in PD patients over time.



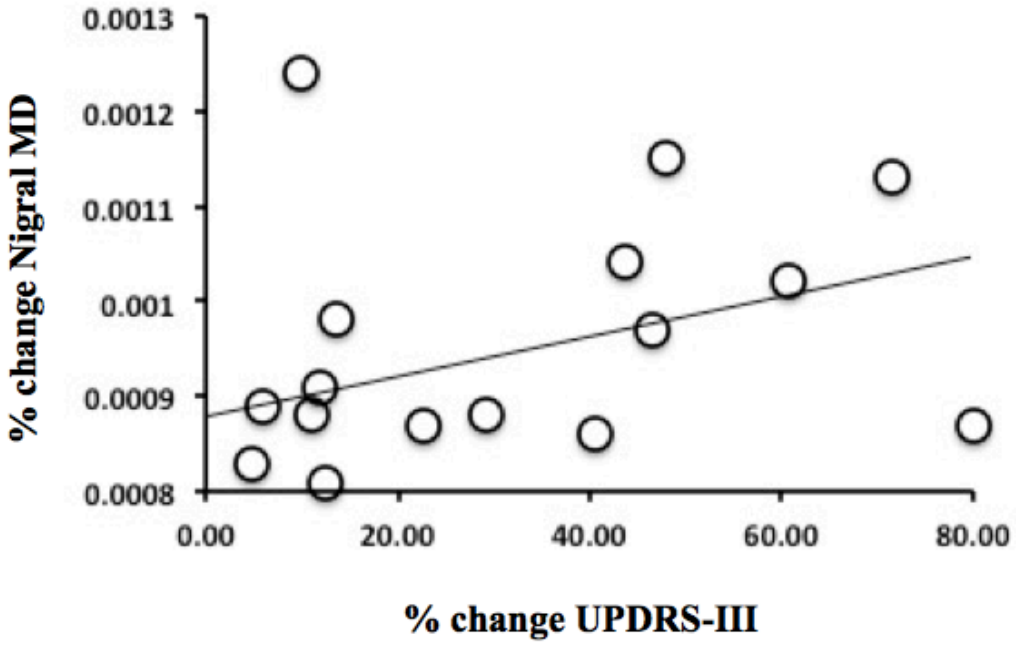

*Alteration of nigral diffusion in PD patients from visit 1 to visit 2 showing significant increases of nigral FA and significant decreases of nigral MD. A : Mean nigral MD values for PD patients at baseline and follow-up. ** = p< 0.01, paired t test. B: Mean nigral FA values for PD patients at baseline and follow-up. ** = p< 0.01, paired t test. MD = mean diffusivity; FA = fractional anisotropy.*

## 5.3 Clinical Correlations

Nigral MD values at follow-up significantly correlated with % increase of UPDRS-III from baseline to follow-up ($r = 0.39$, $p = 0.05$) (Figure 18). No significant correlation was found with caudate or putamen MD.

Nigral, caudate or putamen FA values at follow-up did not significantly correlate with increase of UPDRS-III.

Figure 18. Correlation between nigral MD and % change of UPDRS-III at follow-up.




*Significant correlation for % change nigral MD with % change of UPDRS-III change from visit 1 to visit 2 in PD patients. r = 0.39, p = 0.05; UPDRS = Unified Parkinson Disease Rating Scale, Part III; MD = mean diffusivity.*

## 5.4 VBA

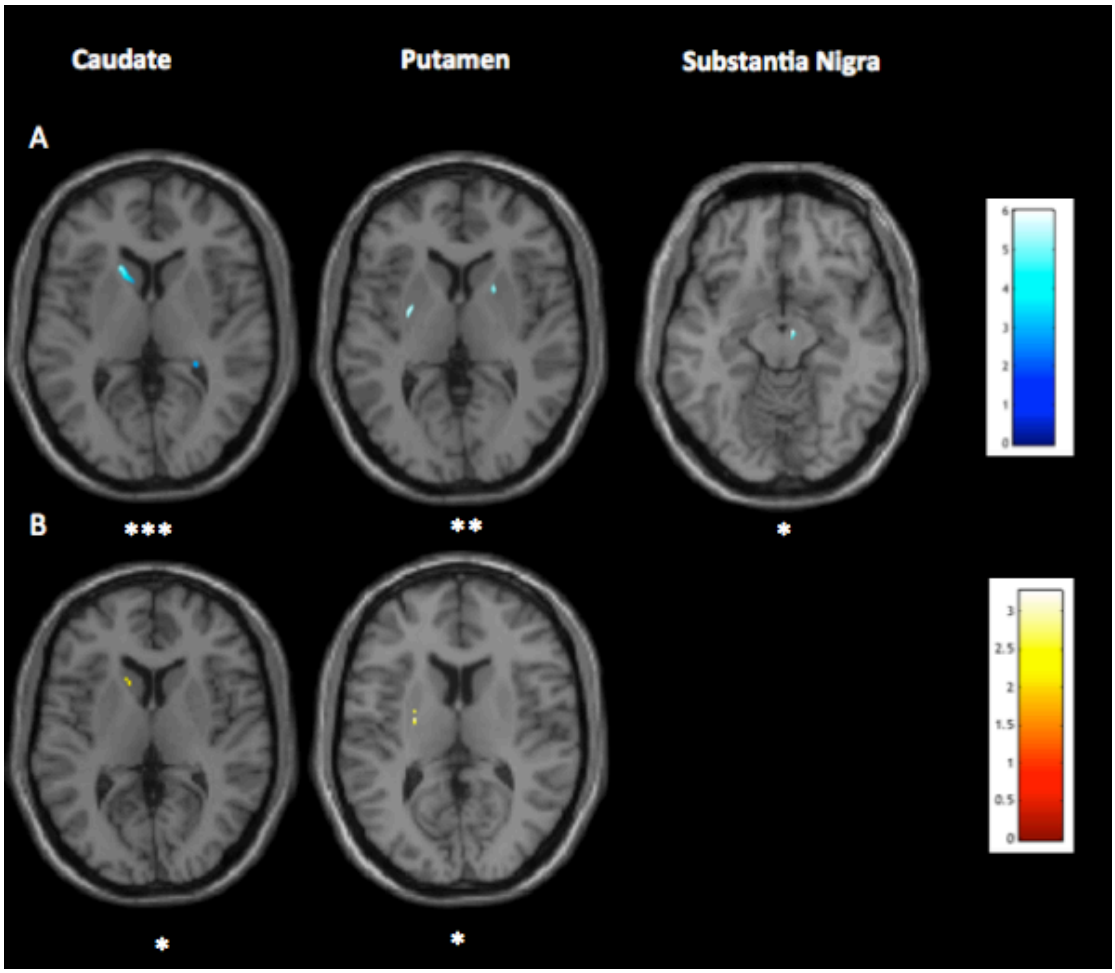
There were significant FA reductions within left caudate, bilateral putamen and right SN in the PD patients at follow-up compared to baseline. Significant increases in MD were detected in left caudate and left putamen but not in SN (Table 11, Figure 19).

Table 11. VBA of FA and MD over time in PD patients

| Diffusion Index | Region | MNI | Z score | P value [c] |
|---|---|---|---|---|
| FA[a] | Caudate | -16, 18, 5 | 4.33 | 0.001 |
| | Putamen | 21, 9, 3 | 2.73 | 0.01 |
| | SN | 7, -12, -10 | 2.35 | 0.05 |
| MD[b] | Caudate | 6, 8, 2 | 1.79 | 0.05 |
| | Putamen | -28, -6, 14 | 2.21 | 0.05 |
| | SN | - | - | ns |

*VBA results showing significant changes in FA within the caudate, putamen and SN and significant changes in MD within caudate and putamen. [a] thresholded at 20 voxels, [b] thresholded at 10 voxels c paired t test; SD = standard deviation; FA = fractional anisotropy; MD = mean diffusivity; SN = substantia nigra.*

Figure 19. Significant regional alterations of diffusion indices in PD patients.




*Significant changes detected by VBA in FA and MD in the PD patients from visit 1 to visit 2. A = Transverse sections of parametric maps showing significant FA decreases (blue-white) in PD patients over time: left caudate***; bilateral putamen**; right substantia nigra*. B = Transverse sections of parametric maps showing significant MD increases (red-yellow) in PD patients over time: left caudate*; left putamen*. Colour bar indicates z scores. * = p < 0.05; ** = p < 0.01; *** = p < 0.001, cluster corrected, thresholded at 20 voxels for FA and 10 voxels for MD.*

## 6. Discussion

Using manual ROI analysis and VBA microstructural changes of subcortical grey matter in patients with PD over time were investigated. Here we have demonstrated alterations of both nigral FA and MD with the latter correlating with percentage change of UDPRS-III scores indicating increased disease severity. With VBA, significant regional decreases in FA within the SN and striatum as well as significant increases of MD within the striatum were demonstrated

The current cohort can be considered relatively mild regarding disease severity (mean disease duration and UPDRS-III at baseline: 3.9 years, 26.2 and at follow-up: 5.5 years, 34.6), which is in line with most previous cohorts studied with DTI. As such, we consider our results as a novel extension of previous reports of nigral FA and MD alterations through our longitudinal study design, which considers disease progression. Identifying the nature of early progression in PD is vital for the generation of suitable imaging biomarkers.

Our findings of striatal alterations of diffusion are in line with concepts demonstrated in previous PET reports (Playford et al. 1992) and are likely related to the progressive degeneration of nigrostriatal DA neurons. Previous DTI reports of striatal diffusion in PD are less consistent. Microstructural degradation in the striatum has been reported, particularly the increase of MD (Péran et al. 2010; Kim et al. 2013) in PD patients. Conversely, other studies failed to find alterations within the striatum and report white matter alterations in fibre bundles such as the genu of the corpus callosum and superior longitudinal fasciculus (Gattellaro et al. 2009)and frontal areas (Karagulle Kendi et al. 2008).

Nigral diffusion alterations have been investigated in slightly more detail and although there are conflicting reports, it appears that a decrease of FA and increase of

MD is the prevailing conclusion of microstructural alterations in PD. Decreases of nigral FA have been demonstrated in several studies (Vaillancourt et al. 2009; Rolheiser et al. 2011; Chan et al. 2007). To date only two studies have identified a significant correlation of nigral FA and disease severity (Chan et al. 2007; Zhan et al. 2012). Here, we also failed to find a significant correlation with our nigral FA changes over time. This is in line with previous lack of correlation (Vaillancourt et al. 2009; Menke et al. 2010; Du et al. 2011) and may indicate that nigral FA alterations do not possess the predictive power to track disease progression in PD. A recent meta-analysis highlights the problematic nature of using nigral FA as a predictor for PD pathology stating a high degree of variability in the published reports of nigral FA changes (Schwarz et al. 2013). The same meta-analysis reported a case control study that failed to identify nigral FA changes but did report significant nigral MD increases. These increases were detectable only following an ROI analysis and not with VBA. Similarly, we were unable to detect nigral MD alterations with VBA. The differences between differing analysis methods are not clear however, it seems that VBA is less sensitive at detecting alterations of microstructural indices with previous studies also failing to replicate, or require liberal thresholds to confirm ROI or TBSS findings with VBA (Rae et al. 2012). Furthermore, due to variability in normalisation procedures for FA and MD maps, partial volume effects in the SN (sue to its small size) and striatum (due to the internal capsule) could lead to inconsistent findings. Here, we detected differences only with statistically thresholds and not more stringent corrections, thus VBA results should be treated with caution.

However, considering the importance of subcortical structures in PD, it is rational to omit TBSS, which is more suitable to the assessment of white matter regions and fibre bundles. Nonetheless, methodological differences in study planning, scan acquisition,

analysis methods need to be elucidated to ensure the variance of results of studies is reduced. Further inconsistencies may arise due to subject characteristics and small sample sizes.

Unlike Schwarz et al., (2013), our nigral MD alterations were significantly correlated with percentage change of UPDRS-III over time. Previous studies generally report a marginal increase in MD but lack clinical correlates. It is known that MD can distinguish atypical parkinsonisms from PD (Blain et al. 2006; Schocke et al. 2002; Seppi et al. 2003) thus our finding indicates that nigral MD may suggest a microstructural change as a direct result of disease progression. This is the first report of a microstructural clinical correlate in PD.

Our study used DTI to assess microstructural alterations in important subcortical areas in PD pathophysiology. We show that there are significant decreases of FA and increases of MD in the SN and striatum of relatively mild PD patients followed over time. Furthermore, we demonstrate a longitudinal clinical correlation of nigral MD and disease severity. These results provide for the first time, valuable information of the microstructural changes in the PD brain progressing over time. Further longitudinal studies are required to elucidate if our findings are consistent in larger sample sizes before a consensus on the use of DTI as an imaging biomarker in PD can be concluded.

# CHAPTER 6: DISCUSSION

## Discussion and future directions

### 1. Summary of Key Results

PD is a common and debilitating neurodegenerative motor disease, which is known to result from the loss of DA-ergic neurons in the SN extending to the striatum and cortical regions as the disease progresses. Neuroimaging techniques have been applied to study the PD brain in relation to its motor deficits and have revealed relatively consistent findings of loss of amplitude activation in key motor related brain regions. However, it is not clear how the structural and functional connectivity between these regions are affected in the disease and if any compensatory mechanisms are in place, which would aid understanding of the disease processes, its effect on motor symptomatology or provide potential information for future interventional clinical trials or treatment guidance. Moreover, the study of PD over time has been lacking in the literature and limits understanding of how PD brain networks are affected as a function disease progression within subjects. Recent advances in neuroimaging techniques and methodological approaches have allowed scientists to investigate brain networks, not only during task-based activities but also at rest, thus assessing the intrinsic neural activity of an individual's brain. Diffusion MRI has also permitted the assessment of brain microstructure previously not possible in the living brain.

This body of research set out to investigate in a comprehensive, multimodal fashion, how motor networks are affected in PD both in relation of activated and resting connectivity (Chapters 3 and 4) as well as microstructure (Chapter 5).

In Chapter 3, I conducted a cross-sectional study in four groups of PD patients divided according to disease burden (n = 19 each group). All patients underwent a

baseline scanning session involving a motor task-based fMRI and rs-fMRI. In-scanner behavioural data was also collected to assess motor execution and motor amplitude performances. One of the most important findings from Chapter 3 is that PD patients appear to possess compensatory mechanisms coming into effect while disease burden is still relatively low. Here, due to the collection of in-scanner behavioural data it appears that the compensatory mechanisms are more likely a function of motor reserve rather than a mechanism permitting enhanced motor functioning compared to patients with higher disease burdens. The increased amplitude activity and connectivity in both the task based and resting state motor networks indicate interplay or dependency between the intrinsic and activated neural networks. For instance, PD patients with low disease burdens appear to have generalised dysfunctional connectivity across both neural networks. As the disease burden increases, the activated motor network compensate for the increased difficulty in performing the task, which is only evident in the resting motor network later on.

In Chapter 4, I conducted a longitudinal study of Chapter 3 in a sub-set of patients. Twenty-nine PD patients returned for a follow-up scanning session approximately 19.8 months after baseline.

Similarly, following PD patients over time indicates that the activated and resting motor network possess a dynamic in general opposition to each other. The exact underlying reason for this neural behaviour requires further investigation with larger sample sizes and a wider range of disease burdens followed over time. Nonetheless, these findings suggest dynamic neural systems in PD that appear to be making attempts to cope with the disease processes.

Finally, Chapter 5 presents longitudinal DTI data in eighteen PD patients. This study demonstrates significant alterations of nigral FA and MD measures over time and that nigral MD alteration is significantly correlated with % change of UPDRS-III. This study did not detect any significant changes or clinical correlations with striatal diffusion measures suggesting that alterations within the SN may be a better indicator of disease processes in PD.

**2. Compensation mechanisms in PD motor networks**

It is known that the pathophysiological processes of PD lead to altered activations in motor related regions as measured by fMRI. Previous studies have typically used regional BOLD signal changes in PD compared to healthy controls or other non-PD patient groups, thus assessment of connectivity between motor related regions is lacking. Furthermore, investigations of compensatory mechanisms or motor reserve capacity are lacking.

The use of sequential motor tasks, which focus on motor planning and execution, appear to be particularly well suited for studying compensatory mechanism. Previous reports demonstrate a relative increases in premotor and parietal activity compared to controls using both fMRI (Sabatini et al. 2000) and PET techniques (Samuel et al. 1997). These effects are generally interpreted as a compensatory effect to counterbalance the defective striato-frontal motor circuits. Motor deficits in PD patients appear to be improved when provided with external cues, thus it has been hypothesised that compensation effects can be observed following additional processing such as enhanced attention (Bloem et al. 2004). Compensatory mechanism may be interpreted at a neuronal level i.e. synaptic plasticity or systems level i.e. neural changes supporting a cognitive processes. Degeneracy is a term used to

describe compensation as occurring due to the ability of the elements of a circuit to reorganize in order to yield the same output (Edelman & Gally 2001). Degeneracy may provide an explanation why a profound number of DA-ergic neurons within the SN can be lost prior to the onset of symptoms. For instance, the PD brain may possess the ability to engage other brain regions within the motor network or in neighbouring regions thereby preserving the behavioural, functional output. A report of increased connectivity between cingulate and premotor area in presymptomatic gene carriers of PD indicates that compensatory mechanisms may well be in place before symptomatic disease (Buhmann et al. 2005).

The current thesis presents data, which indicates compensatory mechanisms are in place within both the active and resting motor network. The current data would also suggest that investigations of functional connectivity are particularly important to understand the dynamic alterations of the PD brain in response to pathophysiological processes. For instance, Chapter 4 reports the active motor network demonstrating only significant decreases in regional BOLD signal change over time, whereas the functional connectivity analysis demonstrates a trend towards reorganisation of connectivity relationships. It is currently unknown whether compensation occurs at a particular stage of PD i.e. once a certain number of DA-ergic a loss or whether it is a process initiating at early disease stage or even pre-symptomatically. The current thesis suggests both the active and resting motor networks are continuously undergoing dynamic alterations in an attempt to cope with disease processes. Defining the nature of compensation in PD motor networks may have a significant impact on therapeutic intervention. Indeed, in the case that the PD brain is employing mechanisms to overcome the pathophysiological processes and recruiting less affected, unaffected brain regions to maintain functional output then it would be

sensible to consider focusing therapeutic interventions not on the neurons that are lost but those which survive.

The behavioural in-scanner data contained in the current thesis would point toward a situation whereby the PD brain is re-recruiting motor related regions to maintain motor performance.

**3. Studying networks longitudinally**

Although diagnosis of PD is primarily a clinical decision, neuroimaging is a promising tool for early disease detection and measure of disease progression. Advances in neuroimaging techniques have enabled detection of alterations in diffusion properties, anatomical and functional connectivity as well as neural-clinical correlates. However, literature to date has been lacking in relation to studying regional and networks changes over time, thus defining the effect disease processes have on neural mechanisms, either pathological or compensatory. Thus, current cross-sectional findings, although opening the door to understanding intrinsic changes to neural networks in PD compared to the non-PD brain must be viewed with caution as without robust longitudinal studies, results may reflect pathological effects, compensatory mechanisms or indeed medication effects in the cases whereby subjects are scanned ON medication or failed to withdraw adequately.

The results presented in this thesis confirm the importance of using a longitudinal design to investigate the dynamics of motor networks in PD as a function of disease progression. Both the active and resting motor networks in a sizable sample (n = 29) demonstrated that both increases and decreases across the motor network are altered over a period of approximately 19 months in a group of relatively mild–moderate PD patients. Using traditional regional amplitude measures of BOLD signal changes, only

significant decreases were detected across the motor network in the active state as a function of disease course. However, assessment of functional connectivity in both the active and resting networks indicates that compensatory mechanism may well be in place. It is likely that a larger period of time is required between follow-up or a third follow-up is required to detect significant increasing alterations to confirm compensatory mechanisms. These longitudinal results are preliminary and form part of an on-going study within TransEuro whereby completion of the second follow-up and initiation of a third follow-up scan is planned within the next 12 months in more than 40 PD patients. It is expected that increasing the sample size as well as the period of time between the baseline scan will be critical in revealing robust compensatory mechanisms serving as a motor reserve capacity to cope with disease progression and increasing symptomatology.

**4. Nigral diffusion indices in PD**

Conclusive evidence supporting the use of diffusion measures as a biomarker for PD is strongly awaited to aid premotor diagnosis and perhaps the development of disease-modifying therapies. However, the relationship between diffusion parameter alteration and clinical symptomatology such as motor dysfunction is not clear. There are some evidence of using diffusion measures to quantify disease processes in PD, although there are debates in the literature regarding the reliability of diffusion measures such as FA and MD at capturing the microstructural changes of motor pathways. The study presented in Chapter 5 is the first to follow a group of PD patients over time to investigate nigro-striatal changes in FA and MD in PD. It is concluded from this study that measures of nigral MD may be a better predictor of diffusion related alterations due to disease processes than nigral FA or striatal

diffusion indices. It is appreciated that due to the small sample size and perhaps less than optimal acquisition sequence, these data should be considered as preliminary and further studies should seek to improve sample size and scanning protocols.

## 5. Limitations of thesis studies and building on the current work

### 5.1 Limitations of current studies

The current studies have provided information regarding the alteration of motor brain networks in PD. In particular, the potential compensatory reserve capacity of the PD brain to cope with difficulties performing movements due to disease processes has been highlighted. However, these studies have been limited by a number of factors:

- **Sample size**: Although sample sizes in Chapter 3 were reasonable, future studies should aim to increase them for power and sensitivity at cross-sectional level. Similarly, despite increased sensitivity due to a longitudinal design, fMRI results, in particular robust identification of compensatory mechanisms in Chapter 4 could potentially be enhanced and with a larger sample size. Chapter 5, certainly requires larger sample sizes to delineate diffusion property alterations over time.
- **Comparable samples:** In order to fully investigate structure-function relationships in a true multimodal fashion, comparable sample sizes for both modalities are required. In this thesis, diffusion data were available for fewer patients due to compromised data as discussed below. In order to increase power for multimodal fMRI-DTI comparisons, future follow-up data as part of the on-going TransEuro study will provide a larger sample size enabling these analyses.

- **DTI sequence protocol:** Unfortunately, only a single b0 was collected during data acquisition. B0 images enable division of baseline signal of tissues and remove sources of signal variance, such as movement. Due to the nature of PD, movements during the DTI scan lead to a loss of signal in frontal brain areas. As such, a large proportion of the data were compromised and deemed invalid for analysis purposes. As previously mentioned, further data will be acquired with the aim of increasing the useable data set.

## 5.2 Considerations for building on the current studies

Based on the above limitations, there are several improvements that could be made to future studies intending to build on the work presented here.

First and foremost, as with all neuroimaging studies, sample sizes should be increased. This is particularly pertinent for the cross-sectional fMRI motor study and DTI study. The former has a reasonable number of subjects per group (n=16) however, due to the cross-sectional design, multiple comparisons across groups consisting of a larger number of subjects per group would increase power and lead to more reliable results. Furthermore, the ability to then confirm results found with a longitudinal design (such as that conducted in Chapter 4) would be increased. The current DTI study (Chapter 5) was a longitudinal design, which in itself increases power however, the sample size of n=18 which could be considered a small study, increases the possibility of reported averages, standard deviations and effect sizes being quite variable and affecting results. Secondly, future studies should include not just ore PD patients, but patients with a wider range of disease severity. The current studies focused on relatively early PD thus later disease processes could not be considered.

Future studies should also consider including additional and alternative methods when for functional connectivity analyses. Here, seed ROI correlation analyses were used and although this was justified due to the strong *a priori* hypotheses, this approach can be prone to detecting spurious correlations when sufficient de-noising is not implemented. A relatively new method of de-noising which models the motion, physiological (if data collected at the time) and scanner artefacts can be regressed out leaving behind data which is a more 'true' representation of BOLD signal (FMRIBs ICA-based Xnoiseifier; FIX). Applying such a tool on the current dataset would have produced cleaner and more reliable results. However, FIX is predominately designed to deal with rs-fMRI data and although theoretically can be applied to task data, the group have not announced any testing or documentation of using this method for task data. Another approach that could be considered in future studies is that of effective connectivity. Ultimately the aim of the functional connectivity analyses is to make claims regarding causality. Several approaches maybe taken to achieve this: structural equation modeling and dynamic causal modeling for example. However, there are challenges to casual inference in fMRI data such as the size of the model space. To complete an exhaustive search of the entire model space for all possible relationships between regions, is impossible with modern computers and as such, a portion of the model space can be interrogated only.

Future studies should consider the influence of medication more closely in particular when considering longitudinal studies. It is logical that as disease severity increases with time, so does LED in patients. How this increase of mediation interacts with the measured BOLD signal has not been investigated in the current studies and should be considered in future.

The current studies detected increases in activity within many motor related regions, which are also part of the attention network. Due to PD patients experiencing increasing difficulty of motor performance, it may be possible that increases are due to an increased load on the attention network not only due to a motor reserve capacity. This aspect was unexplored in the current studies but future studies could easily include an attention cue during the motor task to model this aspect into the analysis design.

## 6. Implications for future research

*Multimodal imaging studies*

Unimodal imaging studies are still the predominant method to assess brain changes in PD. However, advances in neuroimaging techniques, which permit investigation of the interplay between anatomical, functional and physiological alterations in the diseased brain, and should lead to greater understanding of structure-function relationships. To date, no study has been undertaken to combine multimodal technique to investigate motor control in PD. The closest has been conducted by Wu et al., (Wu et al. 2012) who used task-based fMRI to identify ROIs for investigation of the resting network. Correlational analyses are an important element of multimodal studies with distinction between pure correlations and predictive correlations such as multivariate regression, which are restricted to linear observations and may miss important information regarding non-linear connectivity. Structural equation modelling also assumes the interactions are linear and, furthermore, instantaneous in the sense that structural equation models are not time-series models. Dynamic causal modeling is an alternative to these approaches by accommodating the nonlinear and dynamic aspects of neuronal interactions. Causal or explanatory

variables that comprise the conventional design matrix become the inputs and the parameters become measures of effective connectivity. As such, non-linear interaction between modalities could be included in the design making integration of modalities within a study more comparable. Finally, there has been an increased interest in dynamic bivariate correlations in quantifying possible dynamic changes in FC during fMRI experiments, as it is thought that this may provide insight into the fundamental workings of brain networks. In this work we focus on the specific problem of estimating the dynamic behaviour of pair-wise correlations between time courses extracted from two different regions of the brain.

It is clear that much work remains to be done in order to characterize the promising multimodal approaches. It is helpful to consider unimodal results in comparison to multimodal approaches. In this thesis, a multimodal approach has been attempted, although results of individual modalities have not been directly integrated, i.e. with dynamic causal modeling. A number of study limitations did not allow this within the realm of this thesis and was discussed earlier. Although, this thesis presents for the first time three concurrent imaging techniques with the same endpoint; alteration of brain motor networks due to disease processes.

*Characterisation of a prodromal PD*

PD is a progressive neurodegenerative disease that is characterized by DA depletion. By symptom emergence, invariably approximately 70% of nigral DA neurons will have been lost (Fearnley & Lees 1991). Thus, it is supposed that the loss of these neurons begins perhaps up to 10 years prior to symptom onset. As such, interventions within a prodromal stage of PD may well lead to progression slowing as well as prevention of cardinal symptoms. Using neuroimaging to define biomarkers is

paramount to enabling early PD diagnosis. By fully elucidating the natural course of motor network alteration in PD, on could potentially use a top-down approach to inform preliminary stages of network alteration in a prodromal stage of PD. For instance, this thesis has attempted to comprehensively assess the motor network and should form a basis for future studies to elucidate the staging of motor network dysfunction in both the active and resting brain state as well as from a regional and connectivity point of view. Here, it is demonstrated that in general, inter-motor cortices connectivity significantly declines during earlier disease burdens with striato-cortico connectivity appearing the be the first regions to indicate compensatory changes.

*Implementation of 'well-timed' therapy*

A key aspect of identifying a prodromal PD and for defining periods during established disease progression whereby compensatory reserve processes are initiating, serve to inform the existence of 'windows of opportunities' for future targeted therapies. This may well take the form of timing the introduction or dosage increase of DA-ergic therapies to derive the most benefit or inform new neuro-protective therapy development.

*End-point chatracterisation in clinical trials*

Using neuroimaging techniques to form part of end-point definition in clinical trials has been a mainstay for restorative therapies. Typically, invasive $^{18}$F-Dopa PET imaging has been implemented as the gold standard for measuring DA-ergic function and restoration following surgical interventions. However, to define functional alterations using fMRI will enable cheaper, non-invasive end-point methodology.

Non-invasive MRI techniques have the potential to assess restoration of brain activity during movement and of the structural and functional connectivity changes. As always, definition and characterisation of the motor networks change sin PD must be established prior to the sole use of MRI techniques as clinical trial end-points. However, combination of PET and MRI techniques should lead to better scheduling, monitoring, and modification of clinical outcomes.

**References**


Bammer, R. & Bammer, R., 2003. Basic principles of diffusion-weighted imaging. *European journal of radiology*, 45(3), pp.169–84.

Basser, P.J., Mattiello, J. & LeBihan, D., 1994. Estimation of the effective self-diffusion tensor from the NMR spin echo. *Journal of magnetic resonance. Series B*, 103(3), pp.247–254.

Baudrexel, S. et al., 2011. Resting state fMRI reveals increased subthalamic nucleus-motor cortex connectivity in Parkinson's disease. *NeuroImage*, 55(4), pp.1728–1738.

Biswal, B. et al., 1995. - Functional connectivity in the motor cortex of resting human brain using. *Magn Reson Med*, 34, pp.537–541.

Blain, C.R. V et al., 2006. Measuring brain stem and cerebellar damage in parkinsonian syndromes using diffusion tensor MRI. *Neurology*, 67(12), pp.2199–2205.

Bloem, B.R. et al., 2004. Falls and freezing of Gait in Parkinson's disease: A review of two interconnected, episodic phenomena. *Movement Disorders*, 19(8), pp.871–884.

Braak, H. et al., 2003. Staging of brain pathology related to sporadic Parkinson's disease. *Neurobiology of Aging*, 24(2), pp.197–211.

Bressler, S.L. & Kelso, J.A.S., 2001. Cortical coordination dynamics and cognition. *Trends in Cognitive Sciences*, 5(1), pp.26–36.

Buhmann, C. et al., 2005. Motor reorganization in asymptomatic carriers of a single mutant Parkin allele: A human model for presymptomatic parkinsonism. *Brain*, 128(10), pp.2281–2290.

Buhmann, C. et al., 2003. Pharmacologically modulated fMRI - Cortical responsiveness to levodopa in drug-naive hemiparkinsonian patients. *Brain*, 126(2), pp.451–461.

Cerasa, A. et al., 2006. Functional changes in the activity of cerebellum and frontostriatal regions during externally and internally timed movement in Parkinson's disease. *Brain Research Bulletin*, 71(1-3), pp.259–269.

Chan, L.-L. et al., 2007. Case control study of diffusion tensor imaging in Parkinson's disease. *Journal of neurology, neurosurgery, and psychiatry*, 78(12), pp.1383–1386.

Chesselet, M.F. & Delfs, J.M., 1996. Basal ganglia and movement disorders: An update. *Trends in Neurosciences*, 19(10), pp.417–422.

Cochrane, C.J. & Ebmeier, K.P., 2013. Diffusion tensor imaging in parkinsonian syndromes: A systematic review and meta-analysis. *Neurology*, 80(9), pp.857–864.

Damoiseaux, J.S. et al., 2006. Consistent resting-state networks across healthy subjects. *Proceedings of the National Academy of Sciences of the United States of America*, 103(37), pp.13848–13853.

Deichmann, R. et al., 2003. Optimized EPI for fMRI studies of the orbitofrontal cortex. *NeuroImage*, 19(2), pp.430–441.

Delaveau, P. et al., 2010. Dopaminergic modulation of the default mode network in Parkinson's disease. *European neuropsychopharmacology : the journal of the European College of Neuropsychopharmacology*, 20(11), pp.784–792.

Desmond, J.E. & Glo, G.H., 2002. Estimating sample size in functional MRI ( fMRI ) neuroimaging studies : Statistical power analyses. , 118, pp.115–128.

Du, G. et al., 2011. Combined R2* and Diffusion Tensor Imaging Changes in the Substantia Nigra in Parkinson's Disease. *Movement Disorders*, 26(9), pp.1627–1632.

Eckert, T. et al., 2006. Increased pre-SMA activation in early PD patients during simple self-initiated hand movements. *Journal of Neurology*, 253(2), pp.199–207.

Edelman, G.M. & Gally, J.A., 2001. Degeneracy and complexity in biological systems. *Proceedings of the National Academy of Sciences of the United States of America*, 98(24), pp.13763–13768.

Van Den Eeden, S.K. et al., 2003. Incidence of Parkinson's disease: variation by age, gender, and race/ethnicity. *American journal of epidemiology*, 157(11), pp.1015–1022.

Esposito, F. et al., 2008. Independent component model of the default-mode brain function: combining individual-level and population-level analyses in resting-state fMRI. *Magnetic Resonance Imaging*, 26(7), pp.905–913.

Essen, D.C. Van et al., 2012. NeuroImage The Human Connectome Project : A data acquisition perspective. , 62, pp.2222–2231.

Fearnley, J.M. & Lees, A.J., 1991. Ageing and Parkinson's disease: substantia nigra regional selectivity. *Brain : a journal of neurology*, 114 ( Pt 5, pp.2283–2301.

Fox, M.D. & Greicius, M., 2010. Clinical applications of resting state functional connectivity. , 4(June).

Frisina, P.G., Haroutunian, V. & Libow, L.S., 2009. The neuropathological basis for depression in Parkinson's disease. *Parkinsonism and Related Disorders*, 15(2), pp.144–148.

Friston, K.J., Holmes, A.P. & Worsley, K.J., 1999. How Many Subjects Constitute a Study ? , 5, pp.1–5.

Gaenslen, A. et al., 2011. The patients' perception of prodromal symptoms before the initial diagnosis of Parkinson's disease. *Movement Disorders*, 26(4), pp.653–658.

Gattellaro, G. et al., 2009. White matter involvement in idiopathic Parkinson disease: a diffusion tensor imaging study. *AJNR. American journal of neuroradiology*, 30(6), pp.1222–1226.

Gavrilescu, M. et al., 2008. Functional connectivity estimation in fMRI data: Influence of preprocessing and time course selection. *Human Brain Mapping*, 29(9), pp.1040–1052.

Georgopoulos, A.P., DeLong, M.R. & Crutcher, M.D., 1983. Relations between parameters of step-tracking movements and single cell discharge in the globus pallidus and subthalamic nucleus of the behaving monkey. *The Journal of neuroscience : the official journal of the Society for Neuroscience*, 3(8), pp.1586–1598.

Gorges, M. et al., 2013. Functional connectivity within the default mode network is associated with saccadic accuracy in Parkinson's disease: a resting-state FMRI and videooculographic study. *Brain connectivity*, 3(3), pp.265–72.

Göttlich, M. et al., 2013. Altered Resting State Brain Networks in Parkinson's Disease. *PLoS ONE*, 8(10).

Grafton, S.T., 2004. Contributions of functional imaging to understanding parkinsonian symptoms. *Current Opinion in Neurobiology*, 14(6), pp.715–719.

Grafton, S.T. et al., 1997. Premotor cortex activation during observation and naming of familiar tools. *NeuroImage*, 6(4), pp.231–236.

Hacker, C.D. et al., 2012. Resting state functional connectivity of the striatum in Parkinson's disease. *Brain : a journal of neurology*, 135(Pt 12), pp.3699–711.

Haslinger, B. et al., 2001. Event-related functional magnetic resonance imaging in Parkinson's disease before and after levodopa. *Brain*, 124(Pt 3), pp.558–570.

Helmich, R.C. et al., 2010. Spatial remapping of cortico-striatal connectivity in parkinson's disease. *Cerebral Cortex*, 20(5), pp.1175–1186.

Herz et al., 2014. Functional Neuroimaging of Motor Control in PArkinson's Disease: A Meta-Analysis. *Hum Brain Mapp, 35, pp3227-3237.*

Hikosaka, O. & Isoda, M., 2010. Switching from automatic to controlled behavior: cortico-basal ganglia mechanisms. *Trends in Cognitive Sciences*, 14(4), pp.154–161.

Holden, A. et al., 2006. Basal ganglia activation in Parkinson's disease. *Parkinsonism and Related Disorders*, 12(2), pp.73–77.

Hughes, A.J. et al., 1992. Accuracy of clinical diagnosis of idiopathic Parkinson's disease: a clinico-pathological study of 100 cases. *Journal of Neurology, Neurosurgery & Psychiatry*, 55(3), pp.181–184.

Ibarretxe-bilbao, N. et al., 2009. Differential progression of brain atrophy in Parkinson disease with and without visual hallucinations. *Journal of neurology, neurosurgery, and psychiatry*, 81(6), pp.650–657.

Jahanshahi, M. et al., 2010. Dopaminergic modulation of striato-frontal connectivity during motor timing in Parkinson's disease. *Brain*, 133(3), pp.727–745.

Jankovic, J., 2008. Parkinson ' s disease : clinical features and diagnosis Parkinson ' s disease : clinical features and diagnosis. *Journal of Neurology*, 79(4), pp.368–376.

Jenkins, I.H. et al., 1992. Impaired activation of the supplementary motor area in Parkinson's disease is reversed when akinesia is treated with apomorphine. *Annals of neurology*, 32(6), pp.749–757.

Jenkinson, M. et al., 2002. Improved optimization for the robust and accurate linear registration and motion correction of brain images. *NeuroImage*, 17(2), pp.825–841.

Kahan, J. et al., 2014. Resting state functional MRI in Parkinson's disease: the impact of deep brain stimulation on "effective" connectivity. *Brain : a journal of neurology*, 137(Pt 4), pp.1130–44.

Karagulle Kendi, A.T. et al., 2008. Altered diffusion in the frontal lobe in Parkinson disease. *American Journal of Neuroradiology*, 29(3), pp.501–505.

Kim, H.J. et al., 2013. Alterations of mean diffusivity in brain white matter and deep gray matter in Parkinson's disease. *Neuroscience Letters*, 550, pp.64–68.

Kish, S.J., Shannak, K. & Hornykiewicz O., 1988. Uneven patterns of dopamine loss in the striatum of patients with idiopathic Parkinson's disease. *New England Journal of Medicine*, 318, pp.876–880.

Kraft, E. et al., 2009. Levodopa-induced striatal activation in Parkinson's disease: A functional MRI study. *Parkinsonism and Related Disorders*, 15(8), pp.558–563.

Krajcovicova, L. et al., 2012. The default mode network integrity in patients with Parkinson's disease is levodopa equivalent dose-dependent. *Journal of Neural Transmission*, 119(4), pp.443–454.

Kwak, Y. et al., 2010. Altered resting state cortico-striatal connectivity in mild to moderate stage Parkinson's disease. *Frontiers in systems neuroscience*, 4, p.143.

Kwak, Y. et al., 2012. L-DOPA changes spontaneous low-frequency BOLD signal oscillations in Parkinson's disease: a resting state fMRI study. *Frontiers in Systems Neuroscience*, 6.

Liu, H. et al., 2013. Altered resting-state functional connectivity of the dentate nucleus in Parkinson's disease. *Psychiatry Research - Neuroimaging*, 211(1), pp.64–71.

Loane, C. et al., 2013. Serotonergic loss in motor circuitries correlates with severity of action-postural tremor in PD. *Neurology*, 80(20), pp.1850–1855.

Luo, C. et al., 2014. Reduced functional connectivity in early-stage drug-naive Parkinson's disease: A resting-state fMRI study. *Neurobiology of Aging*, 35(2), pp.431–441.

Marras, C. & Lang, A., 2008. Invited article: Changing concepts in Parkinson disease: Moving beyond the Decade of the Brain. *Neurology*, 70(21), pp.1996–2003.

Mattila, P.M. et al., 2001. Choline acetytransferase activity and striatal dopamine receptors in Parkinson's disease in relation to cognitive impairment. *Acta Neuropathologica*, 102(2), pp.160–166.

Menke, R.A. et al., 2010. Connectivity-based segmentation of the substantia nigra in human and its implications in Parkinson's disease. *NeuroImage*, 52(4), pp.1175–1180.

Mori, S. et al., 2006. Principles of diffusion tensor imaging and its applications to basic neuroscience research. *Neuron*, 51(5), pp.527–39.

Mulder, T., Zijlstra, W. & Geurts, A., 2002. Assessment of motor recovery and decline. *Gait & posture*, 16(2), pp.198–210.

O'Neill, M.J. & Dix, S., 2007. AMPA receptor potentiators as cognitive enhancers. *IDrugs : the investigational drugs journal*, 10(3), pp.185–192.

Obeso, I. et al., 2013. Bilateral stimulation of the subthalamic nucleus has differential effects on reactive and proactive inhibition and conflict-induced slowing in Parkinson's disease. *Experimental Brain Research*, 226(3), pp.451–462.

Obeso, J.A. et al., 2002. The basal ganglia and disorders of movement: pathophysiological mechanisms. *News in physiological sciences : an international journal of physiology produced jointly by the International Union of Physiological Sciences and the American Physiological Society*, 17, pp.51–55.

Olanow, C.W., Stern, M.B. & Sethi, K., 2009. The scientific and clinical basis for the treatment of Parkinson disease (2009). *Neurology*, 72(21 SUPPL. 4).

Palmer, S.J. et al., 2010. Joint amplitude and connectivity compensatory mechanisms in Parkinson's disease. *Neuroscience*, 166(4), pp.1110–1118.

Palmer, S.J. et al., 2009. Motor reserve and novel area recruitment: Amplitude and spatial characteristics of compensation in Parkinson's disease. *European Journal of Neuroscience*, 29(11), pp.2187–2196.

Péran, P. et al., 2010. Magnetic resonance imaging markers of Parkinson's disease nigrostriatal signature. *Brain*, 133(11), pp.3423–3433.

Pinto, S. et al., 2011. Functional magnetic resonance imaging exploration of combined hand and speech movements in Parkinson's disease. *Movement Disorders*, 26(12), pp.2212–2219.

Playford, E.D. et al., 1992. Impaired mesial frontal and putamen activation in Parkinson's disease: a positron emission tomography study. *Annals of neurology*, 32(2), pp.151–161.

Politis, M. et al., 2010. Depressive symptoms in PD correlate with higher 5-HTT binding in raphe and limbic structures. *Neurology*, 75(21), pp.1920–1927.

Politis, M. et al., 2011. Serotonergic mediated body mass index changes in Parkinson's disease. *Neurobiol Dis*, 43(3), pp.609–615.

Politis, M. et al., 2010. Staging of serotonergic dysfunction in Parkinson's Disease: An in vivo 11C-DASB PET study. *Neurobiology of Disease*, 40(1), pp.216–221.

Popescu, A. & Lippa, C.F., 2004. Parkinsonian syndromes: Parkinson's disease dementia, dementia with Lewy bodies and progressive supranuclear palsy. *Clinical Neuroscience Research*, 3(6), pp.461–468.

Poulopoulos, M., Levy, O.A. & Alcalay, R.N., 2012. The neuropathology of genetic Parkinson's disease. *Movement Disorders*, 27(7), pp.831–842.

Prakash, B.D. et al., 2012. Asymmetrical diffusion tensor imaging indices of the rostral substantia nigra in Parkinson's disease. *Parkinsonism and Related Disorders*, 18(9), pp.1029–1033.

Prodoehl, J. et al., 2010. Blood oxygenation level-dependent activation in basal ganglia nuclei relates to specific symptoms in de novo Parkinson's disease. *Movement Disorders*, 25(13), pp.2035–2043.

Quinn, N. et al., 1996. Core assessment program for intracerebral transplantation in Huntington's disease (CAPIT-HD). *Movement Disorders*, 11(2), pp.143–150.

Rae, C.L. et al., 2012. White matter pathology in Parkinson's disease: The effect of imaging protocol differences and relevance to executive function. *NeuroImage*, 62(3), pp.1675–1684.

Raichle, M.E. et al., 2001. A default mode of brain function. *Proceedings of the National Academy of Sciences of the United States of America*, 98(2), pp.676–682.

Rascol, O. et al., 1992. Supplementary and primary sensory motor area activity in Parkinson's disease. Regional cerebral blood flow changes during finger movements and effects of apomorphine. *Archives of neurology*, 49(2), pp.144–148.

Redgrave, P. et al., 2010. Goal-directed and habitual control in the basal ganglia: implications for Parkinson's disease. *Nature reviews. Neuroscience*, 11(11), pp.760–772.

Riecker, A. et al., 2003. Parametric analysis of rate-dependent hemodynamic response functions of cortical and subcortical brain structures during auditorily cued finger tapping: A fMRI study. *NeuroImage*, 18(3), pp.731–739.

De Rijk, M.C. et al., 2000. Prevalence of Parkinson's disease in Europe: A collaborative study of population-based cohorts. Neurologic Diseases in the Elderly Research Group. *Neurology*, 54(11 Suppl 5), pp.S21–S23.

Rolheiser, T.M. et al., 2011. Diffusion tensor imaging and olfactory identification testing in early-stage Parkinson's disease. *Journal of Neurology*, 258(7), pp.1254–1260.

Rolinski, M. et al., 2015. Aberrant functional connectivity within the basal ganglia of patients with Parkinson's disease. *NeuroImage: Clinical*, 8, pp.126–132.

ROTHWELL, J.C., 2011. THE MOTOR FUNCTIONS OF THE BASAL GANGLIA. *Journal of Integrative Neuroscience*, 10(03), pp.303–315.

Rowe, J. et al., 2002. Attention to action: Specific modulation of corticocortical interactions in humans. *NeuroImage*, 17(2), pp.988–998.

Sabatini, U. et al., 2000. Cortical motor reorganization in akinetic patients with Parkinson's disease A functional MRI study. *Brain*, 123 ( Pt 2, pp.394–403.

Samuel, M. et al., 1997. Evidence for lateral premotor and parietal overactivity in Parkinson's disease during sequential and bimanual movements. A PET study. *Brain*, 120(6), pp.963–976.

Schocke, M.F.H. et al., 2002. Diffusion-weighted MRI differentiates the Parkinson variant of multiple system atrophy from PD. *Neurology*, 58(4), pp.575–580.

Schwarz, S.T. et al., 2013. Diffusion tensor imaging of nigral degeneration in Parkinson's disease: A region-of-interest and voxel-based study at 3 T and systematic review with meta-analysis. *NeuroImage: Clinical*, 3, pp.481–488.

Sen, S. et al., 2010. Dynamic changes in cerebello-thalamo-cortical motor circuitry during progression of Parkinson's disease. *Neuroscience*, 166(2), pp.712–719.

Seppi, K. et al., 2003. Diffusion-weighted imaging discriminates progressive supranuclear palsy from PD, but not from the parkinson variant of multiple system atrophy. *Neurology*, 60(6), pp.922–927.

Sharman, M. et al., 2013. Parkinson's disease patients show reduced cortical-subcortical sensorimotor connectivity. *Movement Disorders*, 28(4), pp.447–454.

Skidmore, F.M., Yang, M., Baxter, L., von Deneen, K., et al., 2013. Apathy, depression, and motor symptoms have distinct and separable resting activity patterns in idiopathic Parkinson disease. *NeuroImage*, 81, pp.484–495.

Skidmore, F.M., Yang, M., Baxter, L., von Deneen, K.M., et al., 2013. Reliability analysis of the resting state can sensitively and specifically identify the presence of Parkinson disease. *NeuroImage*, 75, pp.249–261.

Skorpil, M. et al., 2012. MRI diffusion in Parkinson's disease: Using the technique's inherent directional information to study the olfactory bulb and substantia Nigra. *Journal of Parkinson's Disease*, 2(2), pp.171–180.

Smith, S.M., 2002. Fast robust automated brain extraction. *Human Brain Mapping*, 17(3), pp.143–155.

Spraker, M.B. et al., 2010. Basal ganglia hypoactivity during grip force in drug naive Parkinson's disease. *Hum Brain Mapp*, 31(12), pp.1928–1941.

Supekar, K. et al., 2008. Network Analysis of Intrinsic Functional Brain Connectivity in Alzheimer ' s Disease. , 4(6).

Szewczyk-Krolikowski, K. et al., 2014. Functional connectivity in the basal ganglia network differentiates PD patients from controls. *Neurology*, 83(3), pp.208–214.

Tessa, C. et al., 2013. FMRI changes in cortical activation during task performance with the unaffected hand partially reverse after ropinirole treatment in de novo Parkinson's disease. *Parkinsonism and Related Disorders*, 19(2), pp.265–268.

Tessa, C. et al., 2012. Hypoactivation of the primary sensorimotor cortex in de novo Parkinson's disease: A motor fMRI study under controlled conditions. *Neuroradiology*, 54(3), pp.261–268.

Tessitore, A. et al., 2012. Resting-state brain connectivity in patients with Parkinson's disease and freezing of gait. *Parkinsonism & Related Disorders*, 18(6), pp.781–787.

Tolosa, E. et al., 2009. Diagnosis and the premotor phase of Parkinson disease. *Neurology*, 72(7 SUPPL. 2).

Vaillancourt, D.E. et al., 2009. High-resolution diffusion tensor imaging in the substantia nigra of de novo Parkinson disease. *Neurology*, 72(16), pp.1378–1384.

Wakabayashi, K. et al., 2007. The Lewy body in Parkinson's disease: Molecules implicated in the formation and degradation of alpha-synuclein aggregates. In *Neuropathology*. pp. 494–506.

Wang, J. et al., 2015. Amplitude of Low-frequency Oscillations in Parkinson′s Disease: A 2-year Longitudinal Resting-state Functional Magnetic Resonance Imaging Study. *Chinese Medical Journal*, 128(5), p.593.

Wang, J., Zuo, X. & He, Y., 2010. Graph-based network analysis of resting-state functional MRI. *Frontiers in systems neuroscience*, 4, p.16.

Wiltshire, K. et al., 2010. Corpus callosum and cingulum tractography in Parkinson's disease. *The Canadian journal of neurological sciences. Le journal canadien des sciences neurologiques*, 37(5), pp.595–600.

Wu, T. et al., 2012. Basal ganglia circuits changes in Parkinson's disease patients. *Neuroscience Letters*, 524(1), pp.55–59.

Wu, T., Wang, L., et al., 2009. Changes of functional connectivity of the motor network in the resting state in Parkinson's disease. *Neuroscience Letters*, 460(1), pp.6–10.

Wu, T., Wang, L., et al., 2011. Effective connectivity of brain networks during self-initiated movement in Parkinson's disease. *NeuroImage*, 55(1), pp.204–215.

Wu, T., Long, X., et al., 2011. Functional connectivity of cortical motor areas in the resting state in Parkinson's disease. *Human Brain Mapping*, 32(9), pp.1443–1457.

Wu, T. et al., 2010. Neural correlates of bimanual anti-phase and in-phase movements in Parkinson's disease. *Brain*, 133(8), pp.2394–2409.

Wu, T., Long, X., et al., 2009. Regional homogeneity changes in patients with parkinson's disease. *Human Brain Mapping*, 30(5), pp.1502–1510.

Wu, T. & Hallett, M., 2005. A functional MRI study of automatic movements in patients with Parkinson's disease. *Brain : a journal of neurology*, 128(Pt 10), pp.2250–9.

Yoshikawa, K. et al., 2004. Early pathological changes in the parkinsonian brain demonstrated by diffusion tensor MRI. *Journal of neurology, neurosurgery, and psychiatry*, 75(3), pp.481–484.

Yu, R. et al., 2013. Enhanced Functional Connectivity between Putamen and Supplementary Motor Area in Parkinson's Disease Patients. *PLoS ONE*, 8(3).

Zang, Y. et al., 2004. Regional homogeneity approach to fMRI data analysis. *NeuroImage*, 22(1), pp.394–400.

Zang, Y.-F. et al., 2007. Altered baseline brain activity in children with ADHD revealed by resting-state functional MRI. *Brain & development*, 29(2), pp.83–91.

Zhan, W. et al., 2012. Regional alterations of brain microstructure in Parkinson's disease using diffusion tensor imaging. *Movement disorders : official journal of the Movement Disorder Society*, 27(1), pp.90–7.

Zhou, J. et al., 2010. Divergent network connectivity changes in behavioural variant frontotemporal dementia and Alzheimer ' s disease. , pp.1352–1367.

Ziegler, D.A. et al., 2013. Substantia nigra volume loss before basal forebrain degeneration in early Parkinson disease. *JAMA neurology*, 70(2), pp.241–7.

Zigmond, M.J. et al., 1990. Compensations after lesions of central dopaminergic neurons: some clinical and basic implications. *Trends in neurosciences*, 13(7), pp.290–296.